Topoisomerase II and dynamic microtubules solve sister chromatid intertwinings in anaphase

Iris Titos Vivancos

TESI DOCTORAL UPF / ANY 2013

DIRECTOR DE LA TESI

Manuel Mendoza

Departament of Cell and Developmental Biology, CRG

upf. **Universitat
Pompeu Fabra**
Barcelona

This page intentionally left blank

Acknowledgements

First and foremost, I would like to express my very great appreciation to my PhD advisor, Manuel Mendoza, for his patience, supervision and enthusiastic encouragement during the last years. Thank you Manuel for giving me the freedom to develop my own ideas and for your support and useful critiques that have helped me to be a better scientist. I have enjoyed a lot the time spent in the lab and, although it is time for me to leave, it is really sad to say goodbye!

I would like to thank the members of my Thesis Committee and PhD Defense Board for their valuable and constructive suggestions during the development of this research work. My most sincere gratitude to Francesc Posas, Vivek Malhotra, Ben Lehner, Jordi Torres-Rosell and Isabelle Vernos. Dear Francesc, thanks for giving me the opportunity to start working in your lab during my degree, it has been a pleasure to count on your advice throughout these years. Dear Vivek, I deeply appreciate your counsels during my PhD and your guidance in planning the next step of my career. I want to thank you, Isabelle Vernos, for your support and criticism and all the fruitful lab meetings we have had the pleasure to share with your lab during these years.

I am grateful for the assistance given by the units of Advanced Light Microscopy, Genomics and Bioinformatics from the Core Facilities at the CRG. I would like to specially thank Raquel Garcia and Arrate Mallabiabarrena for their support, training and patience during these years. I wish to acknowledge the essential help provided by Ernesto Lowy, Luca Cozzuto, Toni Gabaldon and Leszek Pryszcz.

During these years I was fortunate to share data clubs, discussions, pro-

tocols and much more with the people from the Cell and Developmental Biology Program. I would like to thank all of them for their help, counsel and enthusiasm. Specially, Hernan Lopez Schier's and Pedro Carvalho's labs for sharing space and long hours in the lab.

In the last years I have had the pleasure of being surrounded by awesome people whose contribution to this thesis is essential. I would like to thank all the past and present lab mates with whom I have shared long lab meetings, protocols, discussions, endless days at the lab, retreats and much more. This work would not have been possible without all of you! Thank you Gabriel, Petra, Nuno, Francesca, Arun and Michael for your enthusiasm, you are great and I will miss you a lot. Evi, it was great meeting you, as you already know, you are a role model for me and I hope we keep in touch despite the distance. Trini, muchas gracias por tu ayuda, tus consejos y tu alegría a lo largo de estos años. Àlex, moltes gràcies per la teva dedicació, ets un molt bon amic que m'ha ajudat a tirar endavant en els moments difícils. Tu més que ningú saps que aquesta tesi no hagués estat possible sense tu! Moltes gràcies Aina pel teu suport durant aquests anys. Juntes hem passat de tot, quan no teníem ni idea de què feiem, els protocols que no funcionaven, els resultats negatius, els canvis de projectes... però també hem passat molts bons moments juntes i hem rigut un munt. Espero que malgrat la distància, la nostra amistat perduri!

Estimats pares, us vull donar les gràcies per tantes coses que no sé ni per on començar. Moltes gràcies pels valors que m'heu transmès. A vosaltres us dec la perseverància i la constància que han sigut essencials per arribar on sóc ara. M'heu donat les eines i, sobretot, l'amor necesari per enfrentar-me als reptes de la vida i per perseguir els meus somnis allà on siguin. Tot el que sóc és gràcies a vosaltres.

Finalment, és difícil trobar les paraules correctes per la persona a qui més he d'agrair. Benjamín, sense la teva paciència infinita, la teva comprensió i el teu amor aquesta tesi no hagués estat possible. Moltes gràcies per haver estat al meu costat tot aquest temps i per voler compartir amb mi totes les aventures futures que ens queden per viure.

Iris Titos Vivancos

This page intentionally left blank

Abstract

At the metaphase-to-anaphase transition, spindle microtubules pull repli-cated chromosomes to the daughter cells, but full separation of long chro-mosome arms is achieved in late anaphase. We have created an allelic series of long chromosomes to elucidate the mechanisms involved in long chromo-some resolution during mitosis. With this method we have shown that long chromosome cells are sensitized to the loss of genes involved in chromosome structure and segregation. We have discovered that Topoisomerase II is needed during anaphase to resolve distal regions of long chromosomes and that the activity of the microtubule polymerase Stu2 is crucial in the resolu-tion of catenations. Moreover, we have identified the nuclear organization as a new source that contributes to the topological stress accumulated in chro-mosomes. Thus, topological constraints imposed by chromosome length and nuclear architecture determine the amount of sister chromatid intertwinings that must be resolved by Topoisomerase II and dynamic microtubules during anaphase.

Resum

A la transició entre metafase i anafase els microtúbuls del fus mitòtic transporten els cromosomes a les cèl·lules filles, tot i això la separació completa dels braços dels cromosomes no succeeix fins al final d'anafase. Amb l'objectiu d'entendre com es resolen els cromosomes llargs durant anafase, hem creat una sèrie al·lèlica de cromosomes artificalment llargs. Amb aquesta metodologia hem demostrat que les cèl·lules que contenen cromosomes llargs estan sensibilitzades a la pèrdua de gens involucrats en l'estructura i la segregació de cromosomes. Hem descobert que la Topoisomerasa II es necesària durant anafase per resoldre les regions distals de cromosomes llargs i que l'activitat de la polimerasa de microtúbuls, Stu2, és essential en la resolució de concatenacions entre cromàtides germanes. A més, hem pogut identificar l'organització nuclear com una nova font que contribueix a l'estrés topològic acumulat als cromosomes. En conclusió, les restriccions topològiques que imposen tant la longitud dels cromosomes com l'arquitectura nuclear determinen la quantitat de concatenacions entre cromàtides germanes que han de ser resoltes per la Topoisomerasa II i els microtúbuls dinàmics durant anafase.

Preface

In this study we present evidence that sister chromatid entanglements are resolved during anaphase by Topoisomerase II and dynamic microtubules. That catenations need to be resolved in order to ensure proper chromosome segregation has been known for a long time. However, it was not clear at what moment during the cell cycle endogenous chromosomes were completely decatenated.

The study of DNA topology has historically been carried out in plasmids. This is due to the fact that these circular molecules retain the topological information after being purified from the cells allowing an easy assessment of the catenations and supercoilings present in the constructs. Linear chromosomes lose their topology during the DNA extraction process. Thus, most of the data accumulated during years is based on circular DNA molecules and the it was assumed that the same processes were taking place in linear chromosomes. Our findings help to understand how endogenous sister chromatids are resolved.

The approach we have used to investigate chromosome segregation has been the creation of an allelic series of long chromosomes by fusing endogenous chromosomes in *Saccharomyces cerevisiae*. The fusion of chromosomes in budding yeast was already described in the laboratory (Neurohr et al., 2011). We have used this tool to look for mutations that decrease long chromosome bearing cell's viability with the aim to get a better understanding on how wild type chromosomes are segregated.

After this short historical perspective, I wish the reader the same pleasure reading this thesis as I had writing it.

This page intentionally left blank

Contents

This page intentionally left blank

1

Introduction

In order to properly partition chromosome arms during mitosis, sister chromatids must be resolved before cytokinesis takes place. Many of the essential components of the segregation machinery have been identified. Notably, the SMC complexes (cohesin, condensin and Smc5/6), Aurora B kinase and Topoisomerase II are required for proper chromosome segregation. However, it is still not well understood how their function is coordinated. In particular, it is known that at the metaphase-to-anaphase transition, upon cohesin cleavage, sister chromatids segregated, but how condensation and decatenation contribute to their segregation at this stage is not fully understood.

In this study, I show that sister chromatids are still connected after the metaphase-to-anaphase transition and that decatenation takes place during anaphase and requires the action of both Topoisomerase II and microtubule dynamics. Moreover, this process is crucial in longer chromosomes because they accumulate more topological stress due to their length and nuclear architecture. We investigated cell cycle progression in normal and artificially

lengthened chromosomes and used these constructs as a tool to gain a better understanding of the molecular processes that occur during chromosome segregation.

This introduction will briefly summarize current knowledge about the changes in the structure of chromosomes occurring during the cell cycle, the role and components of the mitotic spindle, and the principles of nuclear organization. Because the experimental approach used *Saccharomyces cerevisiae* as a model organism, the particularities of this organism will also be considered.

1.1   Cell cycle overview

The cell cycle is a highly regulated series of events that leads to cell reproduction. All cells arise by division of existing cells, and every cell living today descended from a single ancestral cell that lived 3 or 4 billion years ago. Throughout this time, the evolution of cells and organisms has depended on the faithful transmission of genetic information by cell division.

1.1.1   Phases of the cell cycle

There are different stages during the cell cycle that are defined by chromosomal events. In the first phase, named S phase, the DNA is replicated. This process is initiated at the replication origins that are scattered throughout the genome. Sister chromatids are cohesed due to the deposition of cohesion proteins during duplication. In the second phase, mitosis, the duplicated chromosomes are distributed equally to the daughter cells. During this phase, the pairs of sister chromatids are attached to the mitotic spindle, a bipolar array of microtubules. Later in mitosis, sister chromatid cohesion

is destroyed and the microtubules from the spindle pull the separated chromatids to opposite ends of the cell (Figure 1.1) (Morgan, 2007).

Mitosis is typically divided into different phases based on cytological analysis:

- **Prophase:** this phase is initiated by the onset of condensation, that is apparent in the microscope in higher eukaryotes. Also, the centromeres separate and the spindle starts to assemble.

- **Prometaphase:** the nuclear envelope breaks in higher eukaryotes like animals and plants. During this phase the chromatids are completely attached to the spindle.

- **Metaphase:** this is the period during which the sister chromatids are aligned at the center of the spindle, the metaphase plate.

- **Anaphase:** the decohesion of sister chromatids defines anaphase onset, during this phase the sisters are separated and pulled towards opposite poles of the spindle.

- **Telophase:** the chromosomes and other nuclear components are packed into the daughter cells and the spindle disassembles.

After the formation of two daughter nuclei during mitosis, cytoplasmatic division partitions the cell into two daughter cells, this process is known as cytokinesis.

The majority of cycles contain two additional steps, known as gap phases, that occur between S phase and Mitosis. Gap phases provide time for cell growth and serve as regulatory transitions. The first gap phase, G1, occurs before S phase and the second, G2, takes place before Mitosis (Figure 1.1).
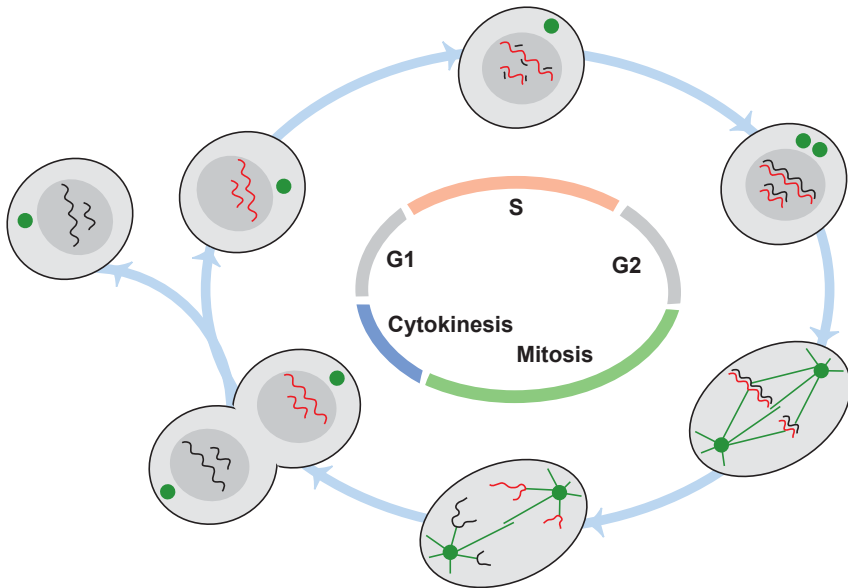
Figure 1.1: The eukaryotic cell cycle. Chromosome duplication takes place in
S phase, followed by chromosome segregation during mitosis and cytokinesis. G1 is
the gap between M and S and G2 is the gap between S and M phases. The figure
is based on (Morgan, 2007).

With the exception of chromosomes, most of the organelles within the
cells are constantly replicated through the cell cycle resulting in the gradual
doubling of cell size at the end of the cell cycle.

1.1.2   Cell cycle control system

There are regulatory mechanisms that ensure that the events of the cell cycle
follow a determined order therefore guaranteeing fidelity in cell reproduction.

The order and alternation of cell-cycle events are reinforced by the de-
pendence of one event on another and by feedback from the cell-cycle ma-
chinery to the control system. If the control system detects problems in the
completion of specific events, it will delay the initiation of later events until

the problems are solved. The stages of the cell cycle whose completion is monitored in this way are known as checkpoints.

Oscillatory mechanism that control cell cycle

The cell cycle control system is governed by cyclin-dependent kinases (Cdks). These kinases phosphorylate, and thus activate, proteins involved in cell-cycle events. Because the concentration of Cdk proteins remains constant along the cell cycle, the oscillations in their activity depend on the expression of their regulatory subunits, the cyclins, which bind to Cdks and stimulate their activity (Morgan, 1997).

The formation of different Cdk-cyclin complexes is a result of the regulation of the expression levels of the different cyclins throughout the cell cycle. The three major cyclin types (G1/S, S and M cyclin) oscillate during the cell cycle in parallel with the Cdk-cyclin complex activity (Figure 1.2).
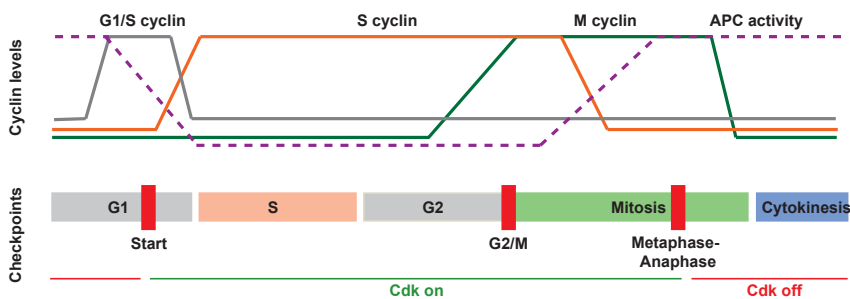
Figure 1.2: The cell-cycle control system. The levels of the three major cyclins oscillate during the cell cycle. The three main cell cycle checkpoints are represented. The figure is based on (Morgan, 2007).

Regulatory checkpoints

The regulatory transitions that ensure correct progression through the cell cycle are called checkpoints (Hartwell and Weinert, 1989). There are three major checkpoints (Figure 1.2):

- **Start**: promotes the G1/S transition activating the G1/S- and S-phase cyclin-Cdk complexes that will phosphorylate proteins involved in DNA replication. Start governs the rate of cell division in most cells and depends both on external and intracellular factors. Yeast cells proliferation depends basically on the nutrients available in the media. However, animal cells proliferation depends on both tissue-specific programming and extracellular proteins produced by other cells (Morgan, 2007).

- **G2/M checkpoint**: G1/S- and S-phase cyclin-Cdk complexes will eventually activate M-phase cyclin-Cdk complexes that will phosphorylate proteins promoting spindle assembly and entry into mitosis. If chromosomal DNA is damaged or not fully replicated the checkpoint will be activated to prevent the distribution of damaged chromosomes. However, it has been shown that yeast cells can enter mitosis with un-replicated DNA (Torres-Rosell et al., 2007). Then, it remains unknown the specific nature of the checkpoint in different organisms.

- **Metaphase-to-anaphase transition**: the checkpoint monitors the correct assembly of the spindle and the proper attachment of the sister kinetochores to microtubules emanating from opposite spindle poles (spindle assembly checkpoint, SAC). Once the SAC is satisfied, the APC complex is activated and ubiquitylates cyclin B (activator of

CDK1) and securin (the inhibitor of separase) promoting their degradation by the proteasome (Figure 1.3). As a consequence, separase is active and cleaves the cohesin complex that was keeping sister chromatids together. Then, the spindle pulls the sister chromatids apart. APC activation is required for chromatid segregation, spindle disassembly and cytokinesis.
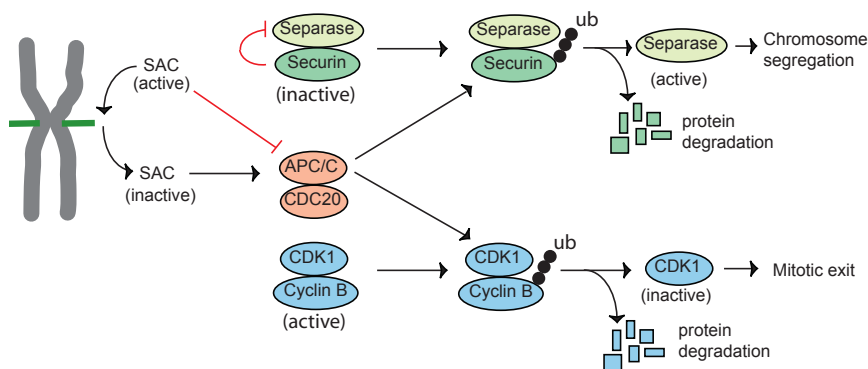
Figure 1.3: The metaphase-to-anaphase transition. Chromosome segregation is restrained by the SAC until chromosome bi-orientation achieved. Then, CDC20 is activated and ubiquitinates (ub) cyclin B and securin targeting them for degradation. As a result, separase is activated enabling chromosome segregation and the low levels of CDK activity promote mitotic exit. The figure is based on (Yanagida, 2009).

In addition to these major checkpoints, other cell cycle transitions might be subject to regulation in at least some cell types, a case in point is the mid-anaphase checkpoint in budding yeast (Introduction 1.4.3).

1.2   The chromosome cycle

The main goal of the cell cycle is to duplicate and segregate chromosomal DNA. Like the rest of cell cycle events, the chromosome cycle is regulated by cyclin-dependent kinases and the ubiquitin ligase APC.
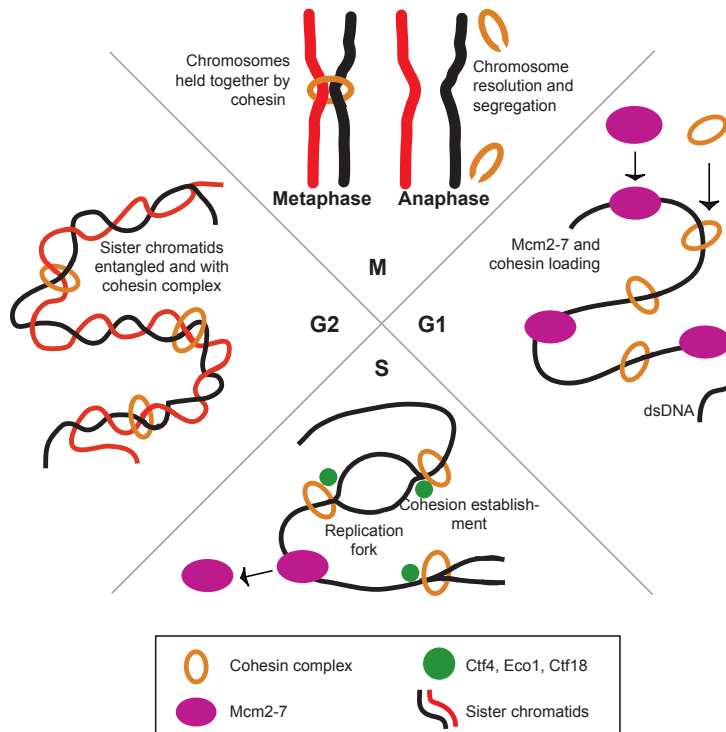
Figure 1.4: The chromosome cycle. DNA strand going through G1 with loading of Mcm2-7 and the cohesin complex and undergoing S phase with strand duplication and loading of cohesion effectors. As a result of replication, sister chromatids are kept together by DNA entanglements and the cohesin complex until the metaphase-to-anaphase transition. The figure is based on (Blow and Tanaka, 2005).

The eukaryotic nucleus is composed by a series of chromosomes that con-

tain long arrays of the DNA sequence. It is crucial to ensure that during each chromosome cycle (1) DNA is replicated only once in all the chromosomes and (2) sister chromatids are sent to different daughter cells. On one hand, cells manage to differentiate replicated and unreplicated DNA by loading of the Mcm2-7 complex in early G1 to mark the replication sites (Figure 1.4). On the other hand, also by means of a protein complex, loading of cohesin allows the cells to keep sister chromatids together from the moment they are replicated to the metaphase-to-anaphase transition (Blow and Tanaka, 2005). In the scheme (Figure 1.4), sister chromatids are decatenated at metaphase, however, as we shall see (Results 4.6.2), budding yeast chromosomes are catenated at metaphase and become decatenated during anaphase.

1.2.1   Chromosome duplication

Replication of chromosomes

The mark involved in DNA replication is the Mcm2-7 complex. This protein complex is loaded onto chromosomal DNA during late mitosis and early G1 in order to mark the sites to use as replication origins in the next S-phase (Blow and Laskey, 1988; Diffley, 2004; Blow and Tanaka, 2005). To avoid re-replication, loading of Mcm2-7 is prevented during late G1, S, G2 and early M phases.

Entanglement of sister chromatids

During chromosome duplication, the unwinding of the parental duplex leads to the accumulation of positively supercoiled DNA in front of the replication fork. This topological stress would difficult the advancement of the repli-

cation forks through the chromosomal DNA. There are two complementary strategies to reduce the accumulation of supercoiling structures and allow fork progression. On one hand, the superhelical tension can be removed enzymatically by topoisomerases that introduce transient DNA breaks (Wang, 2002). On the other hand, positive supercoiling can also be diminished if the advancing fork rotates along the DNA helix. However, the rotation of the DNA helix involves the formation of sister chromatid intertwinings (SCI) (Figure 1.5) (Wang, 2002; Postow et al., 2001).

After replication, sister chromatids must stay together until mitosis, as early separation will lead to unfaithful chromosome transmission due to the inability of the cell to distinguish sister chromatids. Therefore, although catenation of replicated chromosomes is often presented as a problem, the generation of catenated sister chromatids may assist in the proper segregation of duplicated chromosomes (Murray and Szostak, 1985). In this paper the authors propose that the separation of sister chromatids prior to anaphase is prevented by their catenation. However, this idea was overlooked since the discovery of the cohesin complex. Nowadays, new models point to the interplay between catenations and cohesin in maintaining sister chromatids together (Farcas et al., 2011). It has been proposed that the cohesin complex is necessary to maintain catenations between sister chromatids.

Chromosome cohesion

The cohesin complex is involved in the correct segregation of sister strands. At the end of M phase or during G1, the cohesin complex is loaded on the DNA. During S-phase, the cohesin complex establishes a physical link (cohesion) between sister chromatids (Michaelis et al., 1997; Uhlmann et al., 1999;
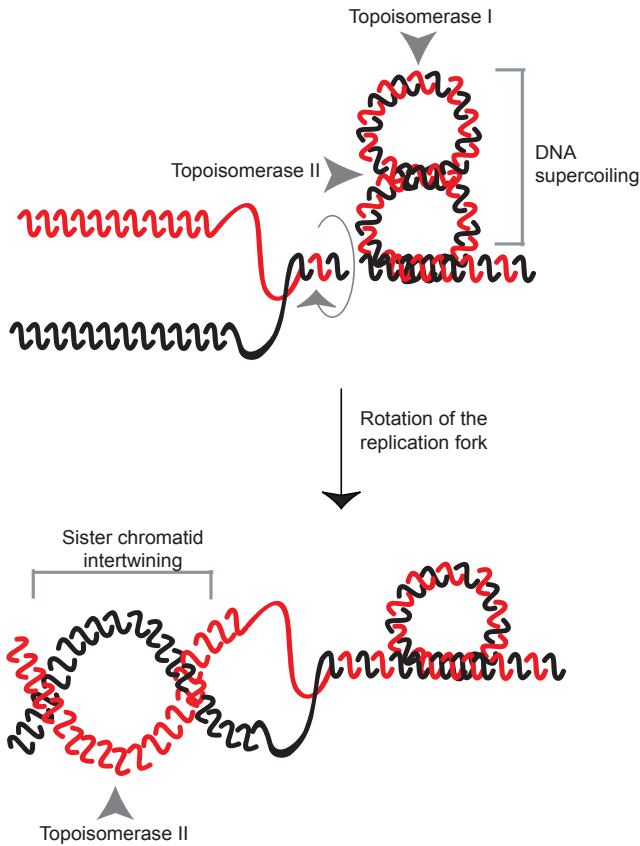
Figure 1.5: Catenations arise during replication. The supercoiling that accumulates in DNA strands during replication can be relaxed by the activity of topoisomerases or by rotating the DNA helix and therefore accumulating sister chromatid intertwinings. Figure adapted from (Kegel et al., 2011).

Tanaka et al., 2000). The cohesin complex consists of four proteins: Smc1, Smc3, Scc1 and Scc3 (Nasmyth and Haering, 2005). The SMC proteins form an intramolecular antiparallel coiled-coil that brings their globular N and C terminal together (Anderson et al., 2002; Haering et al., 2002) forming a ring (Figure 1.9). It is not known how cohesin associates with chromosomes, however, due to its ring shape different models proposed that cohesin embraces

sister chromatids and traps them inside its ring (Nasmyth and Haering, 2005; Haering et al., 2008). Cohesin association to chromosomes is found at specific sites: peri-centromeric regions and sites of convergent transcription.

Other factors also promote chromatid cohesion like: Eco1, Ctf4 and Ctf18 (Skibbens et al., 1999; Tóth et al., 1999; Hanna et al., 2001; Mayer et al., 2001). Loss of these factors produces partial loss of cohesion but does not affect the binding of the cohesin complex to the chromosomes.

Bi-orientation of sister chromatids

Sister chromatid cohesion is essential to ensure sister kinetochore bi- orientation. In order to ensure proper chromosome segregation, centromeres of sister chromatids must attach to microtubules extending from opposite spindle poles achieving sister kinetochore bi-orientation before anaphase onset takes place (Tanaka, 2005). The Aurora B kinase facilitates re-orientation of kinetochore-microtubule attachments by phosphorylation of kinetochore components until proper bi-orientation is achieved (Cheeseman et al., 2002; Tanaka et al., 2002; Hauf et al., 2003; Lampson et al., 2004).

1.2.2   Chromosome segregation

Metaphase-to-anaphase transition

At the metaphase-to-anaphase transition, after all chromosomes bi-orient, separase is activated and proteolitically cleaves cohesin to allow the sister chromatids to be pulled apart (Uhlmann, 2003). The separation of sister chromatids is irreversible, therefore, a number of mechanisms regulate this step.

Separase activity is inhibited by securin (Figure 1.3). Securin is tar-

geted for degradation at the metaphase-to-anaphase transition by the APC complex (Cohen-Fix et al., 1996; Funabiki et al., 1996; Ciosk et al., 1998). Moreover, the Scc1 cohesin subunit is phosphorylated during M phase by Polo-kinase to facilitate its cleavage by separase (Alexandru et al., 2001; Hauf et al., 2005).

The expression of a form of the cohesin complex that cannot be cleaved by separase blocks sister chromatid separation, which is consistent with the notion that chromosome segregation is inhibited if cohesin persists on the sister chromatids. Although mutations that inactivate the complex greatly diminished cohesion, it was not totally abolished (Michaelis et al., 1997). This observation suggests that cohesion could be maintained by multiple mechanisms, with catenanes representing one of them.

Resolution of catenations

As was already mentioned, apart from the cohesin proteinaceous scaffold, sister chromatids are also held together by the presence of entanglements between them that arise during replication. In order to individualize the chromosomes, sister chromatids need to be disentangled by Topoisomerase II, an enzyme that is essential in all organisms (Giménez-Abián et al., 2000; Uemura and Tanagida, 1986; Holm et al., 1989; Shamu and Murray, 1992). However, at which point during the cell cycle are endogenous chromosomes completely decatenated and how decatenation dynamics relate to chromosome length remains elusive.

Compaction of sister chromatids

Since interphase chromosomes are many times longer than the anaphase spindle, compaction of the chromatin fiber to reduce their length is essential to ensure their final segregation. As eukaryotic cells enter mitosis, chromatin condenses resulting in the formation of the mitotic chromosomes (Figure 1.6). The compaction of the mitotic chromosome is thought to involve the gradual folding of chromatin fibers into progressively more compact structures. This hierarchical folding may be guided by a structural protein scaffold that forms at the core of each sister chromatin and organizes the condensing chromatin around (Bazile et al., 2010). Mitotic chromosome compaction helps to organize the chromosomes into individual disentangled units thus assisting proper chromosome segregation and resolution during anaphase. The higher-order structure of condensed mitotic chromosomes is poorly understood.
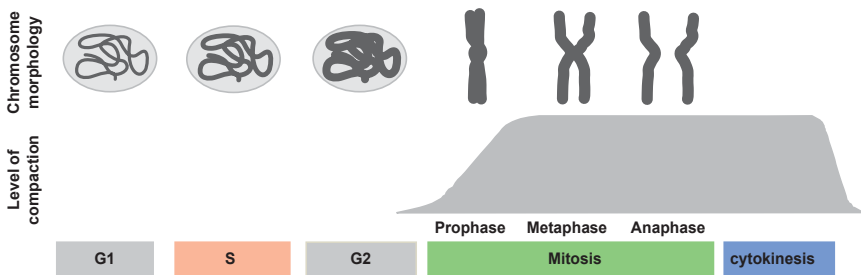
Figure 1.6: Chromosome condensation. The images above depict the changes in the morphology of chromosomes from interphase to the end of mitosis. The bottom graph represents the extent of chromosome condensation seen in mitosis. Stages of mitosis are limited to prophase, metaphase and anaphase for simplicity. The figure is based on (Bazile et al., 2010)

.

1.2.3 The Chromosome cycle in budding yeast

All eukaryotic cells employ similar machineries to duplicate their genome as well as to coordinate cell cycle events. Therefore, a lot of knowledge can be obtained by studying cell division in different species. In this study we have used the budding yeast *Saccharomyces cerevisiae* as a model organism.

Yeast are small, single-celled fungi and are among the simplest eukaryotes. They proliferate rapidly in simple culture conditions. One of the main strengths of yeast is the ease of genetic analysis because they can be grown in haploid state and its genome is fully sequenced and annotated. However, there are some differences to notice when comparing the cell cycle of budding yeast and higher eukaryotes.

First of all, yeast cells undergo closed mitosis, meaning that the nuclear envelope does not break and remains intact throughout the different stages of the cell cycle until it is cleaved in late mitosis. Secondly, in yeast, which have relatively small chromosomes, chromosome condensation is less extensive than in higher eukaryotes. However, condensation is still important to facilitate the resolution and segregation of sister chromatids. Furthermore, cohesin does not dissociate from chromatid arms in prophase like in higher eukaryotes. Instead, budding yeast chromosome arms remain linked along their entire length until anaphase onset. In addition, budding yeast undergo asymmetric cell division, the two daughter cells do not inherit an equal share of cytoplasmic components, the bud cell is always smaller than the mother cell (Morgan, 2007).

In budding yeast and higher eukaryotes segregation of sister chromatids during anaphase is accompanied by their regional stretching and subsequent recoiling (Figure 1.7) (Renshaw et al., 2010; Mora-Bermúdez et al., 2007). In
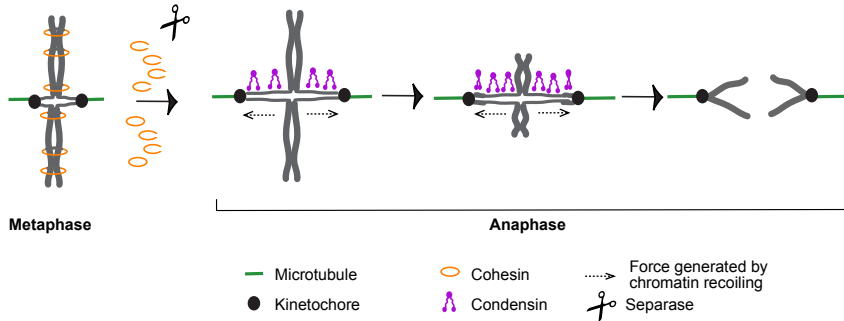
Figure 1.7: Chromosome segregation in budding yeast. Schematic representation of chromosome segregation in budding yeast. At anaphase onset, separase cleaves the majority of cohesin. However, due to a small amount of residual cohesin, sister chromatid cohesion is still present at some loci along chromosome arms, which transiently opposes sister chromatid separation and causes regional chromosome stretching. Stretched chromosome regions are coiled by the action of condensins. Adapted from (Renshaw et al., 2010).

particular, several studies have focused on the regulation of ribosomal DNA (rDNA) segregation in yeast (Freeman et al., 2000) because it is a repetitive region where specific proteins like Net1 are bound. Then, the rDNA can be visualized easily by fusing one of the specific proteins that bind to the array to a fluorescent tag. Separation of rDNA takes place in mid-anaphase independently of cohesins and this process requires the combined action of the condensin complex, Topoisomerase II, and other factors (D'Amours et al., 2004; Sullivan et al., 2004). Although these factors are also required for segregating the other chromosomes that do not carry rDNA (Bhalla et al., 2002), it is still poorly understood how segregation of such chromosomes is regulated. This is due in part to the difficulties in visualizing individual chromosomes in budding yeast.

1.3 Protein components of mitotic chromosomes

Studies of the composition of mitotic chromosomes initially revealed that they are formed by equal amounts of histone and non-histone proteins (Adolph et al., 1977) (Figure 1.8). Imaging of human metaphase chromosomes depleted of histones indicated that condensed mitotic chromosomes comprise successive loops of DNA that are anchored to a proteinacious chromosome axis (Paulson and Laemmli, 1977). This proteinacious skeletal-like structure, originally referred to as "the chromosome scaffold" (Earnshaw and Harrison, 1977) was later shown to be rich in Topoisomerase II (Earnshaw et al., 1985; Gasser et al., 1986) and the structural maintenance of chromosomes 2 (Smc2) protein that is part of the condensin complex (Saitoh et al., 1994). In order to segregate chromosomes, chromatin needs to be compacted and links between sister chromatids removed. Therefore, chromosome compaction, chromosome segregation and DNA topology are intricately interrelated (Koshland and Strunnikov, 1996).
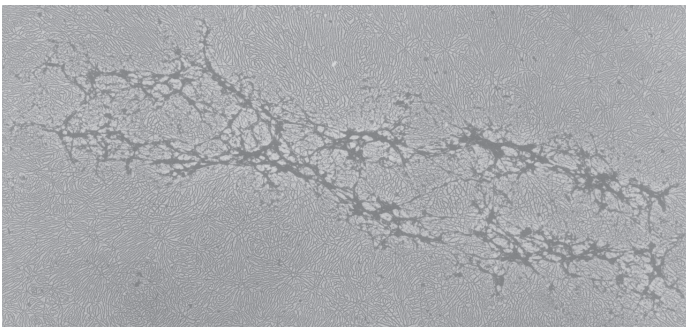
Figure 1.8: The chromosome scaffold. Histone-depleted chromosomes were prepared using dextran sulfate and heparin to visualize them by electron microscopy. The chromosome consists of a central darkly staining scaffold or core surrounded by a halo of DNA. Reproduced from (Paulson and Laemmli, 1977).

It is thought that sister chromatid resolution is achieved by cooperation
between Topoisomerase II and condensins (Coelho et al., 2003; Steffensen
et al., 2001). Indeed, when either Topoisomerase II or condensin is defective
or depleted in cells, similar phenotypes are often observed. Namely, during
anaphase many sister chromatids fail to separate, making bridges between
the two spindle poles. It is generally interpreted that these anaphase bridges
are due to poor resolution and/or abnormal compaction of sister chromatids
in earlier phases of mitosis (Hirano, 2005).

1.3.1   Topoisomerase II

Topoisomerase II enzymes, one of the main components of the mitotic
chromosome scaffold, disentangle the topological stress that accumulates
in double-stranded DNA by the generation and resealing of double strand
breaks (Nitiss, 1998).

Topoisomerase II and its biological functions

Classical studies indicated that Topoisomerase II has a key role in chromo-
some structure and condensation (Belmont, 2006; Xu and Manley, 2007).
The exact role of Topoisomerase II in condensation remains elusive because
its inactivation (either genetically, biochemically or through inhibition) pro-
duces a variety of chromosome morphologies in different organisms (Hirano
and Mitchison, 1993; Giménez-Abián et al., 2000; Uemura and Yanagida,
1984; Buchenau et al., 1993). *In vivo* Topoisomerase II shows a dynamic lo-
calization on mitotic chromosomes (Christensen et al., 2002; Swedlow et al.,
1993; Tavormina et al., 2002). Moreover, treatment with inhibitors that
block topoisomerase II enzymatic activity as a closed clamp on DNA, inhibit

Topoisomerase II mobility demonstrating that Topoisomerase II is catalytically active on chromosomes (Swedlow et al., 1993).

Recent work suggests that decatenation of replicated chromosomes requires a precise choreography that includes regulating Topoisomerase II action both spatially and temporally. Sister chromatid intertwinings are resolved prior to anaphase in circular centromeric plasmids and minichromosomes (Baxter et al., 2011; Koshland and Hartwell, 1987). However, there is evidence that resolution of intertwinings in metaphase linear minichromosomes is prevented by cohesin (Farcas et al., 2011) and it has been shown that the rDNA locus is decatenated during anaphase (D'Ambrosio et al., 2008; Nakazawa et al., 2011). Therefore, it is unclear at which point during mitosis endogenous linear chromosomes are decatenated.

1.3.2   The SMC complexes

As we already mentioned, apart from Topoisomerase II, the chromosome scaffold is rich in Smc2. Structural maintenance of chromosome (SMC) proteins are key regulators of the structural and functional organization of chromosomes. Highlighting their important function is the fact that their origin precedes that of histones. While bacterial genomes contain a single SMC gene whose product forms a homodimer, in eukaryotes there are at least six different SMC proteins (known as Smc1-6) that form heterodimers in specific combinations. *In vivo*, SMC proteins associate with additional non-SMC subunits to form functional complexes.

In eukaryotes, Smc1 and Smc3 form the core of the cohesin complex, Smc2 and Smc4 are components of the condensin complex and Smc5 and Smc6 form a third complex known as Smc5/6 complex. The role of cohesin
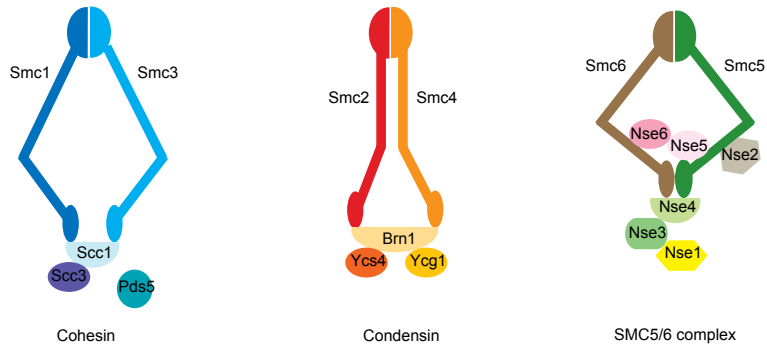
Figure 1.9: The SMC complexes. Schematic representation of the three SMC complexes in budding yeast. Reproduced from (De Piccoli et al., 2009).

has already been described (Introduction 1.2.1), therefore we will focus from now on what is know about the condensin and the SMC5/6 complex function (Figure 1.9).

The condensin complex

Little is known about the structural basis of mitotic chromosome changes, but a central player in this process is condensin. In addition to Smc2, condensin has another SMC subunit (Smc4) and three conserved non-SMC subunits that in budding yeast are named Brn1, Ycs4 and Ycg1 (Hirano et al., 1997; Freeman et al., 2000), which bridge the Smc2-Smc4 heads forming a ring-like structure (Cuylen and Haering, 2011) that traps DNA (Figure 1.9). The first evidence for condensin activity came from studies *in vitro* showing the requirement of the complex to condense sperm chromatin upon addition of *Xenopus laevis* mitotic extract (Hirano et al., 1997). In vertebrate cells, two related condensin complexes exist: condensin I and condensin II (Ono et al., 2003) that share the same pair of SMC subunits but contain different sets of non-SMC subunits. Condensin II participates in an early stage of

chromosome condensation within the prophase nucleus. Condensin I gains access to chromosomes only after the nuclear envelope breaks down, and collaborates with condensin II to assemble metaphase chromosomes with resolved sister chromatids. Interestingly, loss of any condensin subunit inhibits effective chromosome segregation in all organisms where it has been studied so far.

Condensin function is regulated through the cell cycle by phosphorylation. Condensin is activated during prophase, which requires phosphorylation by the mitotic Cdk (Kimura et al., 1998). The drop in mitotic cyclin levels that accompanies the metaphase-to-anaphase transition marks the initiation of a new stage of condensin regulation during the cell cycle that is characterized by the phosphorylation of condensin by Polo/Cdc5 (St-Pierre et al., 2009). An additional level of compaction depends on the Aurora-B kinase (Neurohr et al., 2011; Tada et al., 2011) which phosphorylates histones and condensins in the vicinity of the spindle midzone in anaphase.

The molecular mechanism of action of the condensin complex during anaphase remains unknown. Condensin can induce DNA supercoiling and looping *in vitro* in an ATP-dependent manner (Kimura and Hirano, 1997; Kimura et al., 1999; Strick et al., 2004). The supercoiling activity consists in the induction of positive superhelical tension into double stranded DNA. During chromosome segregation, the DNA fiber stretching is followed by the recoiling of the chromosome when the links that kept sister chromatids together are resolved. The recoiling of chromosomes is impaired in condensin mutants (Renshaw et al., 2010). Therefore, condensin would affect the topology of mitotic chromosomes through the supercoiling and looping of DNA that would promote recoiling of the resolved sister chromatid.

The SMC5/6 complex

The SMC5/6 complex is formed by Smc5 and Smc6 and 4 (humans) or
6 (in yeast) non-SMC proteins (Nse1-6). SMC5 and SMC6 sequences are
substantially divergent from those of SMC1-4 (Cobbe and Heck, 2004). As
we have seen, the main roles of cohesin and condensin in sister chromatid
cohesion and chromosome condensation have been described. However, the
function of the Smc5/6 complex is not yet as well understood.

The Smc5/6 complex binds to distinct sites on chromosomes in a cell
cycle-regulated manner (Lindroos et al., 2006). Chromatin immunoprecip-
itation shows that the loading of the complex occurs during S-phase in a
process that is dependent on DNA replication. In budding yeast, high bind-
ing of the complex is observed at centromeres, telomeres and the ribosomal
gene cluster on chromosome XII (Lindroos et al., 2006; Torres-Rosell et al.,
2005). Analysis of cells arrested at G2/M shows that the frequency of arm-
binding sites increases with chromosome length in budding yeast (Lindroos
et al., 2006). Most of the Smc5/6 peaks are detected in intergenic regions
and colocalize with those of cohesin (Lengronne et al., 2004; Lindroos et al.,
2006) suggesting that the two complexes could work together or in similar
pathways.

The Smc5/6 complex participates in DNA repair and recombination (De
Piccoli et al., 2009). Budding yeast Smc5/6 has been shown to function in
replication termination (Torres-Rosell et al., 2007) and it has been proposed
to be involved in recognizing SCI, maybe to assist their resolution (Kegel
et al., 2011). The complex has been involved in a variety of pathways mainly
by phenotypical description. Biochemistry and genetic analysis will be re-
quired to uncover the different functions of the complex and to understand

them in the different contexts.

1.4   The mitotic spindle

Chromosome segregation is carried out by the mitotic spindle, that pulls the sister chromatids apart and moves a complete set of chromosomes to each pole of the cell, where they are packaged into daughter nuclei. The mitotic spindle is based on a bipolar array of microtubules. All spindles are bipolar, however, the structure of the poles varies in different organisms.

Within the spindle, we distinguish three types of microtubules: (1) kinetochore microtubules that attach to the condensed chromosomes of mitotic cells at their centromeres (2) polar microtubules that emanate from the two spindle poles and are stabilized by overlapping with each other resulting in an antiparallel array in the spindle midzone that pushes the spindle poles apart and (3) astral microtubules that extend outward from the centrosomes to the cell periphery and exert pulling forces that move the spindle poles apart from each other (Morgan, 2007) (Figure 1.10).

The microtubules are formed by the polymerization of α/β tubulin heterodimers that are aligned in a polar head-to-tail fashion constituting the protofilaments. The structure of the microtubule is typically formed by 13 parallel protofilaments. The polymerization of microtubules is initiated from a pool of GTP-loaded tubulin subunits. Once in the polymer, the GTP is rapidly hydrolized to GDP. Therefore, microtubules are polarized with one plus end enriched in tubulin-GTP and the minus end composed by tubulin-GDP (Akhmanova and Steinmetz, 2008).

In the mitotic spindle, the minus end is embedded in the spindle poles where it is stabilized or serves as a microtubule depolymerisation site, for
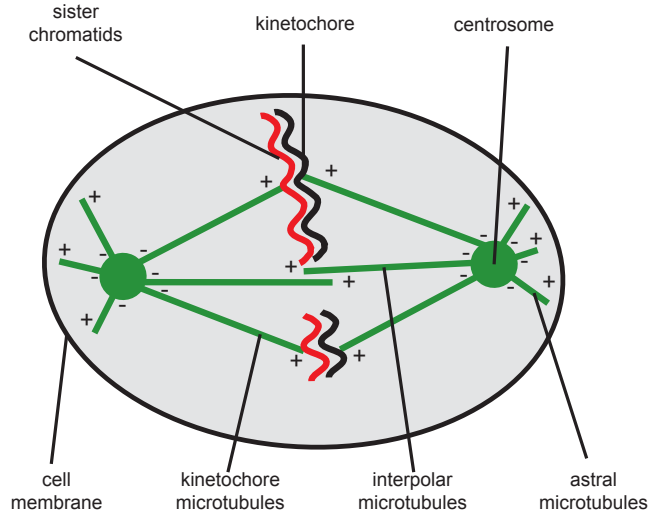
Figure 1.10: Bi-polar spindle organization. Basic features of the mitotic spindle of somatic animal cells in metaphase. Figure based on (Morgan, 2007).

example, during kinetochore microtubule shortening. The plus end of the microtubule is much more dynamic and explores the cellular space thanks to rapid switches between shrinkage (catastrophic events) and growth (rescue events), a behavior called dynamic instability (Desai and Mitchison, 1997). The plus end of the microtubules would determine the attachment to the cell cortex, chromosomes and other microtubules and therefore needs to be tightly regulated. All eukaryotic cells have a wide variety of proteins located at the plus ends of microtubules regulating their dynamics and their interaction with other proteins.

1.4.1   Proteins governing microtubule function

The assembly and function of the spindle depends on accessory proteins that modify the dynamics of microtubules and their association to each other and with other proteins.

The length of microtubules in the spindle can be limited by proteins that promote catastrophic events. The kinesin-13 family of proteins bind to the ends of microtubules and induce catastrophe by triggering a conformational change that disrupts lateral interactions between microtubule filaments (Howard and Hyman, 2003; Ovechkina and Wordeman, 2003). This effect is opposed by other microtubule-associated proteins that promote microtubule polymerization. XMAP215 protein of frogs (called Dis1 in fission yeast, Stu2 in budding yeast and TOG in human cells) promotes microtubule growth by recruiting tubulin dimers and binding to the plus ends of microtubules therefore blocking the attachment of microtubule depolymerases in this area (Akhmanova and Hoogenraad, 2005).

There are three fundamental activities that microtubule motors may contribute to spindle function: motility, microtubule attachment and regulation of microtubule dynamics (Akhmanova and Hoogenraad, 2005). Regarding the microtubule motors, there are two families: (1) the larger family of kinesins and kinesin-related proteins that mainly move towards the plus-ends and (2) dyneins that move toward the minus end.

Therefore, the correct balance of activities of the different proteins involved in microtubule regulation provides a functional mitotic spindle to correctly segregate chromosomes.

1.4.2   Mitotic spindle assembly

Spindle assembly during mitosis depends on two processes (1) the microtubule self organization and (2) the search and capture mechanism of the highly dynamic microtubules that emanate from the poles (Figure 1.11). These processes depend on numerous motor proteins and microtubule stabi-

lizing and destabilizing factors (Wadsworth and Khodjakov, 2004). At the
end of metaphase, the spindle is assembled and the sister chromatids are
attached to opposite poles.
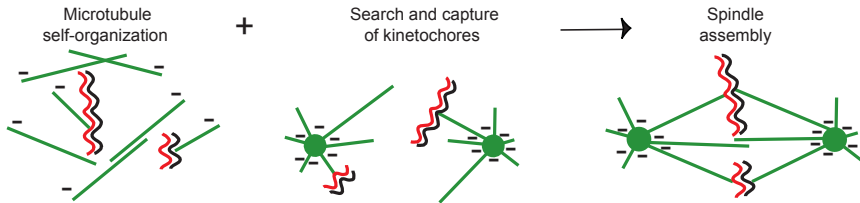
Figure 1.11: General mechanisms of spindle assembly. The bi-polar spin-
dle depends on the search and capture of chromosomes by microtubules and the
self-organization of microtubules around chromosomes. Figure based on (Morgan,
2007).

After separation of sister chromatids, chromosome movement during ana-
phase occurs in two steps: anaphase A, in which chromosomes move towards
the spindle poles; and anaphase B, in which the spindle poles move away
from each other. Anaphase A is assumed to be dependent on shortening of
the kinetochore microtubules that link centromeres to spindle poles. In con-
trast, anaphase B involves pushing forces generated at the spindle midzone
through motor proteins that cause the sliding of interdigitating microtubules
emanating from the opposite spindle poles. At the same time, the spindle
experiences pulling forces generated by motor proteins which are associated
with astral microtubules that connect the spindle to the cell cortex (de Gra-
mont and Cohen-Fix, 2005).

1.4.3   Mitotic spindle in budding yeast

In budding yeast, the spindle is constructed entirely within the nucleus. The
metaphase spindle is formed by microtubules that arise from the nuclear face

of a pair of spindle pole bodies that are embedded in the nuclear envelope. The spindle is composed by 18 microtubules from each pole: one for each of the 16 sister chromatids and 1 to 2 interpolar microtubules. A small number of astral microtubules emanate from the outer part of the spindle pole body and attach to the cell cortex in order to ensure proper orientation of the nucleus in the bud neck (Morgan, 2007).

Protein components of the budding yeast spindle

The *Saccharomyces* genome encodes six kinesin-related proteins (Cin8, Kar3, Kip1, Kip2, Kip3 Smy1) and a single cytoplasmic dynein heavy chain (Dyn1). Of these seven, only Smy1 has not been linked to spindle function, instead, it has been involved in polarized cell growth (Lillie and Brown, 1998). In contrast, mutations in the remaining six motor protein genes show extensive interactions characteristic of gene products involved in a common process.

In the mitotic spindle, Cin8 and Kip1 form tetrameric bipolar complexes that crosslink nuclear microtubules and move toward their plus ends. The effect of Cin8 and Kip1 action is to push spindle pole bodies apart. Kar3 participates in two distinct complexes: the Kar3/Vik1 complex has a nuclear role only and generates a force that opposes Cin8 and Kip1, therefore pulling spindle poles together; the Kar3/Cik1 complex acts in the cytoplasm to position the spindle but can also be found in the nucleus. The Kip3 protein also functions on nuclear microtubules, it is a plus-end directed motor and promotes depolymerization at the tip of the microtubule (Varga et al., 2009). Apart from elongating the spindle, kinesins also control spindle positioning. There are two pathways that mediate nuclear positioning. The first one is composed by dynein and dynactin that operate from the cell cortex in

a pathway that also includes Kip2. The second one includes Kar9/Bni1 and actin and tethers the plus end of a cytoplasmic microtubule to the bud cortex (Hildebrandt and Hoyt, 2000). (Figure 1.12)
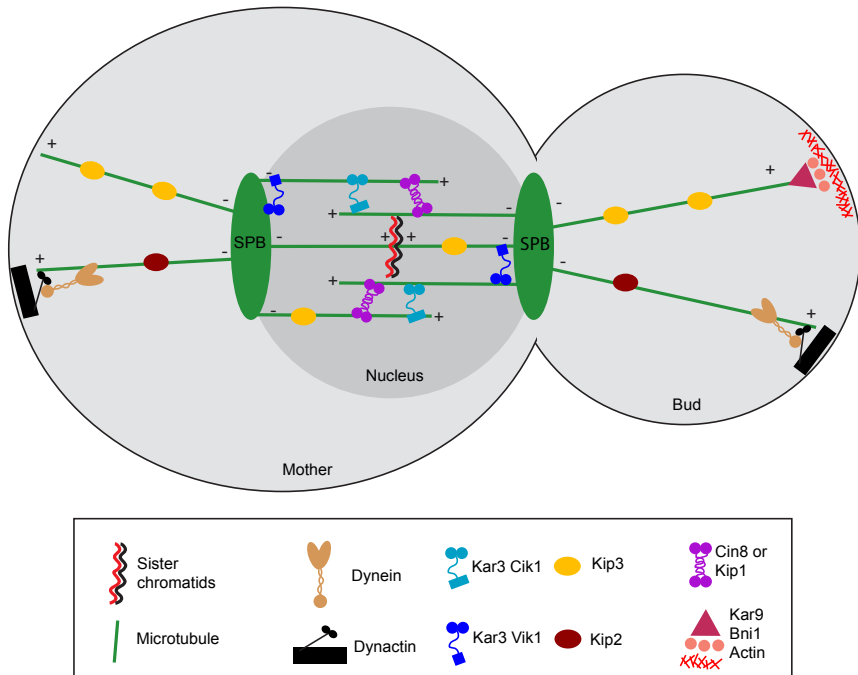
Figure 1.12: Mitotic motors in budding yeast. Proposed roles for the different mitotic motor proteins in *Saccharomyces cerevisiae*. Adapted from (Hildebrandt and Hoyt, 2000).

There are more proteins that regulate microtubules apart from kinesins. The Dis1 family of microtubule-associated proteins plays a central role in the regulation of microtubule polymerization in diverse eukaryotic species. The orthologue of *dis1* in *Saccharomyces cerevisiae* is *STU2*, initially identified as a suppressor of a β-tubulin mutation. *STU2* is an essential gene and its product is localized to the spindle and spindle poles (Wang and Huffaker, 1997). Importantly, microtubule stabilization during anaphase re-

quires Stu2, whose activity is opposed to that of the kinesin-related Kip3 (Severin et al., 2001).

There are also nonmotor proteins that are involved in midzone function. Ase1 is a member of a conserved family of spindle midzone proteins that acts as a homodimer that binds to and bundles microtubules. Ase1 action is required for anaphase spindle elongation and its overexpression is sufficient to induce spindle elongation in S phase-arrested cells. It has been proposed that Ase1 functions as a spindle cross-bridge maintaining anaphase spindle integrity (Schuyler et al., 2003).

Anaphase spindle elongation in budding yeast

In *Saccharomyces cerevisiae*, anaphase A is really fast (it takes between 2 and 4 minutes) compared to anaphase B (around 20 minutes) (Yeh et al., 1995). The spindle elongates in a biphasic fashion during anaphase B. The first phase is fast and is produced by the sliding of antiparallel interpolar microtubules caused by motor proteins. In the second phase, the rate of spindle elongation decreases. During this phase the microtubules have to polymerize to ensure that the interpolar microtubules maintain an overlapping zone as the spindle extends. Thus, the slow phase is set by the rate of tubulin addition to the microtubules (Kahana et al., 1995; Havens et al., 2010). This second phase is related to microtubule polymerases and depolymerases (Figure 1.13).

The mid-anaphase pause

In budding yeast cells, a brief pause between the fast and slow phases of anaphase spindle elongation is often observed (Figure 1.13) (Yeh et al., 1995).
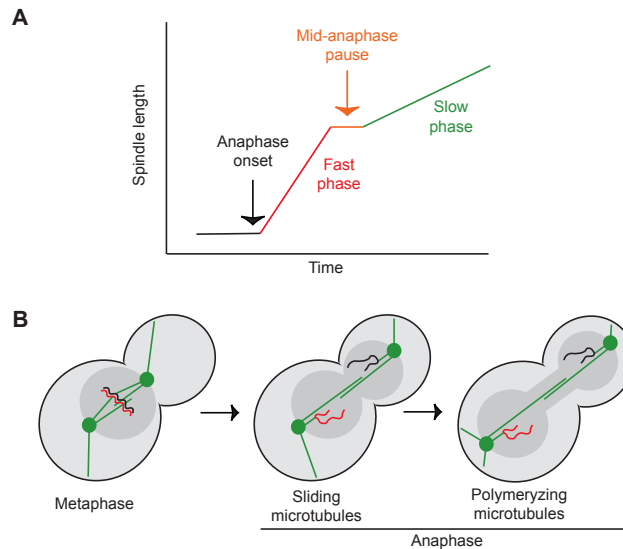
Figure 1.13: Spindle elongation in budding yeast. (A) At anaphase onset
the spindles start elongating. The fast phase is followed by a short mid-anaphase
pause to resume spindle elongation in a second and slower phase. (B) Schematic
showing the different spindle elongation phases in budding yeast. The first fast
phase of elongation depends on the sliding of microtubules while the second slow
phase depends on the polymerization of microtubules.

Upon activation of a facultative dicentric chromosome, this natural transi-
tion of the mid-anaphase pause is greatly extended (Neff et al., 1992; Brock
and Bloom, 1994) (Figure 1.14). No mid-anaphase delay is observed in the
absence of the *RAD9* checkpoint gene, which prevents cell cycle progression
in the presence of damaged DNA (Yang et al., 1997).

   RAD9-dependent DNA damage arrests had been described during G1,
S and G2 cell cycle stages. The observations the authors in (Yang et al.,
1997) did revealed that *RAD9* -dependent events occur well past G2/M
transition, suggesting that chromosome integrity is monitored as late as in
anaphase. However, the need of a mid-anaphase checkpoint in wild type cells

and the perturbations that are monitored in dicentric bearing cells remains
unknown.
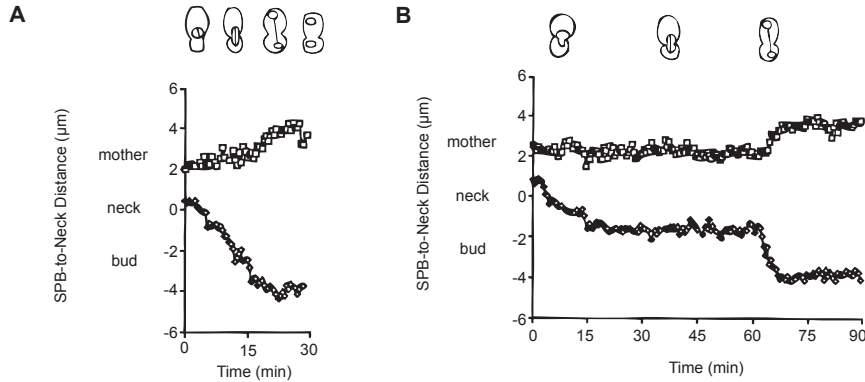
Figure 1.14: The mid-anaphase checkpoint. Kinetic analysis of changes in
nuclear morphology and spindle dynamics in dicentric cells displaying wild-type
kinetics, presumably mono-oriented dicentric chromosomes (A); and mitotic delay,
presumably bi-oriented dicentric chromosomes (B). Reproduced from (Yang et al.,
1997).

1.5 Nuclear organization

As we will see (Results 4.7), the nuclear organization plays a role in deter-
mining the topological stress accumulated in chromosomes. That is why we
consider fundamental to introduce the basic concepts of nuclear organization
and its changes during the cell cycle.

Eukaryotic chromosomes are nonrandomly positioned within the nucleus.
Chromosomes are organized according to two fundamental principles (1) re-
tention of mitotic chromosome geometry, as reflected by polarization of the
nucleus along a centromere to telomere axis and separation of chromosomes
into non-overlapping territories and (2) specific contacts with the nuclear

envelope (Marshall, 2002). The persistence of a polarized anaphase-like ori-
entation of chromosomes in interphase, with centromeres clustered at one
end and telomeres at the other, has been observed in several cell types in-
cluding fruit fly, yeast and mammalian cells. This arrangement is seen most
clearly in rapidly dividing cells. Several studies have confirmed that chromo-
somes do not overlap extensively in interphase but instead remain in separate
nuclear territories (Cremer and Cremer, 2001), again reflecting a persistence
of the mitotic arrangement of chromosomes as spatially separated entities.
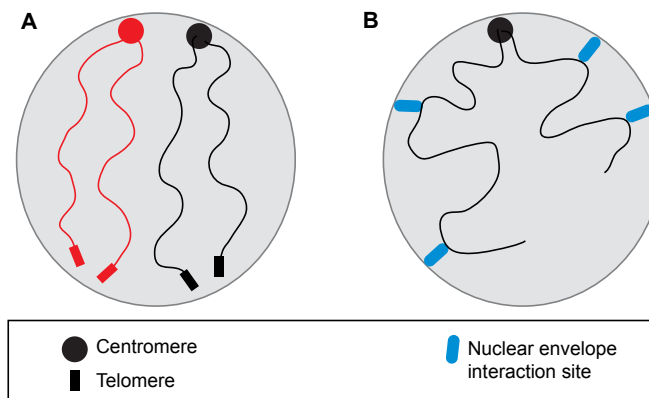
Figure 1.15: The two basic principles of nuclear order. (A) Persistence of
mitotic organization. In mitosis chromosomes are compacted into separate entities,
and during anaphase they are aligned with all centromeres drawn together near
the spindle pole. when chromatin decondenses in telophase, this arrangement is
retained, and persists into interphase. (B) Nuclear envelope contacts. A series of
discrete chromosomal loci interact with the nuclear envelope (red circles), either
through nuclear pores or components of the nuclear lamina. Based on (Marshall,
2002).

On the other hand, as a result of the interactions with the nuclear en-
velope, the entire chromosome is arranged into a series of loops anchored

to the envelope. The nuclear envelope provides a platform to which chromosomes can anchor thus limiting their movement within the nucleoplasm (Chubb et al., 2002; Heun et al., 2001). Settling of a chromosome within its territory creates different subnuclear microenvironments.

Although the function, if any, of chromosome spatial arrangement is largely unknown it has been suggested that it could be related to epigenetic controls of gene expression and cell differentiation (Cockell and Gasser, 1999; Fisher and Merkenschlager, 2002). For example, in budding yeast, artificial perinuclear localization of chromatin promotes its silencing (Andrulis et al., 1998). In higher eukaryotes, the distribution of active and inactive genes within the nucleus is different depending on the cell type. One example are T lymphocytes. In those cells, the silencing of some developmental genes correlates with their translocation to pericentric heterochromatin domains (Reiner and Seder, 1999).

1.5.1   Nuclear organization during the cell cycle

These chromosome-nuclear envelope associations must, however, dissolve in time for mitosis to allow faithful chromosome segregation. In many eukaryotes, the nuclear envelope is broken down prior to mitosis, allowing unhindered chromosome movement directed by the mitotic spindle. The cell cycle regulation of telomere detachment from the nuclear envelope becomes essential in organisms that undergo closed mitosis as *Schizosaccharomyces pombe* and *Saccharomyces cerevisiae*.

Two partially redundant pathways have been identified that mediate tethering of telomeres to the nuclear envelope in budding yeast. The first depends on the yeast Ku (yKu70/80) protein complex and the second on the
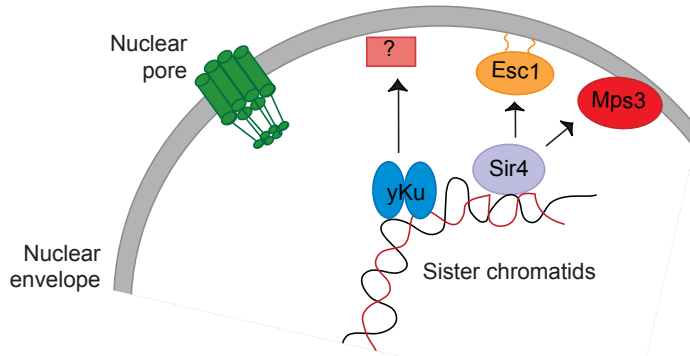
Figure 1.16: Parallel mechanisms lead to yeast telomere attachment at the nuclear envelope. At different stages of the cell cycle the telomere associated proteins mediate different contacts with inner nuclear membrane components. Sir4 binds Esc1 as well as Mps3. There is an unidentified anchor for yKu in G1 phase that is neither Esc1- or Mps3- dependent. Reproduced from (Taddei et al., 2010).

Sir4 and Esc1 proteins (Hediger et al., 2002; Taddei et al., 2004). Experimental evidence suggests that the Ku-dependent pathway tends to dominate during G1, while the Sir4/Esc1-dependent tethering pathway is dominant in the S-phase (Hediger et al., 2002). Budding yeast telomeres are cell cycle regulated, tend to attach to the nuclear envelope but dislodge as cells prepare for mitosis (Laroche et al., 2000). The dislodgement of budding yeast telomeres occurs in late S-phase triggered by telomeric DNA replication (Ebrahimi and Donaldson, 2008). Since telomeres frequently appear to replicate within factories that are at the nuclear periphery, the force that recruits DNA to the replication factory cannot be the sole cause of telomere dislodgment from the nuclear envelope. The negative effect of replication on telomere anchoring is not transient, involves its stable down-regulation to prevent reattachment of telomeres after replication and is mediated by the downregulation of the Ku tethering function (Ebrahimi and Donaldson,

2008).

Telomeres are associated with the nuclear envelope during the inter-phase of the fission yeast cell cycle (Chikashige et al., 2009; Funabiki et al., 1993). It has been recently shown that fission yeast telomeres detach from the nuclear envelope during early stages of mitosis, through G2, and re-main detached until mitotic completion (Fujita et al., 2012). This mitosis-specific telomere dislodgment points to a cell cycle regulated modification in the telomere−nuclear envelope anchoring pathway. The release of chro-mosomes from the nuclear envelope during mitosis is universal among eu-karyotes (Ebrahimi and Cooper, 2012).

1.6   Study of variations in chromosome length

In this study we challenge yeast cells with artificially lengthened chromo-somes in order to understand how mitotic processes are regulated. That is why it is important to summarize current knowledge about the implications of chromosome length in the mitotic machinery.

Eukaryotic nuclear genomes consist of linear chromosomes whose length may vary considerably in dependence on the number of chromosomes and the species-specific amount of nuclear DNA. The first evidence that sterility and even breakdown of the whole organism could be mediated by chromosomes with arms exceeding a defined length was shown in the plant *Vicia faba* (Schubert and Oud, 1997). The chromosome length enlargement was based on crossing individuals carrying translocations that led to an exchange of un-equal parts between chromosomes. Although genetically balanced, some of these plants surprisingly exhibited partial or complete sterility as well as var-ious degrees of disturbances in growth and development. This phenomenon

was confirmed for *Hordeum vulgare* (Hudakova et al., 2002) (Figure 1.17). On the other hand, chromosomes of a much smaller size than average frequently do not segregate correctly during meiosis (Schubert, 2001; Murata et al., 2006).
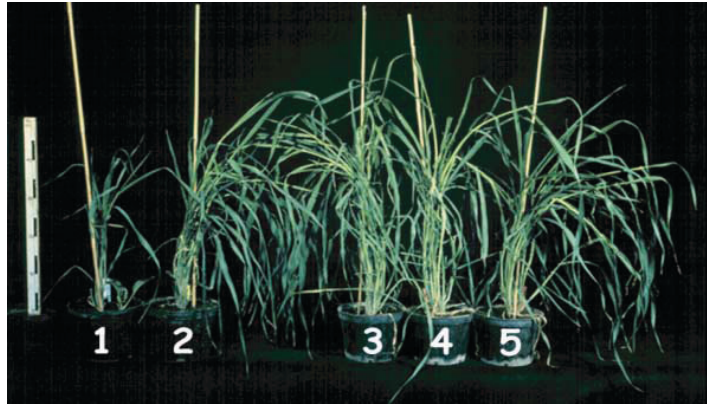
Figure 1.17: Phenotpe of *Hordeum vulgare* plants with altered chromosome lengths. (1) and (2) correspond to homozygous and heterozygous plants respectively with elongated chromosomes. (3) and (4) correspond to the parental genotypes and (5) is wild type. All plants are of the same age. Adapted from (Hudakova et al., 2002).

When yeast cells undergo mitosis, the longer chromosomes are more likely to suffer loss or breakage in the absence of the Topoisomerase II (Spell and Holm, 1994). This finding supports the idea that the DNA topoisomerases evolved to solve the topological problems of circular DNA and later on linear DNA as it became progressively longer; for short linear chromosomes, the topological problems could be alleviated by movements of their ends. It has been proposed that replication-induced superhelical stress increases with the length of *Saccharomyces cerevisiae* chromosomes (Kegel et al., 2011). Indeed, inhibition of either type I topoisomerases or cohesin-

and condensin-related Smc5/6 complex leads to a late replication delay of longer, but not shorter, chromosomes.

Although longer chromosomes may present some difficulties to the mitotic machinery, recently it has been shown that cells have mechanisms to adapt to the presence of long chromosomes both in *Saccharomyces cerevisiae* (Neurohr et al., 2011) and *Drosophila* cells (Kotadia et al., 2012).

Budding yeast can adapt to a 45% increase in chromosome size by enhancing the compaction of the long chromatid during anaphase (Neurohr et al., 2011). Two different chromosomes within the yeast genome were fused to achieve an extralong chromosome and the level of condensation was monitored during mitosis. The long chromosome construct hypercompaction depends on Aurora B activity and serine 10 of Histone H3 phosphorylation. Thus, the anaphase spindle may function as a ruler to adapt the condensation of chromatids promoting their segregation regardless of chromosome or spindle length.

That study showed that budding yeast cells can adapt to an increase in chromosome size by enhancing the compaction of the long chromatid during anaphase in an Ipl1-dependent manner. However, the fusion chromosome was only 45% longer than the longest wild-type arm and, in addition, contained the ribosomal DNA (rDNA) repetitions. The rDNA locus is peculiar because it is subjected to specialized regulation (Clemente-Blanco et al., 2009) and its separation occurs in mid-anaphase and is assisted by condensins and Aurora B (Pereira and Schiebel, 2004) therefore being a potential problem for generalizing conclusions.

One of the goals of this study is to elucidate if the hyper-compaction mechanism was dependent on the rDNA repeats and whether it could act on longer chromosomes. We also wondered whether other processes apart

form hyper-compaction were necessary to deal with longer chromosomes. With the long chromosome approach we seek to get a better understanding of how chromosome arms are segregated during anaphase.

2

Objectives

In order to maintain genome stability chromosomes need to be properly segregated. Exceedingly long chromosome arms product of the fusion of chromosomes IV and XII have been shown to segregate efficiently and to hypercondense during anaphase. However, the Ipl1-dependent hyper-condensation of proximal regions is not essential because anaphase inactivation of *IPL1* slows down but does not abolish chromosome segregation. We thus wandered what other mechanisms are involved in long chromosome segregation.

The objectives of the work presented here were to determine:

- Whether anaphase hyper-condensation takes place in chromosomes devoid of rDNA

- Which are the biological processes affected by chromosome length

- The role of nuclear organization in determining the upper limit of chromosome length

This page intentionally left blank

3

Materials and methods

3.1 Cell growth and synchronization

3.1.1 Growth media

Except when indicated, yeast cells were always grown on rich YP medium (1% Yeast Extract, Becton Dickinson #212720; 2% BactoPeptone, Becton Dickinson #211820), supplemented with 2% sugar (Glucose, Sigma-Aldrich #G7528; Galactose ,Sigma-Aldrich #48260). Rich medium was supplemented with 0.004% adenine (Sigma-Aldrich #A9126).

For antibiotic selection rich medium was supplemented with one of the following compounds: 100 mg/l nourseothricin (ClonNAT, Werner Bioagents #51000), 200 mg/l Geneticin (G418, Invitrogen, #11811023), 300 mg/l hygromycin B (Nucliber, #ant-hm-1) or 40 mg/l phleomycin (Nucliber, #ANT-PH-1).

For selection of auxotrophic markers, cells were grown on synthetic min-

imal medium, lacking the amino acid of choice. Complete synthetic minimal medium was composed of 0.67% Yeast Nitrogen Base w/o ammonium sulfate (Becton Dickinson, #291920), 0.004% adenine (Sigma-Aldrich #A9126), 0.002% uracil (Sigma-Aldrich #U0750), 0.002% tryptophan (Sigma-Aldrich #T0254), 0.002% histidine (Sigma-Aldrich #53319), 0.003% lysine (Sigma-Aldrich #62840), 0.003% leucine (Sigma-Aldrich #61820) and 0.002% methionine (Sigma-Aldrich #M9625).

Solid medium contained 2% agar (Becton Dickinson, #214510). Agar, peptone and yeast extract were mixed with water and autoclaved, all other components were filter sterilized.

To stock strains, cells were scraped directly from 2-3 day old rich solid medium and resuspended in 30% glycerol/70% liquid rich medium. Stocks were kept at -80 ºC.

3.1.2 Cell growth analysis

For growth assays, cells were grown on liquid rich medium to exponential phase ($0.4 <$ OD600 < 0.6). Serial 1 to 5 dilutions were carried out from a stock solution of OD600 = 0.01 ($1.7{\times}10^5$ cells/ml) in rich medium. 3 μl of each dilution were spotted on rich plates, which were inoculated at the indicated temperatures and growth was scored after 48 h and 72 h or longer if indicated.

3.1.3 Cell synchronization

For synchronization in G1, cells were arrested in 15 μg/ml α-factor for 2 h at room temperature (1 mg/ml stock in methanol stored at -20 ºC, α-factor was purified by the in house proteomics facility). To release cells from the

α-factor arrest, cells were washed three times with rich medium.

For synchronization in metaphase, cells were arrested in 10 μg/ml of nocodazole for 2.5 h at room temperature or the precise temperature indicated in the experiment (2 mg/ml stock in DMSO stored at -20 °C Sigma-Aldrich #M1404).

For synchronization in metaphase by Cdc20 depletion the endogenous *CDC20* promoter was replaced by *pMET3*. To arrest in metaphase, exponentially growing cells were transferred to rich medium containing 0.02% (10x) methionine for 3 h. Cdc20 expression and anaphase were induced by washing the cells with minimal synthetic medium lacking methionine.

3.2   Yeast strains

3.2.1   Strain background

All the *Saccharomyces cerevisiae* strains used in the study carry the TetO and LacI arrays on chromosome IV and were derived from a previously described strain (Vas et al., 2007) of a BF264-15 15D background (Reed et al., 1985). The strains derived from YMM409 used in this study have genomic contributions corresponding to 1/2 S288c, 1/4 W303 and 1/4 BF264-15D. As long chromosomes were generated by transformation, they are always isogenic to the corresponding mutant strain with normal karyotype.

3.2.2   Yeast transformation

DNA insertion, gene deletions and gene fusions were generated by transformation of PCR products or linearized plasmids essentially as described in (Janke et al., 2004). Yeast cells were inoculated overnight in rich liquid

medium, diluted to an OD600 = 0.1 in 10 ml until the cultures reached the exponential phase. Then, cells were harvested by centrifugation at 400 g for 5 min at room temperature in a 15 ml tube. Cells were washed in 1 ml transformation buffer (100 mM lithium acetate, 10 mM Tris, 1 mM EDTA pH = 8) and resuspended in 72 μl transformation buffer, 8 μl of denatured and chilled salmon sperm DNA (10 mg/ml salmon sperm DNA (Sigma-Aldrich, #D1626); 10 min denatured at 95 °C, cooled on ice) were added to the cells. 1-10 μl of PCR product or plasmid were added to the cells, followed by 500 μl of PEG buffer (transformation buffer, containing 40% PEG-3350 (Sigma-Aldrich, #P4338)) and incubated on a rotating wheel for 30 min. After addition of 65 μl of DMSO (Sigma-Aldrich, #D2650) cells were heat-shocked for 15 min at 42 °C. Cells were harvested by centrifugation at 400 g for 2 min, resuspended in 100 μl sterile water and plated. To select for auxotrophic markers, cells were plated directly on synthetic minimal medium lacking the amino acid of choice. To select for antibiotic resistances, cells were first plated on rich medium for 1-2 days and replicated on rich medium plates containing the antibiotic of choice. To check the positive colonies that correctly integrated the DNA genomic DNA of transformants was isolated for analysis by PCR essentially as described (Harju et al., 2004).

3.2.3 Generation of chromosome fusions

To fuse chromosomes, *pGAL1-CEN4* cells were grown on rich sucrose medium and transformed with a PCR product encoding an antibiotic resistance cassette flanked by sequences with homology to subtelomeric regions of the two chromosomes to be fused (primer sequences shown in Table 3.1). Transformed cells were grown on galactose plates for 3-4 days to destabilize the

non fused chromosomes and replicated onto galactose plates supplemented with the antibiotic of choice to select transformants. Positive clones were confirmed by different methods, described in Results 4.1.2 including PCR (primer sequences shown in Table 3.2).

3.2.4 Promoter replacement at the CDC20 locus

To replace the endogenous promoter of Cdc20 with *pMET3*, cells were transformed with MscI digested pMM179. Transformants were selected on synthetic minimal medium lacking both methionine (to allow *CDC20* expression) and leucine (to select for positive transformants). Positive clones were confirmed by the accumulation of large budded cells after 5 hours of growth on rich plates supplemented with extra methionine (500 μl of 0.2% methionine stock solution soaked into the plate surface). *pMET-CDC20* cells were stocked in minimal synthetic medium lacking methionine/30% glycerol.

3.2.5 Plasmids and mutant strains

Template plasmids for PCR mediated deletions and fusion protein generation were all from (Janke et al., 2004) except for the fluorescent proteins mCherry and tdTomato which were amplified from plasmids provided by the lab of Karsten Weiss (University of California, Berkeley).

Temperature sensitive mutant alleles were inserted into the used strains. The *smc2-8* and *smc6-9* were provided by Luis Aragón (Imperial College, London). The mutant alleles of *ipl1-321, cdc5-1* and *stu2-13* were provided by Yves Barral (ETH Zurich, Switzerland). The *top2-4* allele was provided by Frank Uhlmann (Cancer Research, London). The plasmid for *CDC20* promoter exchange was a gift from Ethel Queralt (Bellvitge Institute of

PCR product	Forward oligo	Reverse oligo
pGAL:CEN4	ggtaatgaaatgagatgatacttgcttatct catagttaactggcataaacgtacgctgcag gtcgac	ggttttatcgtcacagttttacagtaaataa gtatcacctcttagagttacatcgatgaattc tctgtcg
cen4Δ	acattcttataaaaaagaaaaaaattactgc aaaacagtactagcttttaacttgtatccat ctgtttagcttgcctcgtc	tttactcgacttcaggtaatgaaatgagatg atacttgcttatctcatagttaactggcata aatcgatgaattcgagctcgtt
cen5Δ	attaacaggggaacgcttgcctaccatcaag cccattcaatgcagatgtgatcttgaataat acataactttc	cattgtactttatttttaaggaatagtttag ttgaaacgccaacagtggcttgcgacacctg taagcgttgatttc
cen7Δ	ggtttgagtaacgaatttaggtgctacgcaa attttgaatgtagttcatgatctgtttagct tgcctcgtc	caatattcataccgcattaactttcattgaa ccgaagatctacaaatatctcgatgaattcg agctcgtt
cen15Δ	atccggattttcagaagtcataacgcactta ttgggtgcttataagctgtatctgtttagct tgcctcgtc	agcataagcgacagaaaacacttcgagatga gcttgagaactccatttcatcgatgaattcg agctcgtt
cen16Δ	ttaaagagattatcttgactgatataaaatt tcttatcatggtagtgatcaccttgaataat acataactttc	ccattttcagtgtggagtaagtcatcaaaac tgctatttagccgctttgcgacacctgtaag cgttgatttc
IV:XV fusion	attaagcaattgaacaaaataacgcttcgttt taagttttgtggttattttcaagtttctgat ctgtttagcttgcctcgtc	gattaagcaggtgtgctttagtagttttgcc gctttgcttgatcactgttagtatttcggcc gtacgctgcaggtcgac
XV:V fusion	ctgttactttagcaaggaggattaccgagat acgccgagtaaagtgtgtatgctcatctgtt tagcttgcctcgtc	cagtcacggctgtagagtgtacacagagcct ttgaagtttggtgctttacgaaattcgatga attcgagctcgtt
XV:XVI fusion	ctgttactttagcaaggaggattaccgagat acgccgagtaaagtgtgtatgctcatctgtt tagcttgcctcgtc	cttggttgttttctcggcgattgcagccaaa tcgttcttattcagctaggttacctcgatga attcgagctcgtt
V:VII fusion	gtaacagacgcagttgcggttaaagtcgtag atgattgccctatgcgctaacatctgtttag cttgcctcgtc	caatatctcttgaagactcagaaatgttttt atcctcatttttgaggcagccttcttctcg atgaattcgagctcgtt

Table 3.1: Oligos used for chromosome fusion.

Purpose	Forward oligo	Reverse oligo
CEN4	atagtggttgacatgctggctagt	gtgggaagcaaaggaaattg
CEN15	cggaacctcttgactttgag	gatttcaggtagtatataag
CEN5	gtccacttttcttccttgttg	gcatttccttgatttactgtc
CEN16	catagggatgaaaaagctttatc	gccgttatgttgtcgtaattc
CEN7	gtctgaagtcatatccaaag	gaacaataaacgatctatag
Subtel IV(R)	gcttaaaggtagcgtatagtaagg	gtgggaagcaaaggaaattg
Subtel XV (R)	cagatctagaatgatcacag	gttttaaaatacccaacgtcg
Subtel XV(L)	ggaacagctatgaaaacacc	tcggcatgaagtaagattag
Subtel V(R)	gatttccagaccctttggaag	cattgtggctcacttcaatag
Subtel XVI	gagtttggggagaaaaggctgc	cagacgtcgatacctccttatc
Subtel V(L)	gatttccagaccctttggaag	cattgtggctcacttcaatag
Subtel VII(L)	gcatatatgaagacagttagac	gcgtgtctgatatttggtg

Table 3.2: Oligos used to check chromosome fusion.

Biomedical Research, Barcelona).

3.3   Genome analysis of strains carrying long chromosomes

3.3.1   Pulse-Field Gel Electrophoresis (PFGE)

Pulse-field gel electrophoresis was performed to check the correct fusion of the chromosomes following the protocol described (Herschleb et al., 2007). Approximately 6×10^6 cells were pelleted and washed twice in 0.05 M EDTA (pH = 7.5) keeping the samples on ice. After the last wash, the cells were resuspended in 30 μl 0.125 M EDTA (pH = 7.5) and kept at 37 ºC to warm them up before mixing them with 40 μl of agarose-zymolase solution (1.2% solution of LMP agarose in 0.125 M EDTA pre-equilibrated at 42-50 ºC).

The mixture was quickly pipetted into a casting mold and kept at 4 °C
onvernight to let it solidify completely. Next, the briks were incubated for
at least 12 h in 1 ml of 0.5 M EDTA 7.5% β-mercaptoethanol at 37 °C.
The buffer was drained and replaced with NDSK buffer (0.5 M EDTA, 1%
(w/v) N-laurylsarcosine, 1 mg/ml proteinase K) and incubated overnight
at 50 °C. The bricks were washed 4x drying 30 min with running buffer
(TBE 1x) and molded into a 0.7% agarose gel of 200 ml. The gel running
program was the standard protocol used for both up to 2 Mb of DNA (to
separate chromosomes shorter than IV) and more than 4 Mb (to separate
long chromosomes) in the Bio-Rad CHEF mapper XA System (#170-3672)

3.3.2   Sequencing and *de novo* assembly of whole yeast genome

Whole genome sequencing was performed at the CRG Ultra-sequencing fa-
cility. Sequences of 40 bp, paired-end reads, with an average insert size of
330 bp, were obtained using an Illumina GaIIx sequencer, and preprocessed
with the SCS 2.5 software. Genome assembly was performed with the AMOS
package (Pop et al., 2004), using as a reference the S288c sequence down-
loaded from SGD (Cherry et al., 1997). A minimum region of overlap of 16
nucleotides and a maximum of two mismatches were required to assemble
two reads. This work was done in collaboration with the Ultra-Sequencing
Facility of the CRG, the data was analyzed by Leszek Pryszcz and Toni
Gabaldón from the Bioinformatics and Genomics Program at the CRG.

3.4   Microscopy

Except when specified, time-lapse analysis of the different strains was per-
formed on cells synchronized with α-factor (10 mg/ml) for 2 h, released

in fresh YPD medium for 1 h at 25 °C and placed in a pre-equilibrated temperature-controlled microscope chamber 15 min prior to imaging.

Cells were plated in minimal synthetic medium lacking tryptophan in 8 well Lab-Tek chambers (Nunc #155411). Prior to plating, chambers were coated with concanavalin A (Sigma-Aldrich #C7275) by incubation of 250 μl of an 1 mg/ml solution of concanavalin A in PBS for 20 min. Next, the chambers were washed 6x with 0.5 ml minimal synthetic medium.

Live-cell imaging was performed using an Andor Revolution XD spinning disc confocal microscope equipped with an Andor Ixon 897E Dual Mode EM-CCD camera. Time-lapse images were obtained in series of 4 μm stacks spaced 0.5 μm taken every 2 min. The imaging work was performed in the Advanced Light Microscopy Unit at the CRG.

3.4.1 Image analysis and statistics

Images were analyzed on 2D maximum projections stacks (except when specified) using ImageJ (NIH) and Excel (Microsoft). Graphs and statistical analysis were performed with Prism software (GraphPad) and Excel. On figures, asterisks indicate $p < 0.05$ (*), $p < 0.01$ (**) and $p < 0.001$ (***). To illustrate the data point distribution, measurements are represented in box-plots where the boxes include 50% of data, whiskers 90%, the median is indicated by a line and the mean by a cross.

3.5 Protein analysis

In order to fix cells for protein analysis, 1 ml of liquid yeast cultures was added to 300 μl of 85% trichloracetic acid (TCA, Sigma-Aldrich, #T6399). After 5-30 min of fixation at room temperature, cells were centrifuged twice

at 20,000 g discarding the supernatant. Cells were kept at -20 °C for at least
30 min before processing.

After cold treatment, 100 μl of 1x TCA Sample Buffer (350 mM Tris, 0.1
M dithiotheritol (DTT), 2% SDS, 4% Glycerol, 0.1% Bromophenolblue, pH
= 8.8) was added to each sample to resuspend the cells. In order to facilitate
cell breakage, 300 μl of acid washed beads (Sigma-Aldrich #G8772) were
added to the sample and cells were broken by shaking for 1 min in a FastPrep
FP120 (Thermo Savant). To reduce the foam, tubes were centrifuged at
maximum speed for 1 min. Samples were denatured at 95 °C for 10 min.
To separate the cell lysate from the beads, 1.5 ml tubes were perforated
using a hot needle and placed in a new 1.5 ml tubes for centrifugation.

Of the total lysate, 20 μl were used to run an 8% acrylamide gel and
transferred onto a nitrocellulose membrane using a semi-dry system (Bio-
Rad). Membranes were blocked using 5% milk in TBST (TBS 1x, 0.05%
Tween20) for 30 min at room temperature. Primary antibodies were di-
luted 1:2000 in the same blocking solution and incubated for 4 h at room
temperature or overnight at 4 °C: mouse anti-flag (Sigma-Aldrich #F3165)
and rabbit anti-myc (TEBU-BIO SL #SC789). Primary antibodies were
washed with TBST doing 3 washes of 7 min each. The secondary antibodies
were used in a 1:25,000 dilution in TBS-T and incubated for 1 h at room
temperature: goat anti-mouse (TEBU-BIO SL #SC2005), goat anti-rabbit
(TEBU-BIO SL #SC2004). After 3 washes of 7 min each with TBST,
the membranes were analyzed using ECL (GE Healthcare Europe Gmbh
#RPN2106) and exposed in fils (Agfa curix #RP2 PLUS).

3.6   Chromatin immunoprecipitation and sequencing (ChIP-seq)

3.6.1   Chromatin IP

Chromatin immunoprecipitation was performed as described (Zapater et al., 2007). Yeast cultures were grown to early log phase before 50 ml samples of the culture were arrested in Metaphase using nocodazole (15 μg/ml) and shifted to the indicated temperature for 2.5 h. For crosslinking, yeast cells were treated with 1% formaldehyde for 20 min at room temperature. The crosslinking reaction was stopped adding 5 ml of 0.5 M Glycine for 15 min. Cells were kept on ice and washed 4x in iced-cold TBS. The pellet could be used directly or frozen at -20 °C. Next, the cells were resuspended in 300 μl of lysis buffer (1% deoxycholic acid, 10 mM HEPES, 140 mM NaCl, 1 mM EDTA, 500 μl Triton X-100 and protease inhibitors) and 400 μl of glass beads were added to the mix in order to break the cells using Fastprep during 1 min. Then, 300 μl of lysis buffer were added to the sample and the whole cell extract was transferred to a fresh tube by making a hole in the former tube and spinning down. The samples were kept on ice and sonicated (Branson Digital Ultrasonic Processor Cell Disruptor) twice at intensity 2 for 30 sec.

The whole cell extract was obtained after centrifugation at 4 °C for 5 min at maximum velocity (10 μl were put away to control for input). To immunoprecipitate the protein of interest, 30 μl of incubated and washed dynabeads were added to the cleared lysate. The magnetic beads (Invitrogen #110.41) were previously washed twice with PBS+5 mg/ml BSA and incubated overnight with the appropriate antibody, 50 μl of beads and 4 μl

of antibody were used for each sample. The tubes were kept rotating at 4
°C for at least 3 h. After immunoprecipitating the beads were washed 2x
lysis buffer, 2x lysis buffer + 360 mM NaCl, 2x wash buffer (5% desoxycholic
acid, 10 mM Tris pH = 8, 250 mM LiCl, 0.5% NP-40, 1 mM EDTA pH =
8) and 1x TE (10mM Tric-HCl, 1mM EDTA). The beads were centrifuged
at 1000 g for 1 min to discard the liquid.

To elute the protein from the beads, 50 μl of elution buffer (1% TE,
1% SDS) were added to the beads, vortexed, kept at 65 °C for 10 min and
centrifuged 15 sec at 13,000 rpm. The tube was put into the magnetic stand
in order to remove 30 μl of the sample and add it to a new tube containing
240 μl of elution buffer. To complete the elution, 30 μl more were added
to the beads and the procedure was repeated this time taken all the liquid
from the beads. The samples were kept overnight at 65 °C to reverse the
crosslink.

Next, the samples were treated with proteinase K (279 μl TE, 15 μl
proteinase K and 6 μl of glycogen per sample) for 2 h at 37 °C. Add
600 μl of phenol/chloroform, vortex and centrifugate 25 min at 13,000
rpm. The upper phase was passed into a new tube containing 600 μl phe-
nol/chloroform/isoamyl, vortexed and centrifuged for 15 min at 13,000 rpm.
The upper phase was transferred into a fresh tube containing 600 μl chloro-
form/isoamyl (24:1), vortexed and centrifuged 15 min at 13,000 rpm. Next,
the upper phase was transferred into a new tube. To precipitate the DNA,
22 μl 5 M NaCl and 570 μl of isopropanol were added to the tube that was
kept precipitating the DNA for at least 1 h at -20 °C and centrifuge at 4 °C
for 10 min at 13,000 rpm. The supernatant was removed by vacuum and
the pellet resuspended in 30 μl TE.

3.6.2   Sequencing and bioinformatics analysis

The DNA purified from the different samples was end-repaired, ligated to sequencing adapters, size selected on 2% agarose and amplified with 17 cycles of PCR according to the manufacturer's instructions (Illumina). Amplified libraries with inserts of a 130-330 nt size range were sequenced on the Illumina HiSeq2000 platform using v3 sequencing chemistry to generate 50-bp reads. Sequence reads were aligned to the *Saccharomyces cerevisiae* reference genome (sacCer3) using Bowtie (Langmead et al., 2009) allowing 2 mismatches in the seed. Alignment files were processed using Bedtools (Quinlan and Hall, 2010) in order to create wiggle profiles, displayed as custom tracks in the UCSC genome browser (Kent et al., 2002). More than 11 million reads were mapped for each sample, corresponding to 44- 53x genome coverage. Initial reads were divided into 4 subsamples, each one containing about 4.8 million of reads corresponding to 18x genome coverage. Subsamples were inspected for detecting the genomic portions enriched for mapped tags relative to the untagged control with MACS (version 1.4.2) (Zhang et al., 2008). Regions that were significantly enriched with respect to the background ($p < 1 \times 10^{-5}$) were identified with the nomodel option in order not to estimate the fragment size, a shiftsize of 50 bases to use a fixed fragment size, and sliding windows of 50x2 bases. Only peaks that were common across all subsamples, regardless of their false discovery rate, were considered for analysis. The sequencing of the different samples was performed in the Ultra- Sequencing facility at the CRG. The bioinformatics analysis was carried out by the Bioinformatics Unit Facility at the CRG.

This page intentionally left blank

4

Results

Sister chromatids have to be resolved before cytokinesis takes place to ensure proper segregation of all the genetic material. Although the essential components of the segregation machinery have been identified, is not yet well understood how and when chromosome arm separation occurs and the specific role of the molecules that participate in the process. To investigate the segregation dynamics of extra-long chromosomes, we characterized the segregation dynamics of long compound (LC) chromosomes.

The long chromosomes are constructed by fusing several chromosomes within the budding yeast haploid nucleus. The chromosome fusion allowed us to assess the effect of chromosome length in a sequence-independent manner. Indeed, the effects of a fusion chromosome were described before using a fusion of chromosome IV and XII *LC(IV:XII)*, the last one containing the rDNA repetitive region (Neurohr et al., 2011). Here, we investigate the segregation of extra-long chromosomes independently of the presence of the rDNA by avoiding chromosome XII in the long chromosome constructs.

Moreover, we increased up to 70% the length of the longest wild type chromosome arm.

4.1   Construction of long chromosomes

LCs of comparable length to *LC(IV:XII)* were obtained through fusions between chromosome IV and up to three other chromosomes in haploid yeast cells, by repeated cycles of homologous recombination and simultaneous inactivation of supernumerary centromeres, as previously described (Neurohr et al., 2011). In this study, long chromosomes other than *LC(IV:XII)* derivatives are termed *LC(N)*, with N indicating the length in Mb of the long arm (Table 4.1).

Chromosome name	Chromosomes fused	Centromere active	Chromosome length (Mb)	Chromosome arm (Mb)
LC2.0	IV:XV	*CEN4*	2.6	2.0
LC2.3	IV:XV	*CEN15*	2.6	2.3
LC2.6	IV:XV:V	*CEN4*	3.2	2.6
LC2.9	IV:XV:V	*CEN5*	3.2	2.9
LC3.0	IV:XV:XVI	*CEN4*	3.6	3.0
LC3.1	IV:XV:XVI	*CEN16*	3.6	3.1
LC3.6	IV:XV:V:VII	*CEN4*	4.3	3.6
LC3.7	IV:XV:V:VII	*CEN7*	4.3	3.7

Table 4.1: Long chromosome constructs. Long chromosome constructs created in this study, the centromere that is active in each construct and the length (Mb) of the longest chromosome as well as chromosome arm within the genome.

4.1.1 How to fuse chromosomes

The method to fuse chromosomes consists on using a PCR product with a resistance cassette flanked by sequences homologous to the subtelomeric regions of the chromosomes to be fused. This led to the fusion of two chromosomes and the loss of the subtelomeric regions of both of them.

In order to avoid the formation of dicentric chromosomes while constructing the long chromosomes, a *pGAL1* promoter was inserted in front of one of the centromeres. On galactose the centromere becomes inactivated due to the recruitment of the transcription machinery to the *pGAL1* promoter (Hill and Bloom, 1987). After confirmation of the correct fusion, one of the centromeres was deleted and/or the *pGAL1* promoter was deleted from the strains to restore wild type *CEN4*.

To fuse more chromosomes the process was repeated several times, always using *CEN4* as the conditional centromere. When no more selection markers were available, the transformations were always done using the *URA3* cassette. Next, the transformation was repeated with the same oligomers but this time using a cassette that was already present (like hygromycin, nourseothricin) in the strain to eliminate the *URA3* cassette. Then, colonies were counter-selected on 5-Fluoroorotic Acid (5-FOA) plates for the loss of the *URA3* marker. This method allowed us to reuse the *URA3* marker as many times as needed, achieving the fusion of several chromosomes (Figure 4.1).

As a consequence of the recombination that takes place in the subtelomeric regions in order to fuse chromosomes, some genes were deleted while constructing the strains. These genes were not further considered because most of them had no reported phenotype, are redundant with other genes
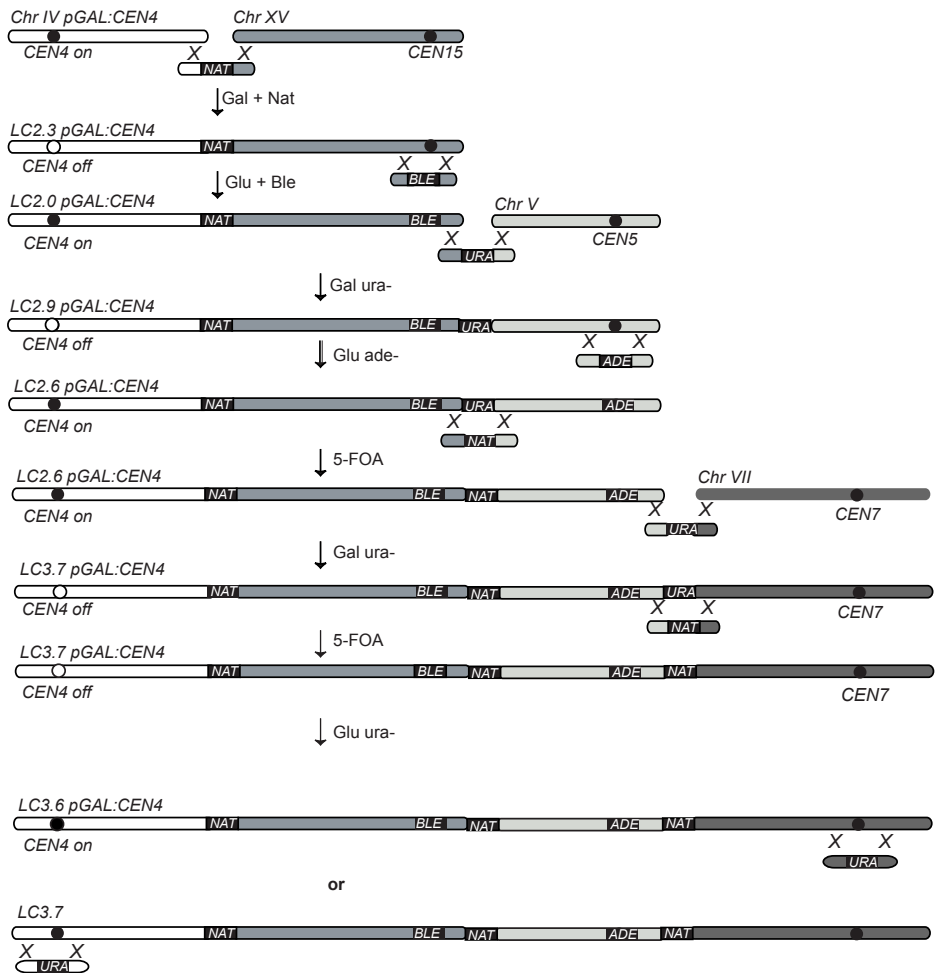
Figure 4.1: Long chromosome construction. Schematic representation of the technique used to fuse chromosomes

present in the genome and are not related to the mitotic cell cycle. A list of the open reading frames deleted in the long chromosome constructs can be found at Appendix A.

4.1.2   Chromosome fusion verification

To verify the correct fusion of the chromosomes, different methods were used. First of all, the presence of the *pGAL1* promoter in front of *CEN4* reduced the viability of wild type karyotype cells growing in plates containing galactose as carbon source due to the loss of chromosome IV. This defect was abolished when chromosomes were fused, indicating that chromosome IV was not missegregating because another centromere was present in the fused construct (Figure 4.2 A).

Second, the fusion was checked by PCR using oligomers that anneal to the subtelomeric region of the fused chromosomes, before and after the site of recombination. In the wild type situation, the oligomers will produce two different short bands corresponding to the two subtelomeric regions (Figure 4.2 B, products A and B). However, when the chromosomes are fused, the PCR product corresponds to one band of higher molecular weight that is due to the amplification of the remaining subtelomeric regions and the cassette inserted by homologous recombination (Figure 4.2 B, PCR product C).

Finally, chromosome fusions were checked by PFGE (see Materials and Methods 3.3.1 and Figure 4.2 C). The electric pulses needed to separate chromosomes up to 1.5 Mb and longer ones are different, meaning that not all chromosomes could be visualized in the same gel. Therefore, two different gels were done in parallel, the first one shows the disappearance of the band corresponding to chromosome IV (Figure 4.2 C i). *LC(IV-XII)cen12Δ* and *LC(IV-XII)cen4Δ* correspond to the fusion of chromosomes IV and XII previously reported (Neurohr et al., 2011). The second gel shows the gain of higher bands that do not correspond to any of the wild type chromosomes and that increase with the length of the chromosomes that are fused (Figure

4.2 C ii). By these three different techniques we were able to show that the chromosomes were correctly fused.

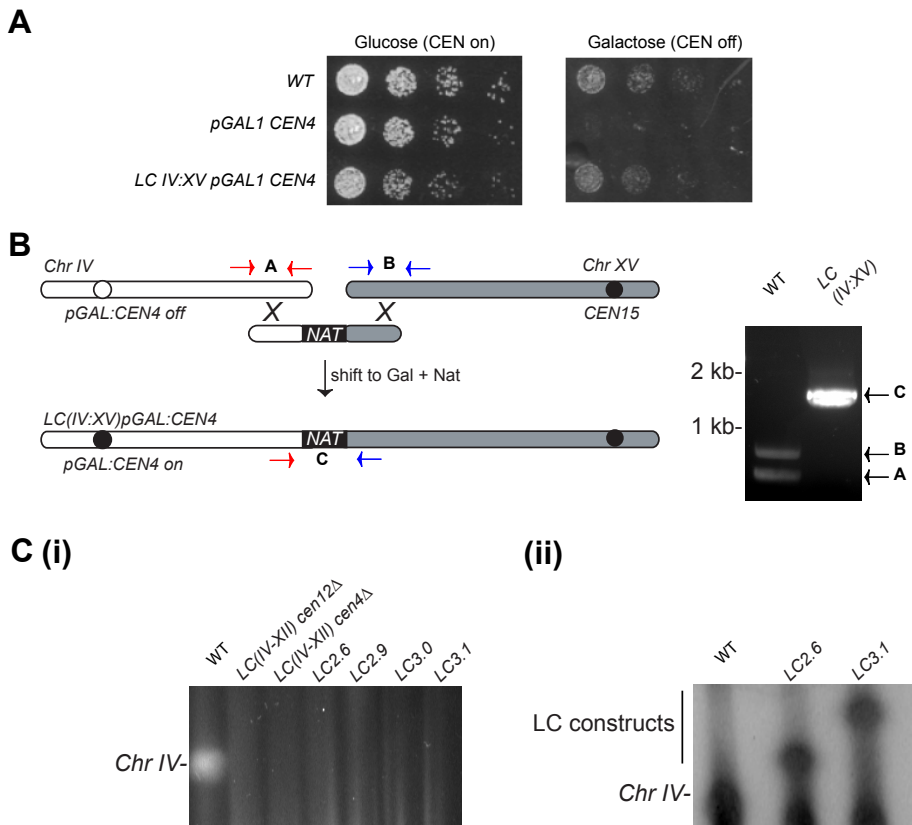**Figure 4.2: Chromosome fusion verification.** (A) Serial dilutions of the indicated strains grown in galactose and glucose. Chromosome fusion was verified by gain of viability in galactose. (B) Scheme and PCR products of subtelomeric regions to check chromosome fusion. (C) Pulse-field gel electrophoresis of the indicated strains in different conditions, to separate short chromosomes (i) and to identify long chromosomes (ii).

4.1.3 Sequencing of long chromosome strains

In order to ensure that the process of chromosome fusion was not causing any major chromosome rearrangement and to discard the appearance of additional mutations, whole genome sequencing of wild type and fusion chromosome strains *LC2.6*, *LC2.9*, *LC3.0* and *LC3.1* was performed on an Illumina GAIIx sequencer. The analysis carried out by Leszek Pryszcz and Toni Gabaldón (Bioinformatics and Genomics Program at the CRG) revealed no genomic re-arrangement between the different strains (data not shown). Moreover, there were no genomic duplications found and the only deletions detected corresponded to repetitive subtelomeric regions, which are known to be difficult to assemble properly. To assess variation at the single nucleotide level, all reads from each strain were mapped onto the wild-type strain assembly. Single nucleotide polymorphisms (SNPs) were called on positions that were highly covered (10x) and unambiguous (90% consistency). This procedure uncovered seven SNPs in total, four of which correspond to the same position in all long-chromosome mutants (Table 4.2).

PHO86 (YJL117W) was found mutated in *LC2.6*, *LC2.9*, *LC3.0* and *LC3.1*. This gene encodes for an endoplasmatic reticulum resident protein required for ER exit of the phosphate transporter Pho84 through COPII vesicles (Lau et al., 2000). There has not been described any cell cycle defect in *pho86Δ* cells so far. Although the mutated residue is conserved among fungi, it is unlikely that the mutation we found causes a gene loss-of-function. This is due to the fact that *pho86Δ* cells have increased sensitivity to heat (Sinha et al., 2008) and increased resistance to methyl methanesulfonate (MMS) (Kapitzky et al., 2010) and we have not observed neither of the phenotypes in cells bearing long chromosomes as we shall see (Results 4.3.1).

Location	Mutation	Description	Strains affected
YJL117W	I268S	Change of a hydrophobic to a polar aminoacid	LC2.6, 2.9, 3.0, 3.1
YPR117W	D366E	Conservative in a protein of unknown function	LC2.6
ChrXIV	T718767G	Non-coding region, 400 bp upstream to start codon of YNR051C	LC2.6
ChrIX	T13444404G	Non-coding region promoter region of YIL120W	LC2.6

Table 4.2: SNPs found in the long chromosome strains by in-deep sequencing.

Therefore, the mutation is unlikely to affect chromosome segregation or cell cycle progress. This mutation is present in all the strains likely because it appeared in one intermediate common to all.

4.1.4   Long chromosome bearing cells are viable

By fusing up to four different chromosomes the maximum chromosome arm length was increased 70% compared to the longest wild type chromosome arm (Figure 4.3 A). In order to assay the viability of this constructs, serial dilutions of exponential growing cultures were plated in rich media and incubated at 30ºC for 48h. There is no difference in growth between wild type cells and cells bearing long chromosomes. Therefore, LCs do not affect cell growth in complete media (Figure 4.3 B).
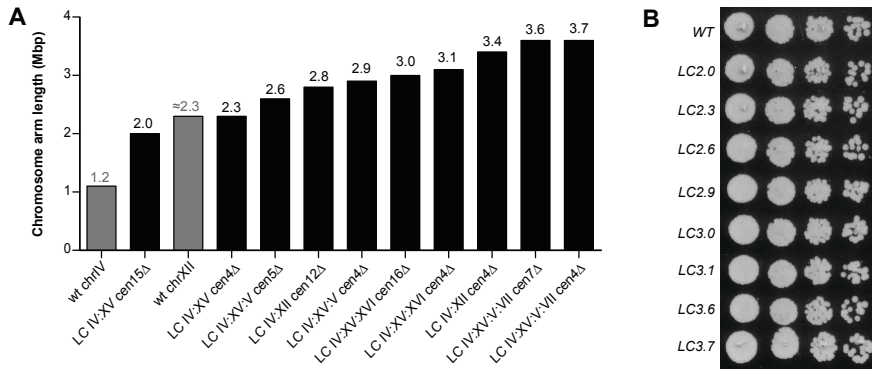
Figure 4.3: Long chromosome constructs' viability. (A) Chromosome arm length of the different LC constructs. (B) Serial dilutions of cells bearing the different long chromosome constructs incubated for 2 days at 30 °C.

4.2   Efficient segregation of long compound chromosomes

To determine anaphase dynamics in wild type and LC cells by live cell imaging, the spindle pole body (SPB) component Spc42 was fused to green fluorescent protein (Spc42-GFP). In addition, two different loci in the same chromosome arm were visualized through TetR-mRFP and LacI-GFP reporters in cells bearing Tet and Lac operator arrays. These were inserted in *TRP1* (distant 10 kb from *CEN4* in wild type chromosome IV) and *LYS4* (in the middle of chromosome IV right arm, 470 kb away from *TRP1*).

Imaging of anaphase cells showed that in wild type chromosome IV, *TRP1* loci segregate to opposite spindle poles during early anaphase, whereas *LYS4* segregation occurred 4-5 minutes later (Figure 4.5 A). Segregation dynamics were similar in LCs where *CEN4* acted as the active centromere, indicating that the segregation of centromere-proximal regions is not affected
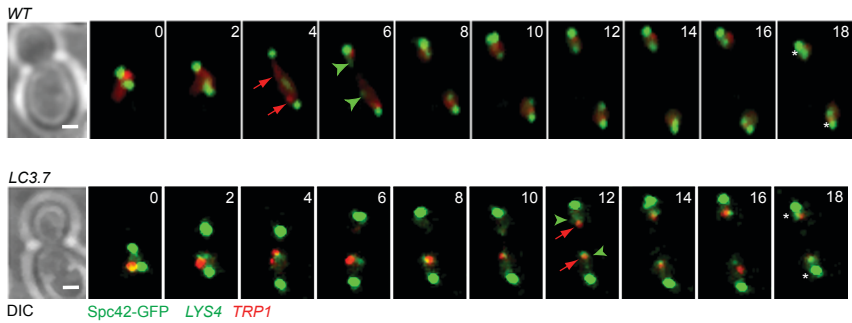
Figure 4.4: Distal loci segregation in long chromosomes. Segregation of wild-type chromosome IV and *LC3.7* imaged in live cells at 30 °C. Spc42-GFP marks the SPBs (bright green dots). The segregation of *LYS4* loci labeled with LacI-GFP (faint green dots) is marked with green arrowheads, and that of *TRP1* (red dots visualized with TetR-mCherry) with red arrows. Asterisks indicate spindle breakdown defined when SPB distance decreased by $> 10\%$ relative to its maximum value. Time 0 is anaphase onset (distance between SPBs>3 μm). Scale bar, 1 μm.

by changes in the length of the chromosome (Figure 4.5 B). Segregation of *TRP1* and *LYS4* occurred in late anaphase when these loci were located distally to the active centromere (Figure 4.5 A and B). Notably, the further away that a locus is from the centromere, the longer it takes to be segregated.

In wild type and LC cells, spindle elongation dynamics and anaphase duration were indistinguishable (Figure 4.5C). The relationship between genomic distance and segregation time was similar in all LCs, including *LC(IV:XII)* (Figure 4.5 D white circles), indicating that the main determinant of segregation time for a genomic locus is its distance from the centromere.
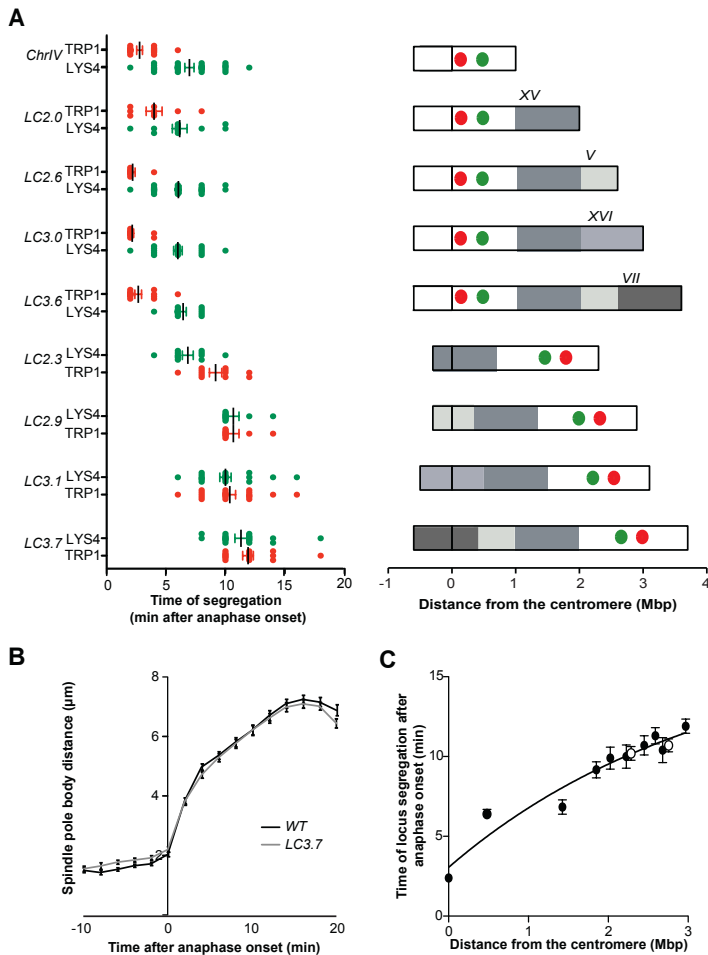
Figure 4.5: Distal loci segregation in long chromosomes. (A) The time of segregation of *TRP1* and *LYS4* loci was determined for the indicated strains. (B) The distance between SPBs (Spc42-GFP) in wild type and *LC3.7* cells was determined during spindle elongation. (C) Time of segregation of *TRP1* and *LYS4* loci in LC, plotted as a function of genomic distance to the centromere White circles correspond to *LC(IV:XII)*. Data in B and C are shown as mean and SEM (N>25 cells).

4.2.1   Anaphase hyper-condensation occurs independently of rDNA sequences

Aurora-B mediates hyper-condensation of *LC(IV:XII)* in anaphase (Neurohr et al., 2011). To establish if LCs lacking rDNA also undergo anaphase hyper-condensation, the distance between *TRP1* and *LYS4* loci was used as a readout for compaction. The *TRP1-LYS4* distance was measured in cells carrying either wild type chromosome IV, or *LC3.6* in which *CEN4* is the active centromere (Figure 4.6).
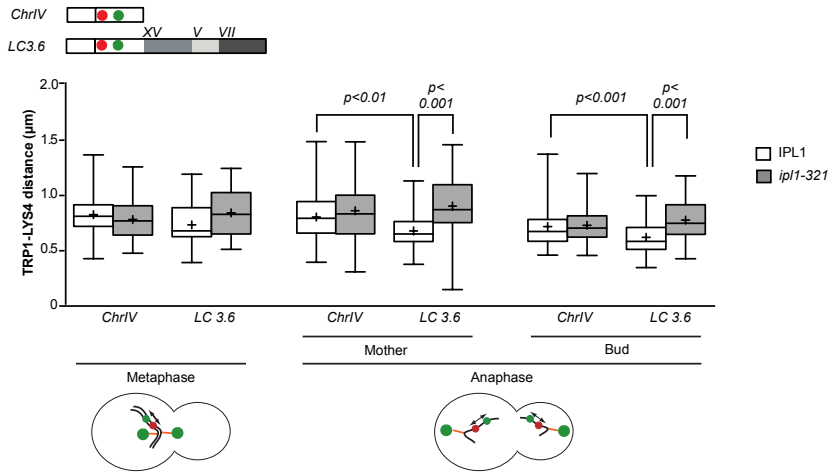
Figure 4.6: Long chromosome hypercondensation.   Cells containing the indicated chromosomes and either *IPL1* or *ipl1-321* alleles were released from a G1 block at 25 °C, shifted to 35 °C after 1 h, and imaged in a temperature-controlled chamber at 35 °C. Only cells that initiated anaphase within the first 20 min of imaging were considered. The distance between *TRP1* and *LYS4* loci was measured in metaphase (10 min before spindle elongation) and in anaphase (after their segregation). Boxes include 50% of data, whiskers 90%. Median (lines) and mean (crosses) are shown (N>20 cells).

To test the role of Aurora-B/Ipl1 in anaphase compaction, wild type

and cells carrying the temperature-sensitive *ipl1-321* allele were arrested in G1 with mating pheromone, released into a new cycle at 25 °C and shifted to 35 °C after 1 h, to inactivate Aurora-B during anaphase without affecting its function in chromosome biorientation (Tanaka et al., 2002). In wild type cells, mean *TRP1-LYS4* distances in late anaphase daughter cells were reduced to 85% of their metaphase value (compare metaphase and anaphase bud of chromosome IV in Figure 4.6; p<0.01), as described previously (Neurohr et al., 2011). *TRP1-LYS4* metaphase distances were not significantly altered in *LC3.6*, but anaphase compaction was further increased in both mother and bud compartments in *LC3.6* cells (Figure 4.6). Furthermore, anaphase hyper-compaction of the *TRP1-LYS4* region in *LC3.6* was defective in *ipl1-321* mutants, establishing that Aurora-B dependent anaphase hyper-condensation is a general response to extra-long chromosomes.

Thus, these data show that the Ipl1-dependent hypercondensation does not depend on the rDNA locus. In addition, this mechanism can deal with chromosomes 70% longer than the longest wild type chromosome.

4.3 Perturbation of long chromosome cells' viability

The construction of long chromosomes alters the karyotype of the cells. In order to investigate if long chromosomes present a challenge to the cell we assayed growth of LC strains in stress conditions and upon gene inactivation.

4.3.1 Long chromosome bearing cells' growth in the presence of drugs

Viability of LC cells was assessed in different stress conditions as increased temperature or drug treatment. Growth assays of long chromosome bearing cells were performed at 37 °C and in the presence of hydroxyurea (HU), methyl methanesulfonate (MMS), rapamycin and benomyl (Figure 4.7).

Long chromosome bearing cells are not susceptible to changes in temperature; either increasing at 37 °C (Figure 4.7 A) or decreasing at 16 °C (data not shown) the temperature does not affect cell growth. In order to check if long chromosome bearing cells present major defects in replication, the different constructs were grown in the presence of low concentrations of MMS and HU. MMS is a drug that stalls replication forks and HU reduces the production of deoxyribonucleotides via inhibition of the enzyme ribonucleotide reductase. None of the long chromosome constructs were affected more than wild type by the presence of these drugs (Figure 4.7 B). Long chromosome bearing cells are also not affected by sub-lethal concentrations of rapamycin, a drug that inhibits the TOR pathway, conferring a G1 arrest (Figure 4.7 C).

Benomyl is a drug that binds to microtubules and interferes with cell functions such as mitosis, meiosis and intracellular transport. In the presence of benomyl, the viability of long chromosome bearing cells is improved when compared to wild type karyotype strains (Figure 4.7 D). Interestingly, the resistance to benomyl of longer chromosomes is rather proportional to the number of fused chromosomes than the length of the chromosomes (the number of chromosomes fused is shown in brackets Figure 4.7). Strains carrying fused chromosomes contain fewer centromeres per cell. Thus, we
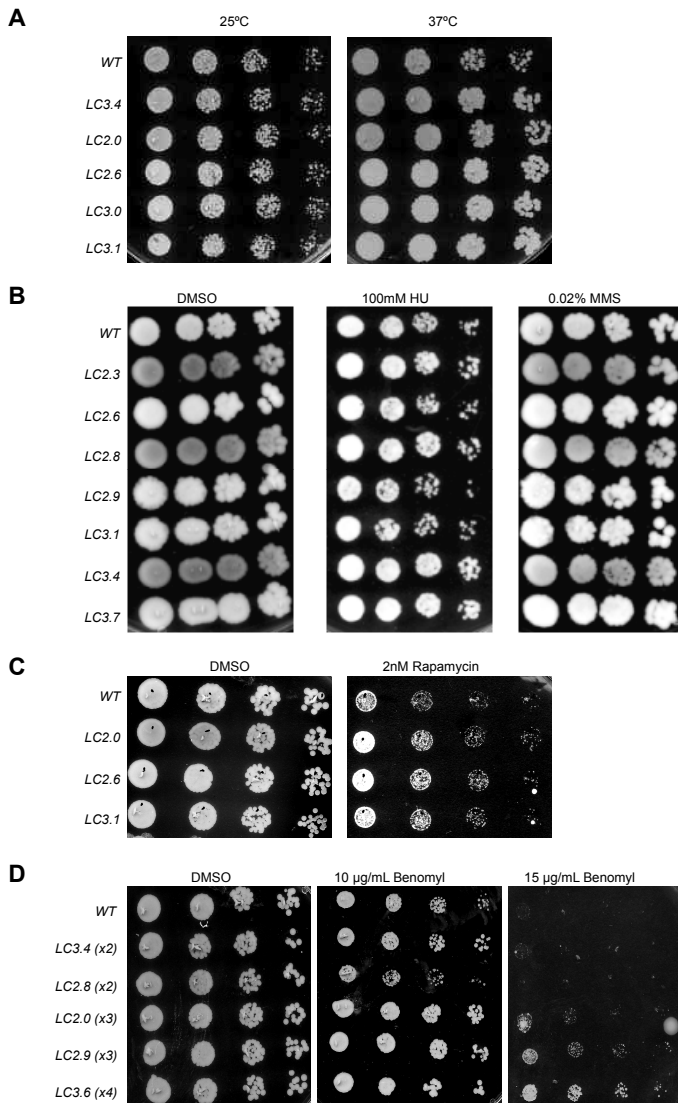
Figure 4.7: Growth assays in the presence of stress conditions. Serial dilutions of long chromosome bearing cells at 37 °C (A) and in the presence of hydroxyurea (HU), methyl methanesulfonate(MMS) (B), rapamycin (C) and benomyl (D) at the indicated concentrations. Cells were grown for 2 days.

hypothesize that the more chromosomes that are fused (decreasing the number of active centromeres), less microtubules are needed to achieve correct kinetochore attachment to the spindle. Thus, by fusing chromosomes the number of centromere is reduced and more resistance to benomyl is observed.

4.3.2 Genetic interactions with long chromosomes

We have observed that distal parts of long chromosomes segregate later than proximal ones even when the hypercondensation adaptive mechanism is active. Moreover, long chromosome bearing strains do not show any synthetic lethality upon *ipl1-321* allele inactivation (Figure 4.8). Therefore, additional processes other than *IPL1*-dependent anaphase hyper-compaction could be essential to segregate distal parts of long chromosomes.

Figure 4.8: *IPL1* **and long chromosomes**. Serial dilutions of wild type karyotype and long chromosome strains containing *ipl1-321* thermosensitive allele were grown at the indicated temperatures during 2 days.

In order to understand the molecular processes involved in long chromosome segregation we performed a candidate-based small scale screen looking for deletions or mutations that would affect the viability of long chromosome bearing cells. We selected genes mainly involved in mitosis, replication, cell cycle progression, microtubules and chromosome structure (Appendix B).

Out of the 52 genes, only 8 of them showed genetic interaction with

long chromosomes. Interestingly, these genes are related to mitotic progression (*SMC6*, *CDC5*, *SMC2* and *YCG1*), microtubule dynamics (*STU2* and *KIP3*) and topological stress (*PIF1* and *TOP2*).

4.3.3 The SMC5/6 complex and long chromosomes

The *smc6-9* allele perturbs the function of the SMC5/6 complex. We have found that only the long chromosome bearing cells that contain the chromosome XII are synthetic sick with the *smc6-9* allele (Figure 4.9). Importantly, *LC(IV-XII)* is the only construct that contains chromosome XII and, therefore, the rDNA repeats. This suggests that the genetic interaction of long chromosomes and the SMC5/6 complex is due to the presence of the rDNA in a longer chromosome but not solely to the length of the chromosome arm *per se*. The SMC5/6 complex has been involved in rDNA resolution during anaphase (Torres-Rosell et al., 2005). Therefore, one possibility is that the Smc5/6-mediated resolution of the rDNA becomes more challenging when the repeats are located in a longer chromosome. As we will see (Results 4.6.3), longer chromosomes accumulate more topological stress. This stress could influence the ability of Smc5/6 in resolving the ribosomal DNA.
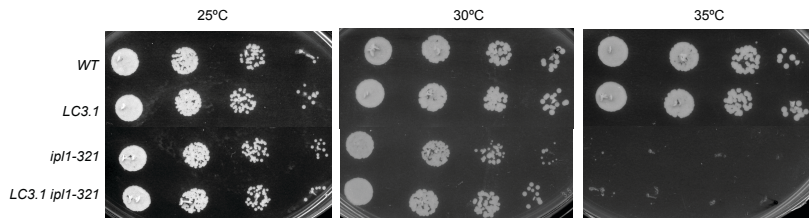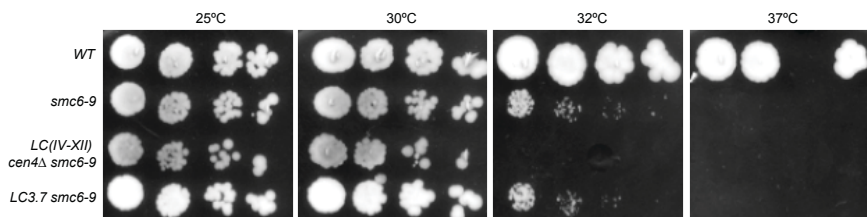

Figure 4.9: SMC5/6 and long chromosomes. Serial dilutions of wild type karyotype and long chromosome strains containing *smc6-9* thermosensitive allele were grown at the indicated temperatures during 4 days.

4.4   Condensin is needed for long chromosome cells viability

The polo-like kinase (Cdc5) is involved in anaphase progression and mitotic exit. We found that long chromosome bearing cells are synthetic sick with the thermosensitive allele of the polo-like kinase *cdc5-1* already at semi-permissive temperature (Figure 4.10).

Figure 4.10: Polo-like kinase is essential to adapt to a long chromosome. Serial dilutions showing the genetic interactions between long chromosomes and Polo-like kinase *cdc5-1* thermosensitive allele.

CDC5 is responsible for the phosphorylation and activation, among others, of the condensin complex during mitosis (Bazile et al., 2010). Therefore, we wondered if long chromosomes were synthetic sick with condensin complex mutants. The condensin complex is involved in the proper compaction of chromosomes during mitosis. It has already been reported condensin is necessary for the adaptation to long chromosomes (Neurohr et al., 2011). Long chromosome bearing cells' viability is reduced when the thermosensitive alles *smc2-8* and *ycg1-2* (subunits of the condensin complex) are partially inactivated at semipermissive temperature (Figure 4.11 A and B). Using live-cell imaging we could confirm that the long chromosome cells

bearing the *ycg1-2* mutation are unable to segregate 95% of the LYS4 locus at semipermissive temperature (Figure 4.11 C). Thus, condensin is essential for long chromosome adaptation and it is possible (but not proven) that the interaction of *CDC5* in LC cells is due to deficient condensin activity in those cells.

4.5 Perturbation of microtubule dynamics blocks anaphase progression of cells with extra-long chromosomes

In order to identify additional processes important for the segregation of long chromosomes, we next addressed whether perturbation of spindle function specifically impairs the growth of LC cells.

4.5.1 Genetic interactions between long chromosome bearing cells and spindle components

Deletion of genes encoding non-essential spindle motors (*CIN8, KIP1, KIP3*) or microtubule-associated proteins (*ASE1, BIM1, CIK1, IRC15*) did not impair growth of *LC3.1* cells to a greater extent than in cells with normal chromosomes (Figure 4.12).

In contrast, partial inactivation of the essential microtubule polymerase Stu2 specifically affected growth of long chromosome cells, as *LC3.1 stu2-13* mutants showed slight growth defects at 25 °C and strongly reduced viability at 30 °C, whereas *stu2-13* mutants with a normal karyotype grew as well as wild type under the same conditions (Figure 4.13 A, left). This suggested that microtubule dynamics are particularly important for LC segregation.
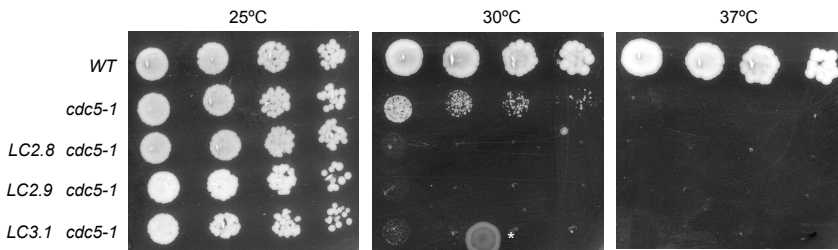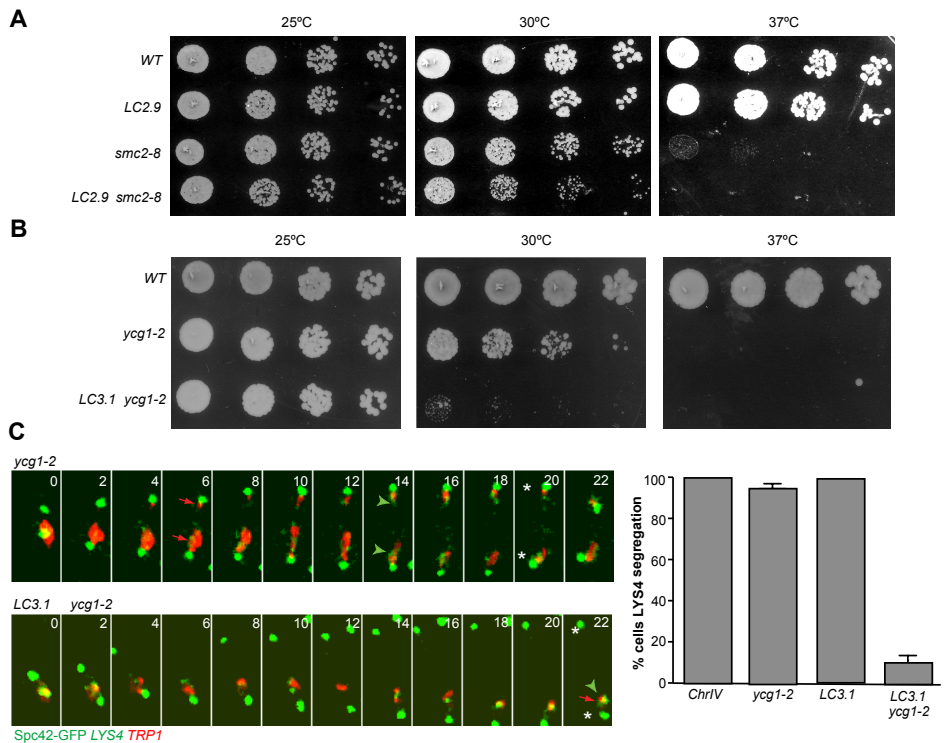
Figure 4.11:   Condensin is essential to adapt to a long chromosome.
Serial dilutions showing the genetic interactions between long chromosomes and
two thermosensitive alleles of the condensin complex: *smc2-8* (A) and *ycg1-2* (B).
(C) Live-cell imaging of *ycg1-2* cells and long chromosome cells bearing *ycg1-2* was
performed on cells grown at permissive temperature and shifted to 30 °C for 15
min before imaging. Double arrows and arrowheads show segregation of *TRP1*
and *LYS4* respectively.   Single arrows and arrowheads indicate missegregation.
The percentage of cells segregating the *LYS4* locus was quantified (N>20 in three
independent experiments). Mean and SEM are plotted.

Supporting this view, over-expression of the microtubule depolymerase Kip3
from the strong *pGAL1* promoter also impaired growth of *LC3.1* cells but
not of cells with wild type karyotype (Figure 4.13 A, right).
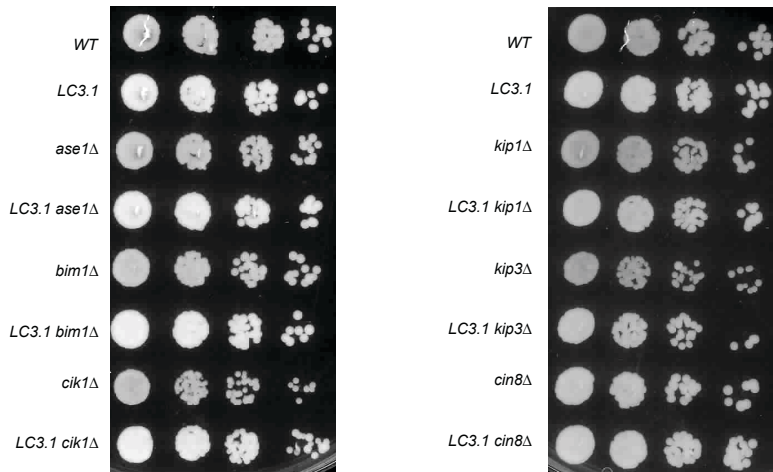
Figure 4.12: Genetic interactions between LCs and spindle components.
Growth tests showing no genetic interaction between long chromosome bearing cells
and the spindle components *ASE1, BIM1, CIK1, KIP1, KIP3* and *CIN8*.

4.5.2   Stu2 function is essential for segregation and anaphase progression in LC bearing cells

To gain insight into the specific defect of *LC stu2-13* cells, wild type and
mutant cultures were synchronized in G1 at 25 °C, released into a new cycle
at 30 °C, and cell and nuclear morphology were assessed at time intervals
by DIC microscopy and DAPI staining (Figure 4.13 B and C). In wild type
and *LC3.1* cells, elongated nuclei indicative of mid-anaphase were briefly
detected 1 h after release from the G1 block. These cells correctly parti-
tioned their nuclei between mother and bud within 30 min of anaphase onset.
Likewise, most *stu2-13* mutants with normal chromosomes completed nu-
clear division albeit with a 15 min delay. In contrast, nuclear division was
severely delayed in *LC3.1 stu2-13* mutants. These mutants initiated nuclear
elongation at the same time as wild type cells, but displayed a high frequency

Figure 4.13: Microtubule dynamics are essential to segregate long chromosomes. (A) Cultures were grown to mid-log phase in YPD, and serial dilutions plated at the indicated temperature and media were incubated for 2 days. (B) Cultures of the indicated strains were arrested in G1 at 25 °C, released at 30 °C, fixed at time intervals and stained with DAPI. Graphs show the frequencies of cells with elongated or divided nuclei in the mother or daughter cell compartments, as shown in the schemes. (C) Representative DAPI-stained cells showing the phenotypes quantified in B.

of elongated nuclei for more than 1h after initiation of anaphase (Figure 4.13 B and C). In addition, nuclear migration into the bud was defective in many *LC3.1 stu2-13* cells, as indicated by the appearance of divided nuclei in the mother cell compartment (4.13 B and C). Thus, mild perturbation of Stu2 severely affects anaphase progression in cells with extra-long chromosomes.

The phenotype of *LC3.1 stu2-13* mutants was further characterized by

Figure 4.14: Long chromosomes with *stu2-13* mutation trigger a mid-anaphase delay. (A) Spindle elongation and chromosome segregation dynamics in representative cells of the indicated genotypes. Cultures were grown at 25 °C to mid log phase, shifted to 30 °C and imaging started within 15 min. Double arrows and arrowheads indicate the segregation of *TRP1* and *LYS4* loci respectively; single arrow and arrowhead indicate defective segregation . Asterisks show the time of spindle breakdown. The graphs show the distances between SPBs and *LYS4* loci in the corresponding cells. Scale bar, 1 μm. (B-C) Analysis of spindle breakdown (B) and *LYS4* segregation (C) in cells treated as in A. Boxes include 50% of data points and whiskers 90%. A line indicates the median and a cross the mean.

live-cell imaging. Cells expressing Spc42-GFP and fluorescently tagged *LYS4* and *TRP1* loci were grown to mid-log phase at 25 °C and shifted to 30 °C 15 min prior to start of imaging. Cells starting anaphase within the first 20 min of imaging were analyzed for spindle elongation and chromosome segregation dynamics. Consistent with its role in anaphase spindle elongation (Severin et al., 2001), partial Stu2 inactivation caused a mild reduction in the final length of anaphase spindles in cells with both normal and extra-long chromosomes (wild type: mean 8.4 μm, SD 0.1μm; stu2-13: 7.3±0.3μm; LC stu2-13: 7.2±0.3μm; N=23 cells/strain). The *stu2-13* mutants showed a 5 min delay in the time of *LYS4* segregation relative to wild type cells, and disassembled their spindles approximately 25 min after anaphase onset, similar to wild type cells (see example in Figure 4.14 A). In contrast, *LC3.1 stu2-13* mutant spindles paused in mid-anaphase (4-5μm length) with unsegregated *LYS4* loci for an extended time (compare *LC3.1* and *LC3.1 stu2-13* cells in Figure 4.14 A). Spindles resumed elongation and reached their maximal length after an average time of 35 min (18/36 cells; see example in Figure 4.14 A, third row) or collapsed, with SPBs moving towards each other and chromosomes remaining in the mother cell (6/36 cells). In addition, in a third of anaphase cells (12/36) the mid-anaphase pause lasted for more than 60 min and did not resolve within the imaging time. Due to either extended anaphase pause or spindle collapse, *LYS4* segregation did not occur within 60 min of anaphase onset in 56% of *LC3.1 stu2-13* mutants (Figure 4.14 B and C).

4.5.3 The mid-anaphase delay of *LC stu2-13* mutants is partially dependent on the DNA damage checkpoint component *RAD9*

The mid-anaphase pause in *LC3.1 stu2-13* was reminiscent of that observed upon activation of a conditionally dicentric chromosome. Dicentric cells arrest transiently in mid-anaphase with spindles partially elongated, before eventually resuming spindle elongation and completing anaphase; this mid-anaphase delay depends on the DNA damage checkpoint component *RAD9* (Yang et al., 1997) (see Introduction 1.4.3). Therefore, we wondered whether *RAD9* also mediates the anaphase delay of *LC3.1 stu2-13* cells.

Live cell imaging of *rad9Δ* mutant cells showed a reduction in the number of cells with mid-anaphase pauses longer than 60 min, from 33% of cells in *LC3.1 stu2-13* to 7% in *LC3.1 stu2-13 rad9Δ*, and an advancement in the time of spindle disassembly in the remaining cells (see example in Figure 4.14 A, bottom). Notably, deletion of *RAD9* did not rescue the chromosome segregation defects in LC3.1 stu2-13 cells, as spindle breakage occurred prior to segregation in almost half of the cases (Figure 4.14 B and C). Thus, the mid-anaphase delay in *LC stu2-13* cells might be caused, at least partially, by chromosome aberrations similar to those occurring after dicentric activation.

4.5.4 *LC stu2-13* anaphase defects can be rescued by *kip3Δ*

The activity of the microtubule depolymerase Kip3 counteracts the activity of Stu2, and simutaneous inactivation of Kip3 and Stu2 restores anaphase elongation (Severin et al., 2001). In order to investigate if the *LC stu2-13* defects were caused by a defect in microtubule polymerization and not by

other possible functions of Stu2, *KIP3* was deleted in *LC stu2-13* cells. The
growth of these cells was severely impaired as reported (Severin et al., 2001)
due to impairment in satisfying the spindle assembly checkpoint.
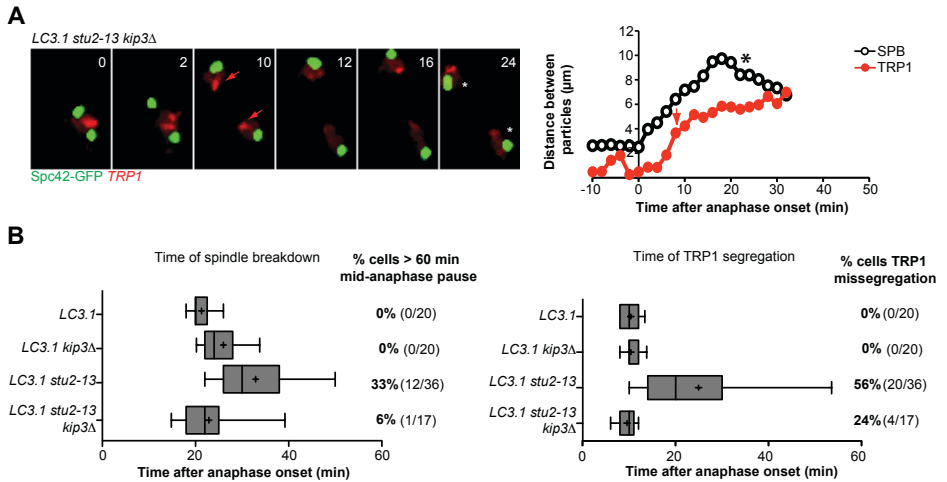
Figure 4.15: *kip3Δ* partially restores the defects of *LC stu2-13*. (A)
Time series of a representative *LC stu2-13 kip3Δ* cell undergoing anaphase. In
these cells, the *LYS4*-associated LacI-GFP signal was not visible in all time points,
and *TRP1* dots were tracked instead. Cultures were grown at 25 °C to mid log
phase, shifted to 30 °C and imaging started within 15 min. Double arrows indicate
TRP1 segregation and asterisks show spindle breakdown. The graphs show the
distances between SPBs and *TRP1* loci. Scale bar, 1 μm. (B-C) Analysis of
spindle breakdown (B) and *TRP1* segregation (C) in cells treated as in A. Boxes
include 50% of data points and whiskers 90%. A line indicates the median and a
cross the mean.

Despite the growth defects, live-cell imaging showed that a portion of
the cells managed to undergo anaphase (Figure 4.15 A). Those cells were
analyzed for anaphase progression and chromosome segregation following the
same protocol as in Figure 4.14. *LC stu2-13 kip3* mutants do not present

an elongated mid-anaphase pause like *LC stu2-13* and their spindles break with a timing more similar to wild type (Figure 4.14 B). Regarding *TRP1* segregation, *LC stu2-13 kip3Δ* mutants manage to segregate *TRP1* locus in 76% of the cells and with a timing undistinguishable from wild type cells. Therefore, the defect in *LC stu2-13* cells is likely caused by an unbalanced rate between polymerization and depolymerization of tubulin that affects microtubule dynamics.

4.6   Segregation of long chromosome ends requires Topoisomerase II activity in anaphase

Long chromosome bearing cells containing the *stu2-13* mutation show an extended mid-anaphase pause at semi-permissive temperature and present severe defects in spindle elongation and long chromosome segregation. Together, these observations raise the possibility that *LC stu2-13* cells are impaired in the resolution of connections between sister-chromatids. Which kind of chromosome linkages might impede chromosome segregation in *LC stu2-13* mutants? It is unlikely that cohesin accounts for unresolved linkages specifically in long chromosomes, since its cleavage by separase occurs simultaneously along chromosome arms (Yaakov et al., 2012). On the other hand, it has been suggested that unresolved DNA catenations could trigger a Rad9-dependent mid-anaphase delay (Yang et al., 1997), and that sister chromatid intertwinings (SCI) accumulate in chromosomes in a length-dependent manner (Kegel et al., 2011). We therefore considered the possibility that *LC stu2-13* defects might be related to unresolved DNA catenations.

4.6.1   Viability of long chromosomes is perturbed upon increase in topological stress

First, to determine whether long chromosomes increase topological stress we introduced mutations in proteins involved in dealing with DNA torsional stress. We checked if long chromosomes presented a viability defect when deleting genes encoding for DNA helicases. Long chromosome bearing cells growth is not affected by *rrm3Δ, hmi1Δ, sgs1Δ*. However, the viability is compromised in *pif1Δ* specially in long chromosome bearing cells (Figure 4.16 A).

PIF1 encodes a DNA helicase that exists in a nuclear form and as a mitochondrial form involved in repair and recombination of mitochondrial DNA (Foury and Lahaye, 1987). The nuclear form is involved in different processes. On one hand, Pif1 acts as an inhibitor of telomerase ensuring telomere homeostasis, its deletion causes longer telomeres and *de novo* formation of telomeres (Zhou et al., 2000). On the other hand, Pif1 has been involved in replication fork progression in the rDNA repeats (Ivessa et al., 2000)

There were no viability defects in long chromosome cells with mutations in genes involved in telomere homeostasis (*RIF1, RIF2, YKU70, ESC1, SIR2* check Appendix B.1). This suggests that telomere length maintenance function of *PIF1* is not the reason for the genetic interaction. We have not find any other helicase that decreases the viability of long chromosome bearing cells when compared to wild type karyotype. Therefore, although there is no evidence that LC suffer mitochondrial stress, we cannot rule out that the mitochondrial function is also necessary for viability in cells bearing long chromosomes.
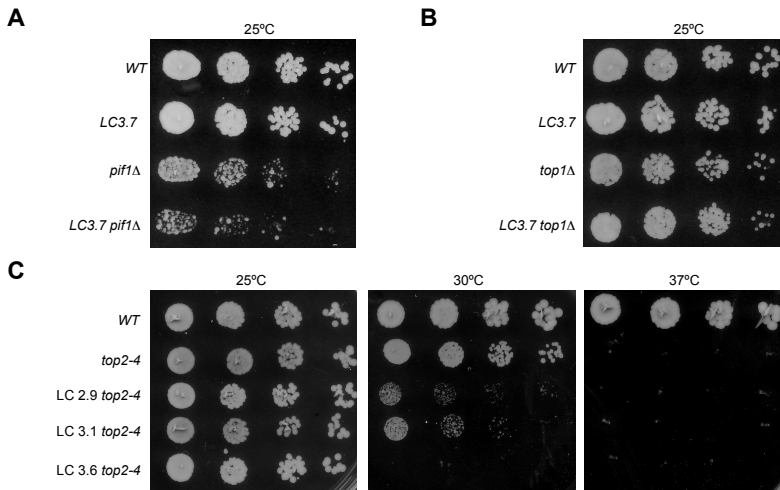
Figure 4.16: Long chromosomes are synthetic sick with genes involved in resolving topological stress. Serial dilutions showing the genetic interactions between long chromosome bearing cells and mutations related to torsional stress: *pif1Δ* (A), *top1Δ* (B) and *top2-4* (C).

Long chromosomes are not susceptible to the loss of Topoisomerase I (*TOP1*) that resolves both positive and negative DNA supercoils (Thrash et al., 1985) (Figure 4.16 B). *TOP1* is not essential in yeast cells because *TOP2* can take over its function, however, *top1Δ* mutants present a delay in late replication (Kegel et al., 2011). *TOP2* is an essential gene due to the fact that is the only topoisomerase in yeast that has the catalytic activity necessary to cut and religate dsDNA. To determine whether long chromosome constructs accumulate more SCI, the topoisomerase II thermosensitive allele *top2-4* was introduced in strains containing long chromosomes to determine their viability at different temperatures. Serial dilutions of the different strains with *top2-4* mutation showed that already at semipermissive temperature there was a severe growth defect specifically in the

strains containing both a long chromosome and the mutation (Figure 4.16 C).

Long chromosome strains are susceptible to the loss of Topoisomerase II activity. Topoisomerase II is involved in resolution not only of sister chromatid intertwinings but also of the supercoilings generated during replication. The fact that long chromosomes are not affected by to the loss of Topoisomerase I enzyme and are not sensitive to HU or MMS (Figures 4.16 and 4.7) implies that these cells do not have a replication-associated defect. This suggests that long chromosome bearing cells have to deal with an increased level of topological stress.

4.6.2   Topoisomerase II is needed during anaphase for chromosome segregation

To establish the time of SCI resolution in normal and long chromosomes, we studied the consequences of inactivating Topoisomerase II during anaphase, using the *top2-4* temperature-sensitive mutation. Wild type and *top2-4* cells with fluorescently labeled SPBs and chromosome markers were arrested in metaphase by depletion of the APC activator Cdc20 at 25 °C, and released into anaphase at 37 °C. Segregation of centromere-proximal *TRP1* loci was only mildly affected by Topoisomerase II inactivation under these conditions; in contrast, *LYS4* failed to segregate in approximately 50% of *top2-4* cells, and unsegregated loci remained in either mother or daughter cell after spindle breakdown (Figure 4.17). A similar defect was observed in freely cycling cells grown at 25 °C, and which started anaphase within the first 20 min of imaging at 37 °C. Therefore, Topoisomerase II activity is needed at the time of anaphase to ensure proper chromosome arm segregation.

Topoisomerase II could be required during anaphase because the cells do not have enough time to disentangle the chromatids before the metaphase-to-anaphase transition as replication is rapidly followed by mitosis in yeast cells. However, this possibility seems unlikely as Cdc20 synchronized cells which arrest for 3h in metaphase, show a similar percentage of *LYS4* missegregation than asynchronous cells in which Topoisomerase II is inactivated.
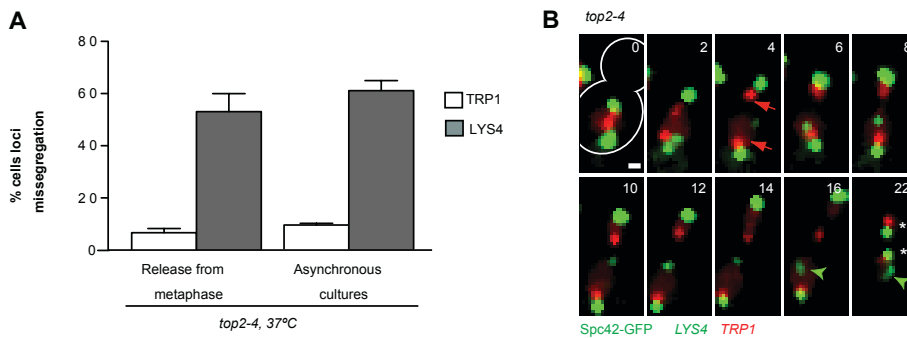
Figure 4.17: Topoisomerase II is essential during anaphase. (A) The percentage of *LYS4* missegregation was determined by live imaging of *top2-4* cells expressing Spc42-GFP and labeled *TRP1* and *LYS4* loci. Cells were arrested in metaphase at 25 °C by depletion of Cdc20 for 3 hours, and released into anaphase at 37 °C. Separately, asynchronous cultures grown at 25 °C were shifted to 37 °C and imaging started after 15 min; segregation was scored for cells that initiated spindle elongation within 20 min of imaging start. Graphs represent mean and SD. N> 20 cells in each of the three independent experiments. Asterisks show the time of spindle breakdown. Scale bar, 1 μm. (B) A representative *top2-4* cell from an asynchronous experiment is shown. Sister *TRP1* spots segregate in early anaphase (red arrows) but *LYS4* loci do not (green arrowhead).

4.6.3 Topoisomerase II is necessary to segregate distal parts of long chromosomes

To characterize the mechanism by which long chromosome bearing cells are more sensitive to Topoisomerase II inactivation, we followed spindle elongation and chromosome segregation of *top2-4* mutants in both wild type karyotype and long chromosome constructs. Imaging of anaphase at 30 °C showed that *LYS4* loci segregated efficiently when located at 480 kb from the centromere, in both *top2-4* and *LC3.6 top2-4* mutants (Figure 4.18A). In contrast, *LYS4* and *TRP1* segregation was defective in 60% of *LC2.9 top2-4* and in 90% of *LC3.7 top2-4* cells, in which *LYS4* is placed at 1.8 and 2.6 Mb from to the centromere, respectively (Figure 4.18). In these cells, unsegregated sister loci oscillated between the spindle poles and remained together in either the mother or daughter cell after spindle breakdown. Thus, segregation of centromere-proximal regions was unaffected by inhibition of Topoisomerase II during mitosis, but that of distal regions was severely impaired. This suggests that centromere-proximal regions lack catenations at anaphase onset, and/or that centromere-proximal SCI are displaced towards distal regions during spindle elongation.

Topoisomerase II mutants increase the number of sister chromatid catenations, which at the same time would increase the tension in the chromosome fiber during anaphase. However, the time of spindle breakdown is not majorly delayed in *top2-4* mutants (Figure 4.18 C), suggesting that the *RAD9*-dependent mid-anaphase checkpoint is not active.

Together, these results indicate that defective Topoisomerase II activity compromises long chromosome-bearing cells' viability due to an impairment in chromosome segregation that affects specifically the distal regions of long
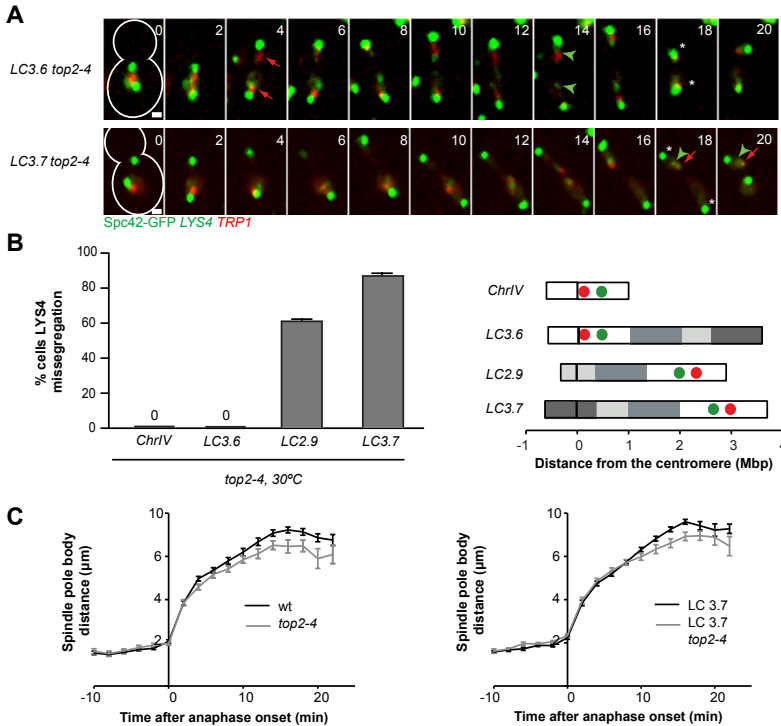
chromosomes.

Figure 4.18: Topoisomerase II is essential for long chromosome segregation. (A) Spindle elongation and chromosome segregation in representative *LC top2-4* mutants shifted from 25 to 30 °C, 15 min before imaging start. Double arrows and arrowheads show segregation of *TRP1* and *LYS4* respectively. Single arrows and arrowheads indicate missegregation. (B) Quantification of LYS4 missegregation in cells of the indicated genotype at 30 °C, treated as in A. Mean and SD are shown. N> 20 cells in each of three independent experiments. Asterisks show the time of spindle breakdown. Scale bar, 1 μm. (C) The spindle dynamics were followed using Spc42-GFP. Mean and SEM are shown for the indicated strains.

4.6.4   Topoisomerase II defects are not rescued with longer spindles

Both *top2-4* and *LC top2-4* cells sow a slight reduction in the maximum spindle length relative to wild type strains. One possibility is that this decrease affects segregation of specifically long chromosomes while not perturbing the segregation of *LYS4* locus in wild type chromosome IV. To investigate if the defect in *LC top2-4* was due to the shortening of the spindles, we created longer spindles by deleting *KIP3*.
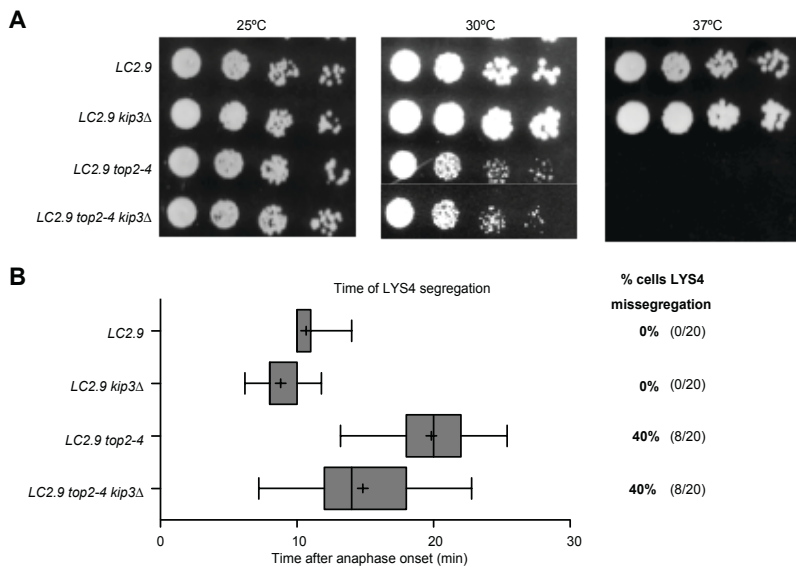
Figure 4.19: *kip3Δ* does not rescue *top2-4* segregation defects. (A) Serial dilutions of the indicated strains were grown for 2 days at the indicated temperatures. (B) Analysis of spindle breakdown and *LYS4* segregation in cells grown at 25 °C to mid log phase, shifted to 30 °C and imaged starting within 15 min. Boxes include 50% of data points and whiskers 90%. A line indicates the median and a cross the mean.

Deletion of *kip3Δ* did not improve the viability of *LC top2-4* mutants

(Figure 4.19 A). To investigate if the deletion had any effect on chromosome segregation we performed live-cell imaging of the different strains and quantified the time of *LYS4* segregation (Figure 4.19 B). Both in *LC* and *LC top2-4* cells, *kip3Δ* advanced the time of *LYS4* segregation. However, the increase in microtubule length could not rescue the percentage of cells that missegregated *LYS4* in *LC top2-4*. Therefore, the defects in segregation observed in *LC top2-4* mutants are not due to the shortening of the spindles but to incomplete sister chromatid resolution.

4.6.5 Long chromosomes accumulate higher levels of SCI markers

In order to investigate if long chromosomes accumulate more sister chromatid intertwinings, we determined the chromosome-binding pattern of the condensin- and cohesin-related Smc5/6 complex. Multiple aspects of Smc5/6 association with chromosome arms, such as its increase upon chromosome lengthening and after inactivation of Topoisomerase II, suggests that its enrichment reports on topological stress (Kegel et al., 2011), and that Smc5/6 binding sites mark SCI.

We assessed the number of peaks of Smc6-FLAG in *WT* and *LC2.9*. Wild type and *LC2.9* were shifted to 33 °C for 2.5 h in the presence of nocodazole to arrest the cells in metaphase. Chromatin immunoprecipitation followed by DNA sequencing (ChIP-seq) was then used to determine the chromosomal association of epitope-tagged Smc6. As reported previously (Kegel et al., 2011; Lindroos et al., 2006), Smc6-FLAG was enriched in intergenic regions (Table 4.4); furthermore, its frequency of association was higher in longer chromosomes. The number of peaks per chromosome was

Strain	No of reads (M)	No of mapped reads (M)	% mapped reads	Genome coverage	Peak bases mapped to intergenic regions (%)	Peak bases expected to map to intergenic regions if random(%)
No tag	14.27	12.17	85	46.05	NA	NA
Smc6-FLAG	12.81	11.65	91	44.07	74.78	29.67±0.98
LC2.9 no tag	19.48	17.52	89.91	66.28	NA	NA
LC2.9 Smc6-FLAG	16.52	15.17	91.57	57.38	69.5	25.7±3.5

Table 4.3: Statistics for ChIP-sequencing experiment in LC strains. To simulate the fraction of peak bases expected to map to intergenic regions, the shuffle tool from Bedtools was used, keeping the number of peaks per chromosome and the length of the peaks. Simulations were done in triplicate, data shown are mean and SEM.

similar between *WT* and *LC2.9* with the notable exception of three chromosomes that are enriched in peaks in the *LC2.9* strain that correspond to chromosomes V, XV and IV. Importantly, those are the chromosomes fused in the *LC2.9* construct. Thus, long chromosome strains specifically increase the presence of Smc5/6 complex in the fused chromosomes.
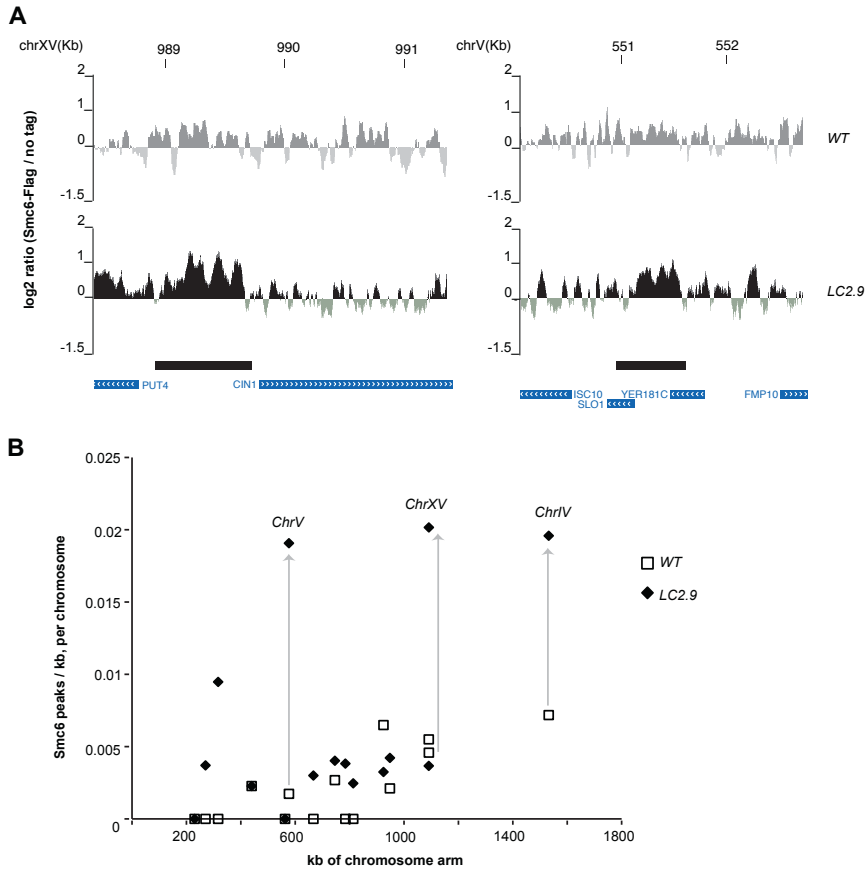
Figure 4.20: Topological stress increases in fused chromosomes. (A) Chromosomal association of Smc6-FLAG in cells of the indicated genotype, shifted from 25 °C to 33 °C for 2.5 h in the presence of nocodazole. The y axis shows the log2 of the number of mapped reads in Smc6-FLAG samples relative to untagged Smc6; the x axis shows chromosomal coordinates in kilobases. Solid bars highlight Smc6 peaks identified with MACS (see Chapter 3.6). ORFs are shown at the bottom of each graph. (B) Correlation between Smc6 binding sites per kb per chromosome and chromosome length in the indicated strains. Chromosome XII, containing the variable length rDNA locus, was excluded from this analysis.
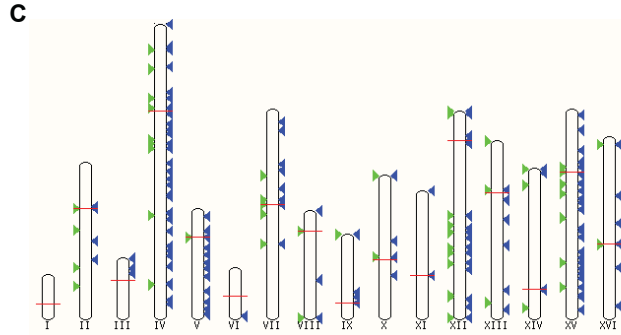
Figure 4.21: Topological stress increases in fused chromosomes. Schemes show the position of Smc6-FLAG peaks identified in: *WT* in green arrowheads, *LC2.9* in blue arrowheads, the centromeres are represented as red lines. The graphs are generated with ENSEMBL (www.ensembl.org)

4.7   Topological stress is relieved by detaching the chromosomes from the nuclear envelope

Replication-induced topological stress, such as supercoiling or SCI accumulation, could be removed by swiveling off the extremities of linear chromosomes. During interphase, telomere anchoring to the nuclear envelope (NE) (Taddei et al., 2010) might prevent passive removal of topological stress. We reasoned that increasing the rotational freedom of chromosomes through detachment from the NE during replication could partially alleviate defects caused by Topoisomerase II inactivation. Likewise, if *LC stu2* defects are caused by unresolved catenations, the same treatment should also ameliorate the segregation defects of these cells.

Two partially redundant pathways have been identified that mediate tethering of telomeres to the nuclear envelope. The first depends on the yeast Ku (Yku70/80) protein complex and the second on the Sir4 and Esc1

proteins (Hediger et al., 2002; Taddei et al., 2004).

4.7.1   *ESC1* and *YKU70* attach chromosome IV to the nuclear envelope

We first examined whether deletion of *YKU70* or *ESC1* alters the subnuclear localization of the right arm of chromosome IV, by determining the distance between GFP-labeled *LYS4* and the nuclear periphery, marked with Nup49-mCherry, as previously reported (Hediger et al., 2002). Due to the folding of chromosome IV, *LYS4* is found in close physical proximity ($<0.1\mu$m) of *TEL4R* in interphase and mitosis, although it is separated from the telomere by >500 kb (Vas et al., 2007). Cells in S/G2 phases were identified by their spherical nuclear shape, and duplicated SPBs separated by $<1.5\mu$m. Spc42-GFP particles were readily distinguished from GFP-labeled *LYS4* loci thanks to the increased fluorescent intensity of the SPB signal (Figure 4.22 A). Consistent with its telomere proximity, *LYS4* was tightly associated with the nuclear periphery in wild type cells, but was displaced away from the nuclear envelope (NE) in *yku70*Δ and *esc1*Δ mutants (Figure 4.22 A). This indicates that *ESC1* and *YKU70* are important for the association with the nuclear periphery of a large chromosome IV region.

To investigate whether nuclear envelope detachment affects anaphase progression, the time of *LYS4* segregation and spindle breakdown was quantified by live-cell imaging in *esc1*Δ and *yku70*Δ strains grown in exponential cultures at 30 °C. Interestingly, *yku70* slightly advances the time of spindle breakdown. However, the time of *LYS4* locus segregation is not affected in these strains (Figure 4.22 B).

Therefore, *esc1*Δ and *yku70*Δ cells detach the telomeres from the nuclear

envelope and change the localization of the *LYS4* locus within the nucleus.
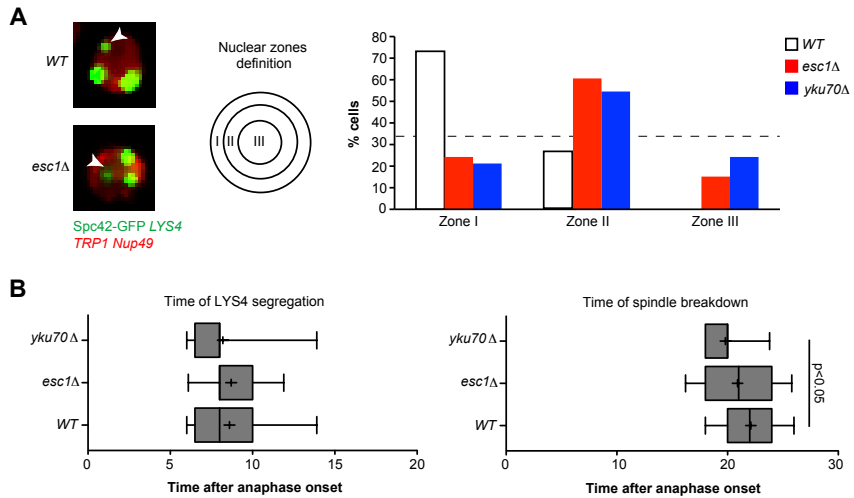
Figure 4.22: ***esc1Δ* and *yku70Δ* detach chromosome IV from the nuclear envelope.** (A) The localization of GFP-labeled *LYS4* relative to the nuclear periphery (Nup49-mCherry) was determined in S/G2 cells at 30 °C. To quantify *LYS4* nuclear localization (marked with green arrowheads) its position in confocal optical slices was mapped to one of three concentric nuclear zones of equal surface. Maximal projections of confocal images are shown. Ten different cells / strain were imaged during 6-8 min every 2 min. Scale bar, 1 μm. (B) Analysis *LYS4* segregation and spindle breakdown in cells grown at 30 °C and imaged. Boxes include 50% of data points and whiskers 90%. A line indicates the median and a cross the mean.

4.7.2   *esc1Δ* and *yku70Δ* alleviate topological stress

To address whether *esc1Δ* or *yku70Δ* alleviates replication-induced topological stress in mitotic chromosomes, we determined the chromosome-binding pattern of the Smc5/6 complex.

We assessed whether the increase in Smc5/6 binding in *top2-4* mutants

Strain	No of reads (M)	No of mapped reads (M)	% mapped reads	Genome coverage	Peak bases mapped to intergenic regions (%)	Peak bases expected to map to intergenic regions if random(%)
No tag	14.27	12.17	85	46.05	NA	NA
top2-4 Smc6-FLAG	15.24	12.99	85	49.17	50.36	26.76±1.09
top2-4 *esc1*Δ Smc6-FLAG	15.31	13.39	87	50.66	61.70	27.82±1.28
top2-4 *yku70*Δ Smc6-FLAG	15.96	12.41	78	46.97	61.01	26.56±6.03
Smc6-FLAG	12.81	11.65	91	44.07	74.78	29.67±0.98

Table 4.4: Statistics for ChIP-sequencing experiments. To simulate the fraction of peak bases expected to map to intergenic regions, the shuffle tool from Bedtools was used, keeping the number of peaks per chromosome and the length of the peaks. Simulations were done in triplicate, data shown are mean and SEM.
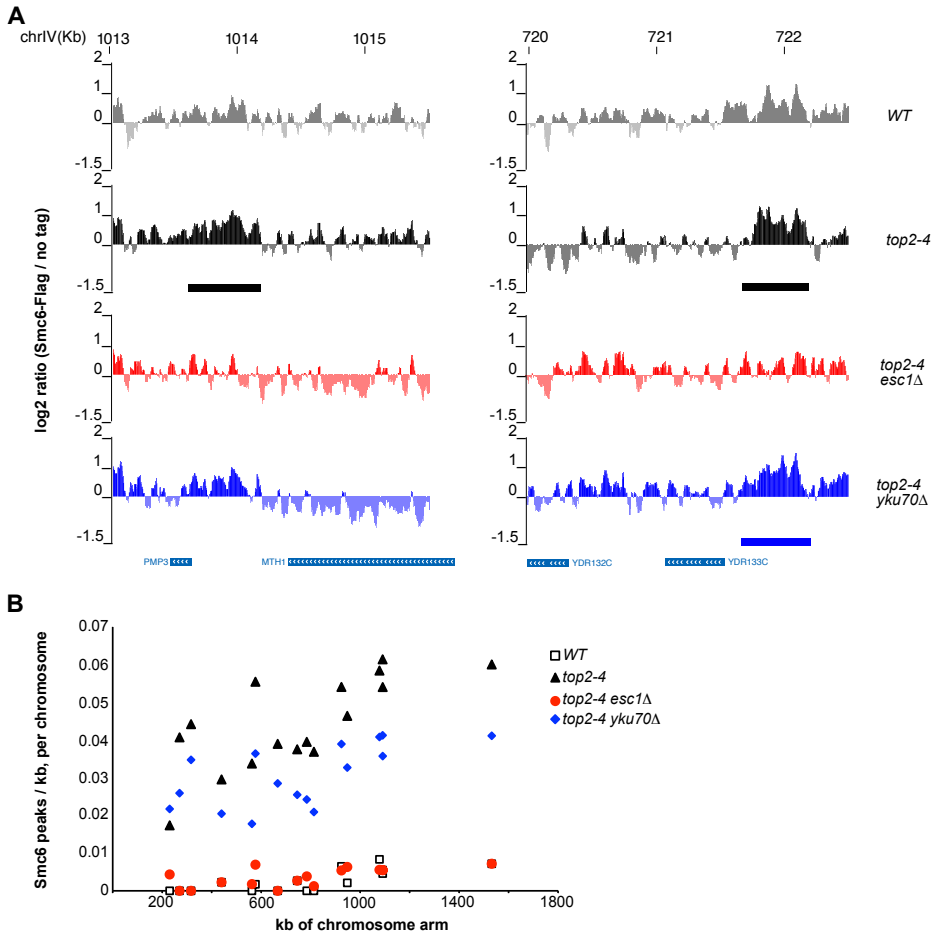
Figure 4.23: Detachment of the chromosomes from the nuclear envelope releases topological stress. (A) Chromosomal association of Smc6- FLAG in cells of the indicated genotype, shifted from 25 to 33 °C for 2.5 h in nocodazole. The y axis shows the log2 of the number of mapped reads in Smc6- FLAG samples relative to untagged Smc6; the x axis shows chromosomal coordinates. Solid bars highlight Smc6 peaks identified with MACS (Chapter 3.6). ORFs are shown at the bottom of each graph. (B) Correlation between Smc6 binding sites per kb per chromosome and chromosome length. Chromosome XII was excluded.
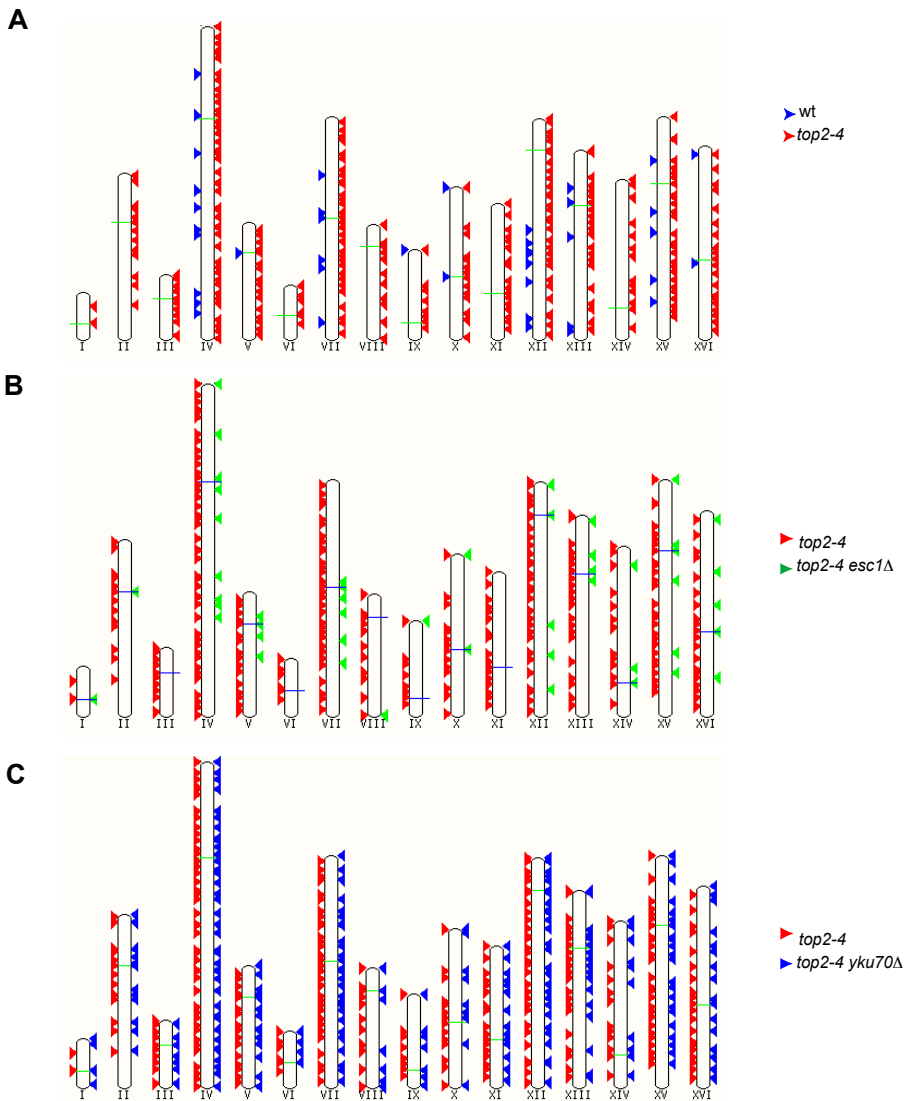
Figure 4.24: Smc6 binding to chromosomes. Schemes show the position of Smc6-FLAG peaks identified in the indicated strains. The graphs are generated with ENSEMBL.

could be reduced by detachment of chromosomes from the nuclear envelope. Wild type, *top2-4* single mutants, and *top2-4 yku70Δ* and *top2-4 esc1Δ*

double mutants were shifted to 33 °C for 2.5 h in the presence of nocoda-
zole, to reduce topoisomerase II activity and arrest cells in metaphase. We
assessed whether the increase in Smc5/6 binding in *top2-4* mutants could
be reduced by detachment of chromosomes from the nuclear envelope. Wild
type, *top2-4* single mutants, and *top2-4 yku70Δ* and *top2-4 esc1Δ* double
mutants were shifted to 33 °C for 2.5 h in the presence of nocodazole, to
reduce topoisomerase II activity and arrest cells in metaphase.

As reported previously (Kegel et al., 2011; Lindroos et al., 2006), Smc6-
FLAG was enriched *top2-4* mutants (Figure 4.23 and 4.24). Importantly,
the chromosome enrichment of Smc6 was reduced in *top2-4 esc1Δ* and *top2-
4 yku70Δ*, with deletion of *ESC1* displaying a stronger effect than that of
YKU70 (Figure 4.23 and 4.24). This suggests that anchoring of telomeres
to the nuclear periphery contributes to SCI accumulation in *top2* mutants.

4.8   Reduction of topological stress rescues *top2-4* and *LC stu2-13* chromosome missegregation

Deletion of *ESC1* and *YKU70* decreases the number of Smc6 binding sites
in chromosomes in *top2-4* mutants suggesting that the topological stress is
alleviated upon detachment of telomeres from the nuclear envelope. If this is
the case, *esc1Δ* and *yku70Δ* should restore the segregation of chromosomes
in *top2-4* mutants to some extent.

Figure 4.25: Detachment of the chromosomes from the nuclear envelope rescues segregation in *top2-4* mutants. (A) Anaphase progression in a representative *LC top2-4 esc1Δ* cell treated as in Figure 4.18. Quantification of *LYS4* segregation is shown for wild type chromosome IV at 33 °C and for *LC2.9* at 28 °C. N>20 cells in three independent experiments. Mean and SD are shown. Asterisks indicate P<0.01 relative to *top2-4* (left) or *LC2.9 top2-4* (right). (B) Cultures were grown to mid-log phase in YPD, and serial dilutions plated at the indicated temperature were incubated for 2 (25 °C) and 6 days (30 and 32 °C).

4.8.1 Telomere detachment rescues missegregation defects in *top2-4 mutants*

We then tested whether reduction of topological stress in *esc1Δ* and *yku70Δ* mutants alleviates the chromosome segregation defects caused by Topoisomerase II impairment during mitosis. Cells expressing fluorescently labeled SPBs and chromosome tags were imaged after reduction of Topoisomerase II function by shifting asynchronously growing cultures to semi-restrictive

temperature. Almost 40% of *top2-4* mutants failed to segregate the *LYS4* locus on wild type chromosome IV after shift to 33 °C (Figure 4.25 A). In contrast, the percentage of *LYS4* segregation defects in *top2-4 esc1Δ* and *top2-4 yku70Δ* under the same conditions was of 7% and 12%, respectively (Figure 4.25 A). Deletion of *ESC1* and *YKU70* also reduced the segregation defects of loci at farther distance from the centromere, in *LC2.9 top2-4* cells shifted to 28 °C (*LC2.9 top2-4 esc1Δ* cell in Figure 4.25 A, top; and quantification, bottom right). Moreover, *esc1Δ* and *yku70Δ* mutations improved the viability of *top2-4* and *LC top2-4* mutants at semi-restrictive temperatures (Figure 4.25 B). We conclude that detachment of telomeres from the nuclear periphery reduces the catenations between replicated chromosomes and thus facilitates their segregation when Topoisomerase II function is compromised.

4.8.2   Telomere detachment rescues missegregation defects in LC stu2-13 mutants

To assess if chromosome-length dependent segregation defects of *stu2-13* mutants are due to unresolved topological stress during anaphase, we tested the effect of deleting *ESC1* or *YKU70* in *LC stu2-13* mutant cells. *LC2.9 stu2-13 esc1Δ* and *LC2.9 stu2-13 yku70Δ* cells shifted to 30 °C showed a significant reduction in both the anaphase delay and the efficiency of *LYS4* segregation (see example of *LC2.9 stu2-13 esc1Δ* cell in Figure 4.26 A, top; and quantifications in Figure 4.26, bottom). In particular, deletion of *ESC1* and *YKU70* in *LC stu2-13* not only reduced the duration of the mid-anaphase pause but also improved chromosome segregation efficiency, reduced the frequency of *LYS4* missegregation events from more than 50%

in *LC stu2-13* cells to 12% in both *LC2.9 stu2-13 esc1Δ* and *LC2.9 stu2-13 yku70Δ* (Figure 4.26 A).

In the case of *LC stu2-13* cells, unlike *top2-4* and *LC top2-4*, the rescue in segregation was not accompanied by an improvement in the viability of the mutants at semi-permissive temperature (Figure 4.26 B).
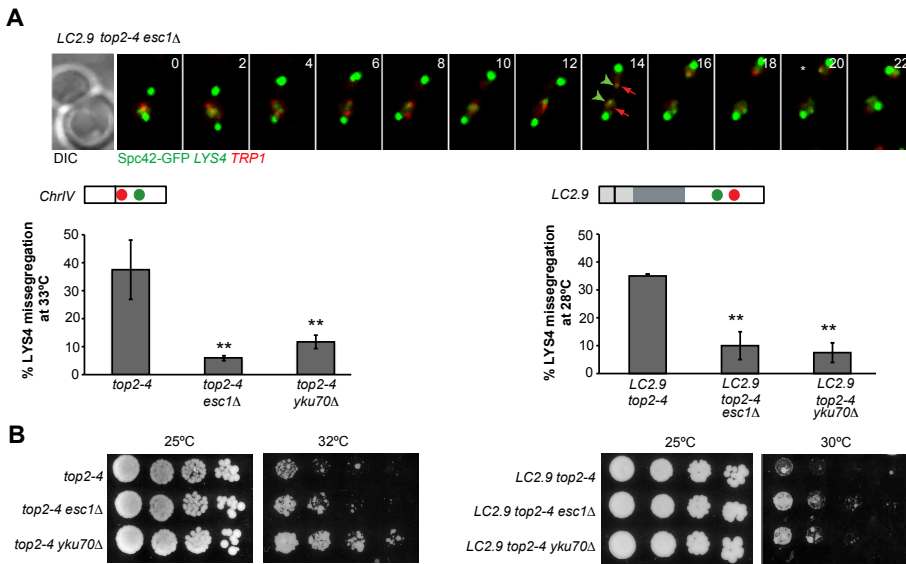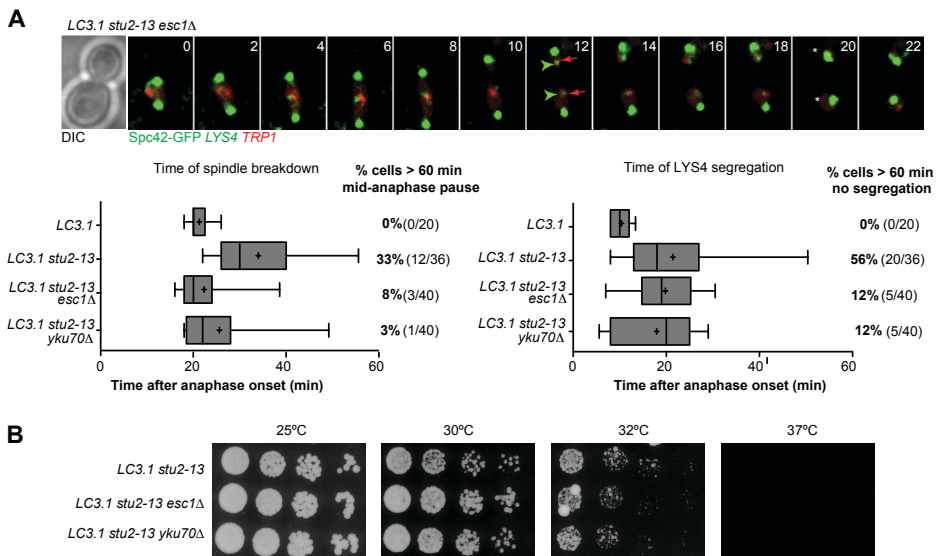

Figure 4.26: Detachment of the chromosomes from the nuclear envelope rescues segregation in *LC stu2-13* mutants. (A) Anaphase progression in a representative *LC stu2-13 esc1Δ* cell. Cells were shifted from 25 to 30 °C as in Figure 4.13. (B) Cultures were grown to mid-log phase in YPD, and serial dilutions plated at the indicated temperature were incubated for 2 (25 °C) and 6 days (30 and 32 °C).

Together, these results show that detaching chromosomes from the nuclear envelope alleviates the topological stress of Topoisomerase II mutants, and reduces the chromosome segregation defects due to Topoisomerase II or Stu2 malfunction. We conclude that *stu2-13* cells are defective in re-

solving SCI from LC, suggesting that microtubule dynamics contribute to *TOP2*-dependent decatenation during anaphase.

5

Discussion

In this study, we have created an allelic series of long chromosomes. We have used the fused chromosomes to sensitize cells and gain a better understanding of how wild type chromosomes are segregated during anaphase. With this tool we were able to:

1. Show that the adaptive hyper-condensation mechanism can occur in all long chromosomes, independently of the presence of the rDNA.

2. Determine that longer chromosomes accumulate more topological stress that needs to be resolved specifically during anaphase by Topoisomerase II and dynamic microtubules.

3. Identify the nuclear envelope attachment of chromosomes as a source of topological stress.

5.1   Long chromosomes hypercondense during ana-phase

We have created a series of long chromosomes by fusing different chromo-somes in yeast haploid cells. The length of the longest chromosome arm has been increased almost 70% by fusing up to four chromosomes (Table 4.1). It is quite remarkable that despite the increase in chromosome length, cells carrying LC do not present any growth defect in rich media (Figure 4.3). This shows that there are mechanisms to adapt to changes in chromosome length.

An increase in chromosome length could be compensated by (1) an ex-tension of the spindle during anaphase (2) a prolongation of anaphase du-ration or (3) an increase in the compaction of chromatin. Our observations show that (1) and (2) do not occur, instead, cells adapt to an increase in chromosome arm length solely by scaling condensation to spindle length (Neurohr et al., 2011). Anaphase hypercondensation occurs in artificially lengthened chromosomes that contain the rDNA (Neurohr et al., 2011) and also in chromosomes devoid of this repetitive region (Figure 4.6). There-fore, hyper-condensation is a general mechanism by which chromosomes are scaled to the length of spindle during anaphase.

It is important to notice that changes in chromosome size are also found in nature. One example is the number of repeats of ribosomal DNA that is constantly changing therefore affecting the total length of chromosome XII. Moreover, translocations and genome rearrangements occur during evolution and speciation (Coghlan et al., 2005) and pathogenic processes like cancer can alter chromosome arm length (Rajagopalan and Lengauer, 2004). Ana-

phase hyper-condensation, if conserved, would favor the viability of cells experiencing these events.

5.2   Factors that determine the upper limit of chromosome size

The approach of this study was to create longer chromosomes. The long chromosomes constructed so far do not cause a viability defect (Results 4.3). Then, is there an upper limit of chromosome size? In order to achieve proper chromosome segregation and organism viability, the longest chromosome arm should not exceed half of the average of the spindle axis at the end of anaphase. Thus, by hyper-condensing long chromosomes, the Aurora B-dependent mechanism increases the limit of maximum chromosome length that can be tolerated by a cell. However, this hyper-condensation might have a physical limit as the DNA is already heavily packed. Moreover, we know now that there are other factors apart from compaction that could determine the upper limit of chromosome size. Longer chromosomes accumulate topological stress that has to be resolved during anaphase with the participation of dynamic microtubules. Therefore, the catenations accumulated could also limit the maximum chromosome length tolerated by an organism.

Despite the variation in chromosome size within a species, mathematic models based on the study of sequenced genomes suggest that there is an upper limit to chromosome size variation in diploid eukaryotes with linear chromosomes (Li et al., 2011). This study predicts that the majority of chromosomes within species are expected to have a base pair length between 0.4 and 1.86 times the average chromosome length.

Experimental data also show that there is an upper boundary of chromosome size for normal development of an organism (Schubert and Oud, 1997). This study determines that organisms, specifically *Vicia faba* plants, exceeding 1.3 times the size in μm of the longest wild type chromosome arm in metaphase present viability defects.

In this study we have used a method to artificially increase chromosome length. Yeast cells bearing these chromosomes are as viable as wild type cells, therefore, we have not reached the upper limit of chromosome size tolerated by budding yeast. However, we know that this increase in chromosome arm length is sufficient to sensitize yeast cells and trigger mechanisms that will ensure cell survival in the presence of this long chromosome construct.

5.2.1   Long chromosomes as a tool to identify genes involved in segregation

We reasoned that cells bearing long chromosomes must be sensitized to the loss of genes important for chromosome segregation. LC bearing cells decrease their viability upon condensin and Polo kinase partial inactivation when compared to wild type karyotype cells carrying the same mutations (Figure 4.11). Thus, proper regulation of the condensation process is crucial in long chromosomes. That is the reason why we started looking for genetic interactions in long chromosome bearing cells (Appendix B.1).

We have identified that long chromosome bearing cells present viability defects upon loss of function of different genes mainly involved in microtubule polymerization (*STU2* and *KIP3*), topological stress (*TOP2* and *PIF1*) and mitotic progression (*YCG1, SMC2* and *CDC5*).

Therefore, long chromosome cells can be used as a tool to identify new processes involved in chromosome segregation and to gain a better understanding of the mechanism by which genes that were already characterized mediate chromosome segregation. It would be interesting to carry out an unbiased screen using long chromosomes in order to discover new genes and pathways involved in chromosome segregation.

5.2.2 Microtubule dynamics are essential for long chromosome segregation

There is a tight regulation between spindle length and the level of chromatin compaction (Neurohr et al., 2011). That is the reason why we investigated how mutations of genes that participate in spindle conformation and dynamics affected the viability of cells bearing long chromosomes. Surprisingly, not all the mutations that decreased spindle length impaired the viability of LC cells. Interestingly, we have found genetic interactions between long chromosomes and partial inactivation of *STU2* and overexpression of *KIP3* (Figure 4.13).

The mitotic spindle is an essential structure for chromosome segregation, and many genes that participate in the regulation of microtubules are redundant, like *CIN8* and *KIP1* (Hildebrandt and Hoyt, 2000). Therefore, one of the reasons why we have not found more genetic interactions with spindle components could be the redundancy between them. Double inactivation of redundant spindle components in long chromosome bearing cells would be enlightening.

There are some differences between *STU2* and *KIP3* and the rest of the spindle components tested. First of all, *STU2* or *KIP3* alter both the spindle

length and the microtubule dynamics. Because other deletions tested decrease the length of the spindle but do not decrease the viability of long chromosome bearing cells, the reason for the genetic interaction could possibly be the alteration in microtubule dynamics. Stu2 microtubule polymerizing activity is opposed by the Kip3 depolymerase factor (Severin et al., 2001). We deleted *kip3* in *LC stu2-13* cells to partially restore microtubule dynamics. If the anaphase defects observed in *LC stu2-13* mutants are indeed a consequence of altered microtubule dynamics, they should be recovered by restoring the dinamicity of microtubules. Accordingly, the anaphase phenotype of *LC stu2-13* cells is alleviated when *kip3* is deleted (Figure 4.15).

The second difference is that, unlike the rest of spindle components tested so far which regulate interpolar microtubules, *STU2* and *KIP3* regulate the three types of microtubules within the spindle: astral, kinetochore and interpolar microtubules. Our preliminary data suggest that kinetochore microtubule dynamics are strongly affected in *stu2* mutants during anaphase (data not shown). Thus, the anaphase defects that we observe in *LC stu2* mutants could be due to the affectation of microtubules other than the interpolar ones.

We know that chromosome condensation scales to the length of the spindle during anaphase. Then, why should *stu2* spindles, only 10% shorter than wild type, affect LC cells viability? With the data we have so far, we hypothesize that the correct dynamicity of kinetochore microtubules and not the final spindle length might be crucial in the resolution of linkages between sister chromatids during anaphase. We can imagine a model where the alternation of pulling force and releasing in the centromere, instead of a constant pulling force, would facilitate the disentanglement of chromosomes in anaphase. Further experiments are needed to prove this hypothesis.

5.2.3   The mid-anaphase checkpoint

When analyzing the phenotype of *LC stu2-13* cells we found that they have defects during anaphase. Those cells present a spindle breakdown delay because most of them arrest with a half-elongated spindle for more than 30 min (Figure 4.14). This phenotype was reminiscent of the *RAD9*-dependent mid-anaphase pause observed in dicentric chromosomes (Yang et al., 1997). That is the reason why we investigated if *LC stu2-13* cells were activating the same checkpoint.

A short mid-anaphase pause is often observed in wild type yeast spindles. However, some DNA lesions can lead to delays in mid-anaphase, like dicentric chromosomes (Yang et al., 1997) and long chromosome bearing cells with defective *stu2* function (Figure 4.14). One possibility is that the tension generated by chromosome bridges in these two cases, mechanically restrains the spindle. However, the response would not be proportional to the tension because dicentric chromosomes of different length, stall the spindles at 4 μm (Yang et al., 1997). Alternatively, a surveillance mechanism could feedback between DNA lesions occurring in both dicentrics and *LC stu2-13* microtubule assembly and motility.

Cells can delay the onset of S phase or mitosis after exposure to agents that damage the DNA. These lesions are recognized by proteins involved in DNA processing (like *RAD9*) or signaling. In a similar way, *RAD9* cells fail to restrain spindle elongation when a dicentric chromosome is present. The mid-anaphase checkpoint could represent the last stage for DNA repair between sister chromatids as the chromosome arms may not be completely disjoined at that stage. It has been proposed that this checkpoint could monitor the final decatenation between sister chromatids and the irreversible

commitment to chromosome separation (Yang et al., 1997). Because LC and dicentrics show a *RAD9* dependent mid-anaphase pause, this suggests that some common DNA insult is present in both situations that is triggering the checkpoint.

Then, if the checkpoint is activated by non-resolved sister chromatids, why are Topoisomerase II mutant cells not triggering the mid-anaphase checkpoint? This could be explained by (1) as the trigger of the checkpoint remains unknown, the tension or structure created in *top2* mutants might be different from the defect present in dicentrics and LC stu2-13 and not able to activate the checkpoint, (2) Topoisomerase II is part of the checkpoint. In higher eukaryotes it has been suggested that the decatenation checkpoint, that occurs during G2, ensures that all catenations between sister chromatids are resolved before entering mitosis and depends on the interaction between MDC1 and a phosphorylated residue of Topoisomerase II (Luo et al., 2009). This results suggest that the decatenation checkpoint in higher eukaryotes could be regulated by Topoisomerase II. Although in a different moment of the cell cycle, it would be interesting to investigate if *LC stu2-13* cells can trigger the mid-anaphase checkpoint in the absence of Topoisomerase II activity.

5.2.4 Topoisomerase II is needed during anaphase for proper chromosome segregation

Looking for genetic interactions in LC cells, we also found that cells bearing the long chromosome constructs are sensitive to Topoisomerase II partial loss of function 4.18. Prior to chromosome condensation and recoiling during anaphase, removal of the linkages between sister chromatids is essential

to ensure proper chromosome segregation. Anaphase linkages include cohesin remnants and sister chromatid intertwinings (SCI) that arise during replication due to the double helix nature of the DNA.

SCI are resolved by Topoisomerase II, the only enzyme that can introduce breaks in dsDNA to pass one double helix through another and is essential for chromosome segregation and the viability of organisms (DiNardo et al., 1984; Holm et al., 1985). However, it remained unclear when SCI are resolved during the cell cycle. In circular centromeric plasmids and minichromosomes, SCI are resolved prior to anaphase (Baxter et al., 2011; Koshland and Hartwell, 1987). However, it has been shown that SCI persist for some time during anaphase in the rDNA locus (D'Ambrosio et al., 2008; Nakazawa et al., 2011) and in linear minichromosomes (Farcas et al., 2011).

The time of resolution of catenations in endogenous linear chromosomes remained elusive largely because of the impossibility to retain topological information in linear chromosomes. That is the reason why all the topological studies have focused on plasmids, that migrate differently in a gel depending on the number of catenations accumulated. We provide live-cell imaging data demonstrating that Topoisomerase II is needed during anaphase to resolve endogenous chromosomes (Figure 4.17).

We have shown that Topoisomerase II activity is essential during anaphase in 50% of the cells in order to segregate chromosome IV (Figure 4.6.2). This could be due to the fact that Topoisomerase II does not have enough time between replication and segregation to solve all the catenations. However, we find this unlikely as we have shown that a similar percentage of cells arrested in metaphase with fully active Topoisomerase II for 3 h, still need the enzyme activity during anaphase to ensure proper chromosome segregation.

Interestingly, our results show that Topoisomerase II is needed to segregate long chromosomes during anaphase and specifically to resolve centromere-distal regions (Figure 4.18). Two different models could explain the fact that only centromere distal regions of long chromosomes are affected upon Top2 partial inactivation (1) either catenations only accumulate in chromosome distal regions or (2) catenations arise in the whole genome but are translocated to the ends of chromosomes during mitosis.

Sister chromatid intertwinings arise during replication due to the unwinding of the DNA double helix and the replication fork progression. Replication starts in the Autonomous Replication Sequences (ARS) that are spread in the chromosomes. Therefore, replication-associated topological stress accumulates in the whole genome. Moreover, in metaphase arrested cells, it has been shown that Smc5/6 localizes along the chromosomes and that it serves as a readout for topological stress (Lindroos et al., 2006; Kegel et al., 2011) (Figures 4.20 and 4.23).

Therefore, it is unlikely that catenations are only created in centromere-distal regions. We favor a model where catenations are created along the whole chromosome and, upon anaphase onset and due to cohesin cleavage and spindle forces, slide along chromosomes and accumulate towards the ends. This model could be confirmed by performing ChIP-seq analysis of the Smc5/6 complex during mid/late anaphase. If what we propose is true, wild type cells should accumulate Smc6-flag peaks at the ends of long chromosomes during anaphase.

5.2.5   Cohesin and SCI resolution

Apart from SCI, the cohesin complex keeps sister chromatids together after replication. The major part of cohesin is cleaved at the metaphase-to-anaphase transition by separase (Uhlmann, 2003). It has been observed that some cohesin remains until anaphase in yeast chromosomes (Renshaw et al., 2010). However, cohesin cleavage occurs independently of the cohesin complex position within the chromosome (Yaakov et al., 2012). In light of these results it is unlikely that cohesin accounts for unresolved linkages specifically in long chromosomes, since its cleavage by separase occurs simultaneously along chromosome arms

Recent experiments done in linear minichromosomes suggest that cohesin is required to maintain SCI but not to form them (Farcas et al., 2011). It remains unkown if in endogenous linear chromosomes SCI are also maintained by the cohesin complex. Therefore, we can not discard that cohesin might contribute to the accumulation of topological stress in long chromosomes prior to anaphase.

Therefore, the increase in SCI observed in long chromosomes should be abolished by impairing cohesin function. As was already mentioned, linear chromosomes do not maintain topological information once they are purified. Therefore, Smc5/6 presence could be used to monitor the presence of SCI in long chromosomes with impaired cohesin function. Cohesin should be inactivated during mitosis because physical proximity of chromosomes, and therefore the action of the cohesin complex, is needed to load the Smc5/6 complex into chromosomes (Lindroos et al., 2006).

5.3   Factors that determine topological stress

We have found that both chromosome length (Figure 4.16) and nuclear organization (Figure 4.23) influence the topological stress accumulated in chromosomes that has to be resolved during anaphase. Long chromosome bearing cells are more susceptible to partial loss of Topoisomerase II function. Moreover, the percentage of missegregation increases as the locus becomes more distal to the centromere. Therefore, long chromosomes accumulate more topological stress and it affects specifically the segregation of centromere-distal regions in anaphase. Then, it is conceivable that the upper limit in chromosome length could be influenced, at least in part, by the number of catenations that can be resolved during anaphase.

The finding that chromatin enrichment of Smc6 in *top2-4* mutants is largely dependent on *ESC1* and to a lesser extent on *YKU70* shows that nuclear organization influences topological stress on linear chromosomes (Figure 4.23). Deletion of *ESC1* or *YKU70* in *top2-4* and *LC stu2-13* mutants restores chromosome segregation to a similar extend. However, *top2-4 esc1Δ* show a stronger decrease of Smc6 binding, almost to wild type levels, than *top2-4 yku70Δ*. This might be related to specific functions of each of these factors, for instance in gene expression and DNA repair (Taddei et al., 2004; Therizols et al., 2006).

Esc1 is required for the assembly of the nuclear basket and for normal localization of the Ulp1 SUMO protease in the nuclear pore complex (Lewis et al., 2007). The Smc5/6 complex is also part of the SUMO pathway. The non-SMC subunit of the complex, Nse2 shows SUMO-ligase activity both in vitro and in vivo (Andrews et al., 2005; Potts and Yu, 2005; Zhao and Blobel, 2005). The Smc5/6 components are majorly found in complex,

suggesting that the enzymatic activity of Nse2 is directed to the complex itself (Taylor et al., 2008). It has been shown that the homolog of Nse2 in humans, hMMS21, sumoylates hSMC6 among other substrates (Potts and Yu, 2005). Therefore, the alteration in Ulp1 localization in *esc1Δ* mutants perturbs the SUMO pathway homeosthasis and could affect the binding of the Smc5/6 complex to chromosomes. That could explain why *top2-4 esc1Δ* mutants show a stronger decrease in Smc6 in the chromosomes than *top2-4 yku70Δ*

These other functions of *ESC1* and *YKU70* could affect DNA topology in non-overlapping ways. Nevertheless, both are involved in telomere anchoring to the nuclear envelope. To ensure that the function of telomere-nuclear envelope attachment of these proteins is the one that rescues both *top2-4* and *LC stu2* phenotype, it could be interesting to re-attach the chromosomes to the nuclear rim in *top2-4 esc1Δ* and *top2-4 yku70 Δ* mutants and assess if this restores missegregation defects and Smc5/6 binding to levels observed in *top2-4* single mutants.

The interactions between proteins form the telomeres and the nuclear envelope ensure that telomeres are more often found in the nuclear rim than in the center of the nucleoplasm. However, anchoring of the telomeres to the nuclear envelope is not an all-or-nothing state. Thus, chromosomes always have certain degree of freedom within the nucleus. By deleting *ESC1* and *YKU70* we might be increasing this rotation freedom of the DNA.

During mitosis, telomeres are detached from the nuclear envelope in order to ensure proper chromosomes segregation (Fujita et al., 2012). Then, why don't chromosomes get rid off all the catenations during mitosis? One possibility is that there is not enough time for the catenations to swivel off. Alternatively, the packed structure of mitotic chromosomes prevents

the freely rotation of the DNA. During replication the DNA is not heavily loaded with complexes promoting their compaction and the advancement of the replication forks increases the topological stress. At that moment, detachment of telomeres from the nuclear envelope could play a pivotal role in assisting DNA rotation and alleviating the topological stress accumulated in the chromosomes.

Therefore, nuclear organization and more specifically telomere attachment to the nuclear rim, are a source of replication-dependent topological stress in linear chromosomes. Telomere detachment could facilitate the rotation of the chromosomes in a way that would reduce the topological stress (as DNA supercoilings) accumulated during replication. Then, this would cause a reduction in the number of catenations to be solved during anaphase (Figure 4.25). Although telomere detachment diminishes the level of SCI in linear chromosomes, it is important to notice that topological stress is not abolished upon *esc1* or *yku70* deletion.

5.4   Model for chromosome resolution during anaphase

We have shown that proper regulation of microtubule polymerization is critical for anaphase progression and chromosome segregation in LC cells. Reduction of topological stress by deletion of *ESC1* or *YKU70* alleviates the anaphase defects of *LC stu2-13* cells suggesting that linkages between sister chromatids are unresolved in these cells (Figure 4.26). Therefore, Stu2-dependent microtubule dynamics might promote the resolution of SCI. This resolution could be achieved by the processing of the SCI by Stu2 to a state than can be later resolved by topoisomerase II enzymatic activity. As men-

tioned earlier (Discussion 5.2.2). Then, impairment of Stu2 function could lead to the formation of aberrant chromatin structures able to trigger the mid-anaphase arrest.

Like proper microtubule dynamics, Topoisomerase II enzyme is also required during anaphase. Cells arrested in metaphase for a long time with intact Top2 activity, still need Topoisomerase II in anaphase to properly decatenate the distal parts of long chromosomes. Why is Topoisomerase II still required for chromosome segregation in anaphase? Topoisomerase II can introduce SCI as well as remove them, the enzymatic activity lacks directionality. However, it is able to fully decatenate centromeric plasmids in metaphase provided that they attach to the spindle, which favors decatenation inducing changes in DNA topology (Baxter et al., 2011). Therefore, it is possible that during metaphase centromere proximal regions are affected by microtubule-dependent topological changes that will not affect chromosomal distal regions until anaphase. This could be due to the action of the cohesin complex, that by keeping the sister chromatids together would prevent the spreading of microtubule exerted forces from the centromere. Consistent with this idea, cohesin inactivation facilitates removal of SCI from linear chromosomes (Farcas et al., 2011) and of Smc5/6 from endogenous chromosomes (Kegel et al., 2011). Then, lack of directionality of topoisomerase II would lead to persistent entanglements. At anaphase onset cohesin is cleaved by separase and as anaphase progresses, centromere distal regions are gradually exposed to the action of spindle microtubules, which would facilitate decatenation in the direction of the chromosome ends.

We have shown that long chromosomes hyper-condense during anaphase in order to be segregated and also that they accumulate more catenations. These two processes are not independent. On one hand, the previous res-

olution of catenations is necessary for hyper-condensation to occur in late anaphase. On the other hand, the resistance to segregation exerted by chromosomes that are highly entangled could promote the faster recoiling of long chromosomes and assist hypercondensation.

From previous knowledge on chromosome segregation and the data presented in this study we propose a model on how chromosomes are segregated (Figure 5.1). During interphase, the sister chromatids become entangled as a product of the semi-conservative nature of replication. The nuclear organization and the attachment of telomeres to the nuclear envelope would restrain the mobility of chromosomes thus impeding the release of catenations by rotation of the DNA fiber. This topological stress is more prominent in longer chromosomes.

Once replication is finished, cells enter mitosis. At metaphase, all the sister chromatids are attached to microtubules emanating from opposite poles of the bipolar spindle. The centromeric regions of the chromosomes sense the pulling tension of the kinetochore microtubules and are decatenated. However, this force from the spindle is not translated to further regions of chromosomes due to the cohesin complex. Thus, sister chromatid arms are not resolved due to the presence of the cohesin complex and the catenations constantly introduced and removed by Topoisomerase II due to the lack of directionality in the enzyme.

The metaphase-to-anaphase transition occurs when cohesin is cleaved by separase. Cohesin release from the chromosomes allows the chromosome arms to progressively sense the pulling force exerted by the microtubules. Then Stu2-dependent microtubule dynamics would process the catenations in a conformation that is favored by Topoisomerase II enzyme. Therefore, thanks to the microtubule dynamicity promoted by Stu2 and to the en-

zymatic activity of Topoisomerase II, sister chromatid intertwinings would be resolved during anaphase achieving a fully decatenated pair of sister chromatids at telophase. This process would ensure complete chromosome resolution before cytokinesis takes place, thus ensuring genome preservation and stability.

Therefore, we propose that Stu2-dependent microtubule dynamics contribute to the step-wise resolution of SCI along chromosome arms during spindle elongation in anaphase, possibly by promoting a resolution-competent state on catenated DNA.

This study provides insights about how cells can deal with extra long chromosomes during segregation, which might reflect a common need of mechanisms designed to ensure proper segregation of specifically longer chromosomes.
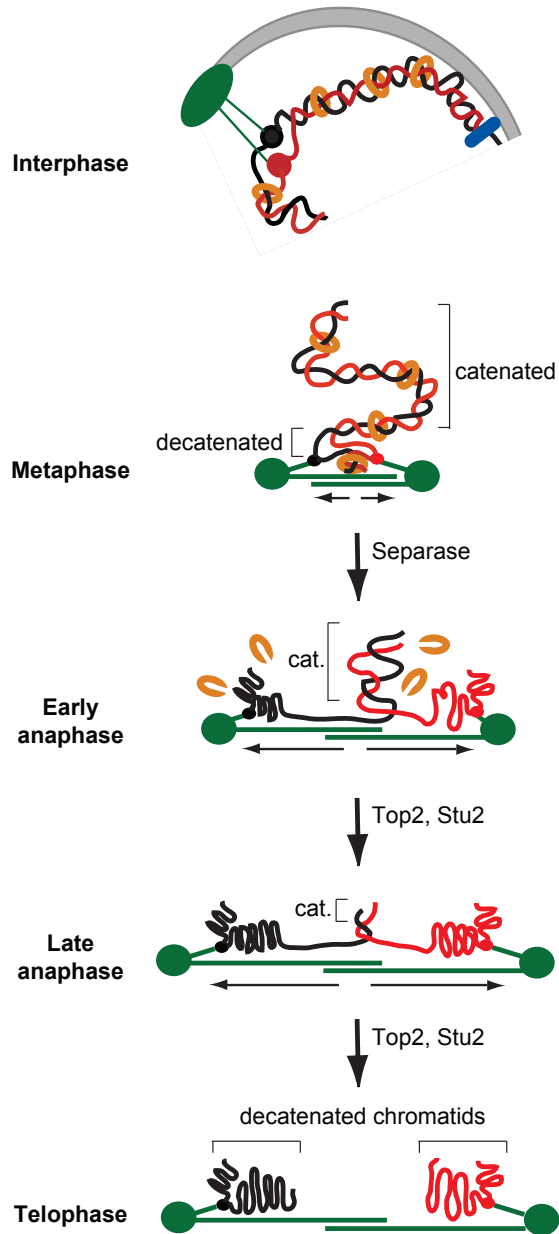
Figure 5.1: Microtubule dynamics and topoisomerase II solve sister chromatid intertwinings during anaphase. See text for details (Discussion 5.4).

6

Conclusions

The conducted research leads to the following major conclusions:

- Yeast cells can adapt to 70% increase in chromosome arm length.

- Aurora B mediated anaphase hyper-condensation is an adaptation mechanism that occurs independently of the presence of the rDNA repeat in the longest chromosome.

- Long chromosome bearing cells are sensitized to the loss of genes involved in chromosome condensation, decatenation and microtubule dynamics.

- Partial impairment of the microtubule polymerase Stu2 in long chromosome bearing cells triggers the *RAD9*-dependent mid-anaphase checkpoint and causes chromosome missegregation.

- Topoisomerase II is needed during anaphase to ensure proper segregation of centromere-distal regions in long chromosomes.

- Telomere detachment from the nuclear envelope decreases the topological stress and partially rescues the segregation defects of *top2-4* and *LC stu2-13* mutants

7

Future directions

The data provided during this research opens up new questions in the field to be solved in the future:

- Long chromosomes can be used as a tool to identify new genes involved in chromosome segregation or to help in the understanding of how previously identified genes work. Therefore, it would be interesting to perform a genetic screen with cells bearing long chromosomes.

- We have not reached the upper limit of chromosome length in budding yeast. Fusing more chromosomes would determine what is the maximum chromosome arm length that yeast can deal with.

- The RAD9-dependent mid-anaphase checkpoint is activated in dicentric chromosomes and *LC stu2-13* but not in Topoisomerase II mutants. It remains unknown what insult is triggering the checkpoint in these cells. Therefore, two scenarios are possible (1) the trigger

of the checkpoint is not present in *top2-4* mutants and therefore it is not simply unresolved catenanes or (2) Topoisomerase II is part of the checkpoint. Then, describing the phenotype of *LC stu2-13 top2-4* mutant would be enlightening.

- Our results suggest that *LC stu2-13* cells accumulate more catenations, however, direct evidence is missing. Performing Smc6-flag ChIP-seq experiments in *stu2-13* mutants would clarify if there is an accumulation of this SCI-associated marker during anaphase in these mutants.

- Our work has focused on the interplay of Topoisomerase II and microtubules during anaphase. However, there are other components to take into account. For example, is not clear yet what is the role of the cohesin complex in the resolution of catenations in linear chromosomes. It would be interesting to investigate if cohesin has a role in SCI resolution in long chromosomes and if this is related to the Topoisomerase II and *stu2* phenotypes.

- The basic principles of cell cycle regulation are conserved throughout species, and it has been shown that there are chromatin remnants during anaphase in mammal cells (namely lagging chromosomes and ultrafine DNA bridges). Therefore, this interplay between Topoisomerase II and microtubules could also be present in higher eukaryotes.

Bibliography

Adolph, K. W., Cheng, S. M., and Laemmli, U. K. (1977). Role of Nonhistone Proteins Chromosome Structure in Metaphase. *Cell*, 12(November):805–816.

Akhmanova, A. and Hoogenraad, C. C. (2005). Microtubule plus-end-tracking proteins: mechanisms and functions. *Current opinion in cell biology*, 17(1):47–54.

Akhmanova, A. and Steinmetz, M. O. (2008). Tracking the ends: a dynamic protein network controls the fate of microtubule tips. *Nature reviews. Molecular cell biology*, 9(4):309–22.

Alexandru, G., Uhlmann, F., Mechtler, K., Poupart, M. a., and Nasmyth, K. (2001). Phosphorylation of the cohesin subunit Scc1 by Polo/Cdc5 kinase regulates sister chromatid separation in yeast. *Cell*, 105(4):459–72.

Anderson, D. E., Losada, A., Erickson, H. P., and Hirano, T. (2002). Con-

densin and cohesin display different arm conformations with characteristic hinge angles. *The Journal of cell biology*, 156(3):419–24.

Andrews, E. A., Palecek, J., Sergeant, J., Taylor, E., Lehmann, A. R., and Watts, F. Z. (2005). Nse2 , a Component of the Smc5-6 Complex , Is a SUMO Ligase Required for the Response to DNA Damage. *Molecular and cellular biology*, 25(1):185–196.

Andrulis, E. D., Neiman, A. M., Zappulla, D. C., and Sternglanz, R. (1998). Perinuclear localization of chromatin facilitates transcriptional silencing. *Nature*, 394(6693):592–5.

Baxter, J., Sen, N., López Martínez, V., Monturus De Carandini, M., Schvartzman, J., Diffley, J. F. X., and Aragón, L. (2011). Positive supercoiling of Mitotic DNA drives decatenation by Topoisomerase II in eukaryotes. *Science*, 331(March):1328–1332.

Bazile, F., St-Pierre, J., and D'Amours, D. (2010). Three-step model for condensin activation during mitotic chromosome condensation. *Cell Cycle*, 9(16):3243–3255.

Belmont, A. S. (2006). Mitotic chromosome structure and condensation. *Current opinion in cell biology*, 18(6):632–8.

Bhalla, N., Biggins, S., and Murray, A. W. (2002). Mutation of YCS4 , a Budding Yeast Condensin Subunit , Affects Mitotic and Nonmitotic Chromosome Behavior. *Molecular Biology of the Cell*, 13(February):632–645.

Blow, J. J. and Laskey, R. A. (1988). A role for the nuclear envelope in controlling DNA replication within the cell cycle. *Nature*, 332:546–548.

Blow, J. J. and Tanaka, T. U. (2005). The chromosome cycle: coordinating replication and segregation. *EMBO reports*, 6(11):1028–1034.

Brock, J. a. and Bloom, K. (1994). A chromosome breakage assay to monitor mitotic forces in budding yeast. *Journal of cell science*, 107 (Pt 4:891–902.

Buchenau, P., Saumweber, H., and Arndt-Jovin, D. J. (1993). Consequences of topoisomerase II inhibition in early embryogenesis of Drosophila revealed by in vivo confocal laser scanning microscopy. *Journal of cell science*, 104 (Pt 4):1175–85.

Cheeseman, I. M., Anderson, S., Jwa, M., Green, E. M., Kang, J. S., Yates, J. R., Chan, C. S. M., Drubin, D. G., and Barnes, G. (2002). Phosphoregulation of kinetochore-microtubule attachments by the Aurora kinase Ipl1p. *Cell*, 111(2):163–72.

Cherry, J. M., Ball, C., Weng, S., Juvik, G., Schmidt, R., Adler, C., Dunn, B., Dwight, S., Riles, L., Mortimer, R. K., and Botstein, D. (1997). Genetic and physical maps of Saccharomyces cerevisiae. *Nature*, 387:67–73.

Chikashige, Y., Yamane, M., Okamasa, K., Tsutsumi, C., Kojidani, T., Sato, M., Haraguchi, T., and Hiraoka, Y. (2009). Membrane proteins Bqt3 and -4 anchor telomeres to the nuclear envelope to ensure chromosomal bouquet formation. *The Journal of cell biology*, 187(3):413–27.

Christensen, M. O., Larsen, M. K., Barthelmes, H. U., Hock, R., Andersen, C. L., Kjeldsen, E., Knudsen, B. R., Westergaard, O., Boege, F., and Mielke, C. (2002). Dynamics of human DNA topoisomerases IIalpha and IIbeta in living cells. *The Journal of cell biology*, 157(1):31–44.

Chubb, J. R., Boyle, S., Perry, P., and Bickmore, W. A. (2002). Chromatin motion is constrained by association with nuclear compartments in human cells. *Current biology*, 12(6):439–45.

Ciosk, R., Zachariae, W., Michaelis, C., Shevchenko, A., Mann, M., and Nasmyth, K. (1998). An ESP1/PDS1 complex regulates loss of sister chromatid cohesion at the metaphase to anaphase transition in yeast. *Cell*, 93(6):1067–76.

Clemente-Blanco, A., Mayán-Santos, M., Schneider, D. A., Machín, F., Jarmuz, A., Tschochner, H., and Aragón, L. (2009). Cdc14 inhibits transcription by RNA polymerase I during anaphase. *Nature*, 458(7235):219–22.

Cobbe, N. and Heck, M. M. S. (2004). The evolution of SMC proteins: phylogenetic analysis and structural implications. *Molecular biology and evolution*, 21(2):332–47.

Cockell, M. and Gasser, S. M. (1999). Nuclear compartments and gene regulation. *Current opinion in genetics & development*, 9:199–205.

Coelho, P. A., Queiroz-Machado, J., and Sunkel, C. E. (2003). Condensin-dependent localisation of topoisomerase II to an axial chromosomal structure is required for sister chromatid resolution during mitosis. *Journal of cell science*, 116(Pt 23):4763–76.

Coghlan, A., Eichler, E. E., Oliver, S. G., Paterson, A. H., and Stein, L. (2005). Chromosome evolution in eukaryotes: a multi-kingdom perspective. *Trends in genetics : TIG*, 21(12):673–82.

Cohen-Fix, O., Peters, J. M., Kirschner, M. W., and Koshland, D. (1996). Anaphase initiation in Saccharomyces cerevisiae is controlled by the APC-

dependent degradation of the anaphase inhibitor Pds1p. *Genes & Development*, 10(24):3081–3093.

Cremer, T. and Cremer, C. (2001). Chromosome territories, nuclear architecture and gene regulation in mammalian cells. *Nature reviews. Genetics*, 2(4):292–301.

Cuylen, S. and Haering, C. H. (2011). Deciphering condensin action during chromosome segregation. *Trends in cell biology*, 21(9):552–9.

D'Ambrosio, C., Kelly, G., Shirahige, K., and Uhlmann, F. (2008). Condensin-dependent rDNA decatenation introduces a temporal pattern to chromosome segregation. *Current biology*, 18(14):1084–9.

D'Amours, D., Stegmeier, F., and Amon, A. (2004). Cdc14 and condensin control the dissolution of cohesin-independent chromosome linkages at repeated DNA. *Cell*, 117(4):455–69.

de Gramont, A. and Cohen-Fix, O. (2005). The many phases of anaphase. *Trends in biochemical sciences*, 30(10):559–68.

De Piccoli, G., Torres-Rosell, J., and Aragón, L. (2009). The unnamed complex: what do we know about Smc5-Smc6? *Chromosome research*, 17(2):251–63.

Desai, A. and Mitchison, T. J. (1997). Microtubule polymerization dynamics. *Annual review of cell and developmental biology*, 13:83–117.

Diffley, J. F. X. (2004). Regulation of early events in chromosome replication. *Current biology*, 14(18):R778–86.

DiNardo, S., Voelkel, K., and Sternglanz, R. (1984). DNA topoisomerase II mutant of Saccharomyces cerevisiae: topoisomerase II is required for segregation of daughter molecules at the termination of DNA replication. *Proceedings of the National Academy of Sciences of the United States of America*, 81(9):2616–20.

Earnshaw, W. C., Halligan, B., Cooke, C. A., Heck, M. M., and Liu, L. F. (1985). Topoisomerase II is a structural component of mitotic chromosome scaffolds. *The Journal of cell biology*, 100(5):1706–15.

Earnshaw, W. C. and Harrison, S. C. (1977). DNA arrangement in isometric phage heads. *Nature*, 268(5621):598–602.

Ebrahimi, H. and Cooper, J. P. (2012). Closed mitosis: A timely move before separation. *Current biology*, 22(20):R880–2.

Ebrahimi, H. and Donaldson, A. D. (2008). Release of yeast telomeres from the nuclear periphery is triggered by replication and maintained by suppression of Ku-mediated anchoring. *Genes & development*, 22(23):3363–74.

Farcas, A.-M., Uluocak, P., Helmhart, W., and Nasmyth, K. (2011). Cohesin's concatenation of sister DNAs maintains their intertwining. *Molecular cell*, 44(1):97–107.

Fisher, A. G. and Merkenschlager, M. (2002). Gene silencing, cell fate and nuclear organisation. *Current opinion in genetics & development*, 12(2):193–7.

Foury, F. and Lahaye, A. (1987). Cloning and sequencing of the PIF1 gene

involved in repair and recombination of yeast mitochondrial DNA. *The EMBO journal*, 6(5):1441–1449.

Freeman, L., Aragon-Alcaide, L., and Strunnikov, A. (2000). The condensin complex governs chromosome condensation and mitotic transmission of rDNA. *The Journal of cell biology*, 149(4):811–24.

Fujita, I., Nishihara, Y., Tanaka, M., Tsujii, H., Chikashige, Y., Watanabe, Y., Saito, M., Ishikawa, F., and Hiraoka, Y. (2012). Telomere-Nuclear Envelope Dissociation Promoted by Rap1 Phosphorylation Ensures Faithful Chromosome Segregation. *Current Biology*, 22:1932–1937.

Funabiki, H., Hagan, I., Uzawa, S., and Yanagida, M. (1993). Cell cycle-dependent specific positioning and clustering of centromeres and telomeres in fission yeast. *The Journal of cell biology*, 121(5):961–76.

Funabiki, H., Yamano, H., Kumada, K., Nagao, K., Hunt, T., and Yanagida, M. (1996). Cut2 proteolysis required for sister-chromatid seperation in fission yeast. *Nature*, 381(6581):438–41.

Gasser, S. M., Laroche, T., Falquet, J., Boy de la Tour, E., and Laemmli, U. K. (1986). Metaphase chromosome structure. Involvement of topoisomerase II. *Journal of molecular biology*, 188(4):613–29.

Giménez-Abián, J. F., Clarke, D. J., Devlin, J., Giménez-Abián, M. I., De la Torre, C., Johnson, R. T., Mullinger, A. M., and Downes, C. S. (2000). Premitotic chromosome individualization in mammalian cells depends on topoisomerase II activity. *Chromosoma*, 109(4):235–44.

Haering, C. H., Farcas, A.-M., Arumugam, P., Metson, J., and Nasmyth,

K. (2008). The cohesin ring concatenates sister DNA molecules. *Nature*, 454(7202):297–301.

Haering, C. H., Löwe, J., Hochwagen, A., and Nasmyth, K. (2002). Molecular architecture of SMC proteins and the yeast cohesin complex. *Molecular cell*, 9(4):773–88.

Hanna, J. S., Kroll, E. S., Lundblad, V., and Spencer, F. A. (2001). Saccharomyces cerevisiae CTF18 and CTF4 Are Required for Sister Chromatid Cohesion. *Molecular and cellular biology*, 21(9):3144–3158.

Harju, S., Fedosyuk, H., and Peterson, K. R. (2004). Rapid isolation of yeast genomic DNA: Bust n' Grab. *BMC biotechnology*, 4(8).

Hartwell, L. H. and Weinert, T. A. (1989). Checkpoints: controls that ensure the order of cell cycle events. *Science*, 246(4930):629–34.

Hauf, S., Cole, R. W., LaTerra, S., Zimmer, C., Schnapp, G., Walter, R., Heckel, A., van Meel, J., Rieder, C. L., and Peters, J.-M. (2003). The small molecule Hesperadin reveals a role for Aurora B in correcting kinetochore-microtubule attachment and in maintaining the spindle assembly checkpoint. *The Journal of cell biology*, 161(2):281–94.

Hauf, S., Roitinger, E., Koch, B., Dittrich, C. M., Mechtler, K., and Peters, J. M. (2005). Dissociation of cohesin from chromosome arms and loss of arm cohesion during early mitosis depends on phosphorylation of SA2. *PLoS biology*, 3(3):419–432.

Havens, K. a., Gardner, M. K., Kamieniecki, R. J., Dresser, M. E., and Dawson, D. S. (2010). Slk19p of Saccharomyces cerevisiae regulates ana-

phase spindle dynamics through two independent mechanisms. *Genetics*, 186(4):1247–60.

Hediger, F., Neumann, F. R., Van Houwe, G., Dubrana, K., and Gasser, S. M. (2002). Live imaging of telomeres: yKu and Sir proteins define redundant telomere-anchoring pathways in yeast. *Current biology*, 12(24):2076–89.

Herschleb, J., Ananiev, G., and Schwartz, D. C. (2007). Pulsed-field gel electrophoresis. *Nature protocols*, 2(3):677–84.

Heun, P., Laroche, T., Shimada, K., Furrer, P., and Gasser, S. M. (2001). Chromosome dynamics in the yeast interphase nucleus. *Science (New York, N.Y.)*, 294(5549):2181–6.

Hildebrandt, E. R. and Hoyt, M. (2000). Mitotic motors in Saccharomyces cerevisiae. *Biochimica et Biophysica Acta (BBA) - Molecular Cell Research*, 1496(1):99–116.

Hill, A. and Bloom, K. (1987). Genetic Manipulation of Centromere Function. *Molecular and cellular biology*, 7(7):2397–2405.

Hirano, T. (2005). Condensins: organizing and segregating the genome. *Current biology*, 15(7):R265–75.

Hirano, T., Kobayashi, R., and Hirano, M. (1997). Condensins, chromosome condensation protein complexes containing XCAP-C, XCAP-E and a Xenopus homolog of the Drosophila Barren protein. *Cell*, 89(4):511–21.

Hirano, T. and Mitchison, T. J. (1993). Topoisomerase II does not play a scaffolding role in the organization of mitotic chromosomes assembled in Xenopus egg extracts. *The Journal of cell biology*, 120(3):601–12.

Holm, C., Goto, T., Wang, J. C., and Botstein, D. (1985). DNA topoisomerase II is required at the time of mitosis in yeast. *Cell*, 41(2):553–563.

Holm, C., Stearns, T., and Botstein, D. (1989). DNA topoisomerase II must act at mitosis to prevent nondisjunction and chromosome breakage. *Molecular and cellular biology*, 9(1):159–68.

Howard, J. and Hyman, A. A. (2003). Dynamics and mechanics of the microtubule plus end. *Nature*, 422(6933):753–8.

Hudakova, S., Künzel, G., Endo, T., and Schubert, I. (2002). Barley chromosome arms longer than half of the spindle axis interfere with nuclear divisions. *Cytogenetic and Genome Research*, 98(1):101–107.

Ivessa, A. S., Zhou, J. Q., and Zakian, V. A. (2000). The Saccharomyces Pif1p DNA helicase and the highly related Rrm3p have opposite effects on replication fork progression in ribosomal DNA. *Cell*, 100(4):479–89.

Janke, C., Magiera, M. M., Rathfelder, N., Taxis, C., Reber, S., Maekawa, H., Moreno-Borchart, A., Doenges, G., Schwob, E., Schiebel, E., and Knop, M. (2004). A versatile toolbox for PCR-based tagging of yeast genes: new fluorescent proteins, more markers and promoter substitution cassettes. *Yeast (Chichester, England)*, 21(11):947–62.

Kahana, J. A., Schnapp, B. J., and Silver, P. A. (1995). Kinetics of spindle pole body separation in budding yeast. *Proceedings of the National Academy of Sciences of the United States of America*, 92(21):9707–11.

Kapitzky, L., Beltrao, P., Berens, T. J., Gassner, N., Zhou, C., Wüster, A., Wu, J., Babu, M. M., Elledge, S. J., Toczyski, D., Lokey, R. S., and Krogan, N. J. (2010). Cross-species chemogenomic profiling reveals

evolutionarily conserved drug mode of action. *Molecular systems biology*, 6(451):451.

Kegel, A., Betts-Lindroos, H., Kanno, T., Jeppsson, K., Ström, L., Katou, Y., Itoh, T., Shirahige, K., and Sjögren, C. (2011). Chromosome length influences replication-induced topological stress. *Nature*, 471(7338):392–6.

Kent, W. J., Sugnet, C. W., Furey, T. S., Roskin, K. M., Pringle, T. H., Zahler, A. M., and Haussler, A. D. (2002). The Human Genome Browser at UCSC. *Genome Research*, 12(6):996–1006.

Kimura, K., Hirano, M., Kobayashi, R., and Hirano, T. (1998). Phosphorylation and Activation of 13S Condensin by Cdc2 in Vitro. *Science*, 282(5388):487–490.

Kimura, K. and Hirano, T. (1997). ATP-Dependent Positive Supercoiling of DNA by 13S Condensin : A Biochemical Implication. *Cell*, 90:625–634.

Kimura, K., Rybenkov, V. V., Crisona, N. J., Hirano, T., and Cozzarelli, N. R. (1999). 13S condensin actively reconfigures DNA by introducing global positive writhe: implications for chromosome condensation. *Cell*, 98(2):239–48.

Koshland, D. and Hartwell, L. H. (1987). The structure of sister minichromosome DNA before anaphase in Saccharomyces cerevisiae. *Science*, 238:1713–1716.

Koshland, D. and Strunnikov, A. (1996). Mitotic chromosome condensation. *Annual review of cell and developmental biology*, 12:305–33.

Kotadia, S., Montembault, E., Sullivan, W., and Royou, A. (2012). Cell

elongation is an adaptive response for clearing long chromatid arms from the cleavage plane. *The Journal of cell biology*, 199(5):745–53.

Lampson, M. A., Renduchitala, K., Khodjakov, A., and Kapoor, T. M. (2004). Correcting improper chromosome-spindle attachments during cell division. *Nature cell biology*, 6(3):232–7.

Langmead, B., Trapnell, C., Pop, M., and Salzberg, S. L. (2009). Ultrafast and memory-efficient alignment of short DNA sequences to the human genome. *Genome biology*, 10(3):R25.

Laroche, T., Martin, S. G., Tsai-pflugfelder, M., and Gasser, S. M. (2000). The Dynamics of Yeast Telomeres and Silencing Proteins through the Cell Cycle. *Journal of structural biology*, 174(129):159–174.

Lau, W. T., Howson, R. W., Malkus, P., Schekman, R., and O'Shea, E. K. (2000). Pho86p, an endoplasmic reticulum (ER) resident protein in Saccharomyces cerevisiae, is required for ER exit of the high-affinity phosphate transporter Pho84p. *Proceedings of the National Academy of Sciences of the United States of America*, 97(3):1107–12.

Lengronne, A., Katou, Y., Mori, S., Yokobayashi, S., Kelly, G. P., Itoh, T., Watanabe, Y., Shirahige, K., and Uhlmann, F. (2004). Cohesin relocation from sites of chromosomal loading to places of convergent transcription. *Nature*, 430(6999):573–8.

Lewis, A., Felberbaum, R., and Hochstrasser, M. (2007). A nuclear envelope protein linking nuclear pore basket assembly, SUMO protease regulation, and mRNA surveillance. *The Journal of cell biology*, 178(5):813–27.

Li, X., Zhu, C., Lin, Z., Wu, Y., Zhang, D., Bai, G., Song, W., Ma, J., Muehlbauer, G. J., Scanlon, M. J., Zhang, M., and Yu, J. (2011). Chromosome size in diploid eukaryotic species centers on the average length with a conserved boundary. *Molecular biology and evolution*, 28(6):1901–11.

Lillie, S. H. and Brown, S. S. (1998). Smy1p, a kinesin-related protein that does not require microtubules. *The Journal of cell biology*, 140(4):873–83.

Lindroos, H. B., Ström, L., Itoh, T., Katou, Y., Shirahige, K., and Sjögren, C. (2006). Chromosomal association of the Smc5/6 complex reveals that it functions in differently regulated pathways. *Molecular cell*, 22(6):755–67.

Luo, K., Yuan, J., Chen, J., and Lou, Z. (2009). Topoisomerase IIalpha controls the decatenation checkpoint. *Nature cell biology*, 11(2):204–10.

Marshall, W. F. (2002). Order and disorder in the nucleus. *Current biology*, 12(5):R185–92.

Mayer, M. L., Gygi, S. P., Aebersold, R., and Hieter, P. (2001). An Alternative RFC Complex Required for Sister Chromatid Cohesion in S . cerevisiae. *Molecular cell*, 7:959–970.

Michaelis, C., Ciosk, R., and Nasmyth, K. (1997). Cohesins: chromosomal proteins that prevent premature separation of sister chromatids. *Cell*, 91(1):35–45.

Mora-Bermúdez, F., Gerlich, D., and Ellenberg, J. (2007). Maximal chromosome compaction occurs by axial shortening in anaphase and depends on Aurora kinase. *Nature cell biology*, 9(7):822–31.

Morgan, D. O. (1997). Cyclin-dependent kinases: engines, clocks, and microprocessors. *Annual review of cell and developmental biology*, 13:261–91.

Morgan, D. O. (2007). *Cell Cycle: Principles of Control*, volume 80. New Science Press.

Murata, M., Shibata, F., and Yokota, E. (2006). The origin, meiotic behavior, and transmission of a novel minichromosome in Arabidopsis thaliana. *Chromosoma*, 115(4):311–9.

Murray, A. W. and Szostak, J. W. (1985). Chromosome segregation in mitosis and meiosis. *Annual review of cell and developmental biology*, 1:289–315.

Nakazawa, N., Mehrotra, R., Ebe, M., and Yanagida, M. (2011). Condensin phosphorylated by the Aurora-B-like kinase Ark1 is continuously required until telophase in a mode distinct from Top2. *Journal of cell science*, 124(Pt 11):1795–807.

Nasmyth, K. and Haering, C. H. (2005). The structure and function of SMC and kleisin complexes. *Annual review of biochemistry*, 74:595–648.

Neff, M. W., Burke, D. J., and Hall, G. (1992). A delay in the Saccharomyces cerevisiae cell cycle that is induced by a dicentric chromosome and dependent upon mitotic A Delay in the Saccharomyces cerevisiae Cell Cycle That Is Induced by a Dicentric Chromosome and Dependent upon Mitotic Checkpoints. *Molecular and cellular biology*, 12(9):3857–3864.

Neurohr, G., Naegeli, A., Titos, I., Theler, D., Greber, B., Díez, J., Gabaldón, T., Mendoza, M., and Barral, Y. (2011). A midzone-based ruler

adjusts chromosome compaction to anaphase spindle length. *Science*, 332(6028):465–8.

Nitiss, J. L. (1998). Investigating the biological functions of DNA topoisomerases in eukaryotic cells. *Biochimica et biophysica acta*, 1400(1-3):63–81.

Ono, T., Losada, A., Hirano, M., Myers, M. P., Neuwald, A. F., and Hirano, T. (2003). Differential contributions of condensin I and condensin II to mitotic chromosome architecture in vertebrate cells. *Cell*, 115(1):109–21.

Ovechkina, Y. and Wordeman, L. (2003). Unconventional motoring: an overview of the Kin C and Kin I kinesins. *Traffic*, 4(6):367–75.

Paulson, J. F. and Laemmli, U. K. (1977). Chromosomes of Histone-Depleted Metaphase Chromosomes. 12:817–828.

Pereira, G. and Schiebel, E. (2004). Cdc14 phosphatase resolves the rDNA segregation delay. *Nature cell biology*, 6(6):473–5.

Pop, M., Phillippy, A., Delcher, A. L., and Salzberg, S. L. (2004). Comparative genome assembly. *Briefings in bioinformatics*, 5(3):237–248.

Postow, L., Ullsperger, C., Keller, R. W., Bustamante, C., Vologodskii, A. V., and Cozzarelli, N. R. (2001). Positive torsional strain causes the formation of a four-way junction at replication forks. *The Journal of biological chemistry*, 276(4):2790–6.

Potts, P. R. and Yu, H. (2005). Human MMS21 / NSE2 Is a SUMO Ligase Required for DNA Repair. *Molecular and cellular biology*, 25(16):7021–7032.

Quinlan, A. R. and Hall, I. M. (2010). BEDTools: a flexible suite of utilities for comparing genomic features. *Bioinformatics (Oxford, England)*, 26(6):841–2.

Rajagopalan, H. and Lengauer, C. (2004). Aneuploidy and cancer. *Nature*, 432(7015):338–41.

Reed, S. I., Hadwiger, J. A., and Lörincz, A. T. (1985). Protein kinase activity associated with the product of the yeast cell division cycle gene CDC28. *Proceedings of the National Academy of Sciences of the United States of America*, 82(12):4055–9.

Reiner, S. L. and Seder, R. A. (1999). Dealing from the evolutionary pawnshop: how lymphocytes make decisions. *Immunity*, 11(1):1–10.

Renshaw, M., Ward, J., and Kanemaki, M. (2010). Condensins Promote Chromosome Recoiling during Early Anaphase to Complete Sister Chromatid Separation. *Developmental cell*, 19:1–26.

Saitoh, N., Goldberg, I. G., Wood, E. R., and Earnshaw, W. C. (1994). ScII: an abundant chromosome scaffold protein is a member of a family of putative ATPases with an unusual predicted tertiary structure. *The Journal of cell biology*, 127(2):303–18.

Schubert, I. (2001). Alteration of chromosome numbers by generation of minichromosomes â Is there a lower limit of chromosome size for stable segregation? *Cytogenetic and Genome Research*, 93:175–181.

Schubert, I. and Oud, J. L. (1997). There is an upper limit of chromosome size for normal development of an organism. *Cell*, 88(4):515–20.

Schuyler, S. C., Liu, J. Y., and Pellman, D. (2003). The molecular function of Ase1p: evidence for a MAP-dependent midzone-specific spindle matrix. Microtubule-associated proteins. *The Journal of cell biology*, 160(4):517–28.

Severin, F., Habermann, B., Huffaker, T., and Hyman, T. (2001). Stu2 promotes mitotic spindle elongation in anaphase. *The Journal of cell biology*, 153(2):435–42.

Shamu, C. E. and Murray, A. W. (1992). Sister chromatid separation in frog egg extracts requires DNA topoisomerase II activity during anaphase. *The Journal of cell biology*, 117(5):921–34.

Sinha, H., David, L., Pascon, R. C., Clauder-Münster, S., Krishnakumar, S., Nguyen, M., Shi, G., Dean, J., Davis, R. W., Oefner, P. J., McCusker, J. H., and Steinmetz, L. M. (2008). Sequential elimination of major-effect contributors identifies additional quantitative trait loci conditioning high-temperature growth in yeast. *Genetics*, 180(3):1661–70.

Skibbens, R. V., Corson, L. B., Koshland, D., and Hieter, P. (1999). Ctf7p is essential for sister chromatid cohesion and links mitotic chromosome structure to the DNA replication machinery. *Genes & development*, 13:307–319.

Spell, R. M. and Holm, C. (1994). Nature and distribution of chromosomal intertwinings in Saccharomyces cerevisiae. *Molecular and cellular biology*, 14(2):1465–76.

St-Pierre, J., Douziech, M., Bazile, F., Pascariu, M., Bonneil, E., Sauvé, V., Ratsima, H., and D'Amours, D. (2009). Polo kinase regulates mitotic

chromosome condensation by hyperactivation of condensin DNA super-coiling activity. *Molecular cell*, 34(4):416–26.

Steffensen, S., Coelho, P. A., Cobbe, N., Vass, S., Costa, M., Hassan, B., Prokopenko, S. N., Bellen, H., Heck, M. M., and Sunkel, C. E. (2001). A role for Drosophila SMC4 in the resolution of sister chromatids in mitosis. *Current biology*, 11(5):295–307.

Strick, T. R., Kawaguchi, T., and Hirano, T. (2004). Real-Time Detection of Single-Molecule DNA Compaction by Condensin I. *Current biology*, 14:874–880.

Sullivan, M., Higuchi, T., Katis, V. L., and Uhlmann, F. (2004). Cdc14 phosphatase induces rDNA condensation and resolves cohesin-independent cohesion during budding yeast anaphase. *Cell*, 117(4):471–82.

Swedlow, J. R., Sedat, J. W., and Agard, D. A. (1993). Multiple chromosomal populations of topoisomerase II detected in vivo by time-lapse, three-dimensional wide-field microscopy. *Cell*, 73(1):97–108.

Tada, K., Susumu, H., Sakuno, T., and Watanabe, Y. (2011). Condensin association with histone H2A shapes mitotic chromosomes. *Nature*, 474(7352):477–83.

Taddei, A., Hediger, F., Neumann, F. R., Bauer, C., and Gasser, S. M. (2004). Separation of silencing from perinuclear anchoring functions in yeast Ku80, Sir4 and Esc1 proteins. *The EMBO journal*, 23(6):1301–12.

Taddei, A., Schober, H., and Gasser, S. M. (2010). The budding yeast nucleus. *Cold Spring Harbor perspectives in biology*, 2(8):a000612.

Tanaka, T., Fuchs, J., Loidl, J., and Nasmyth, K. (2000). Cohesin ensures bipolar attachment of microtubules to sister centromeres and resists their precocious separation. *Nature cell biology*, 2(8):492–9.

Tanaka, T. U. (2005). Chromosome bi-orientation on the mitotic spindle. *Philosophical transactions of the Royal Society of London. Series B, Biological sciences*, 360(1455):581–9.

Tanaka, T. U., Rachidi, N., Janke, C., Pereira, G., Galova, M., Schiebel, E., Stark, M. J. R., and Nasmyth, K. (2002). Evidence that the Ipl1-Sli15 (Aurora kinase-INCENP) complex promotes chromosome bi-orientation by altering kinetochore-spindle pole connections. *Cell*, 108(3):317–29.

Tavormina, P. A., Côme, M.-G., Hudson, J. R., Mo, Y.-Y., Beck, W. T., and Gorbsky, G. J. (2002). Rapid exchange of mammalian topoisomerase II alpha at kinetochores and chromosome arms in mitosis. *The Journal of cell biology*, 158(1):23–9.

Taylor, E. M., Copsey, A. C., Hudson, J. J. R., Vidot, S., and Lehmann, A. R. (2008). Identification of the proteins, including MAGEG1, that make up the human SMC5-6 protein complex. *Molecular and cellular biology*, 28(4):1197–206.

Therizols, P., Fairhead, C., Cabal, G. G., Genovesio, A., Olivo-Marin, J.-C., Dujon, B., and Fabre, E. (2006). Telomere tethering at the nuclear periphery is essential for efficient DNA double strand break repair in subtelomeric region. *The Journal of cell biology*, 172(2):189–99.

Thrash, C., Bankier, A. T., Barrell, B. G., and Sternglanz, R. (1985). Cloning, characterization, and sequence of the yeast DNA topoisomerase

I gene. *Proceedings of the National Academy of Sciences of the United States of America*, 82(13):4374–8.

Torres-Rosell, J., De Piccoli, G., and Aragón, L. (2007). Can eukaryotic cells monitor the presence of unreplicated DNA? *Cell division*, 2:19.

Torres-Rosell, J., Machín, F., Farmer, S., Jarmuz, A., Eydmann, T., Dalgaard, J. Z., and Aragón, L. (2005). SMC5 and SMC6 genes are required for the segregation of repetitive chromosome regions. *Nature cell biology*, 7(4):412–9.

Tóth, A., Ciosk, R., Uhlmann, F., Galova, M., Schleiffer, A., and Nasmyth, K. (1999). Yeast Cohesin complex requires a conserved protein , Eco1p (Ctf7), to establish cohesion between sister chromatids during DNA replication. *Genes & development*, 13:320–333.

Uemura, T. and Tanagida, M. (1986). Mitotic spindle pulls but fails to separate chromosomes in type II DNA topoisomerase mutants: uncoordinated mitosis. *The EMBO journal*, 5(5):1003–10.

Uemura, T. and Yanagida, M. (1984). Isolation of type I and II DNA topoisomerase mutants from fission yeast: single and double mutants show different phenotypes in cell growth and chromatin organization. *The EMBO journal*, 3(8):1737–44.

Uhlmann, F. (2003). Chromosome cohesion and separation: from men and molecules. *Current biology*, 13(3):R104–14.

Uhlmann, F., Lottspeich, F., and Nasmyth, K. (1999). Sister-chromatid separation at anaphase onset is promoted by cleavage of the cohesin subunit Scc1. *Nature*, 400(6739):37–42.

Varga, V., Leduc, C., Bormuth, V., Diez, S., and Howard, J. (2009). Kinesin-8 motors act cooperatively to mediate length-dependent microtubule depolymerization. *Cell*, 138(6):1174–83.

Vas, A. C. J., Andrews, C. A., Matesky, K. K., and Clarke, D. J. (2007). In Vivo Analysis of Chromosome Condensation in Saccharomyces cerevisiae. *Molecular Biology of the Cell*, 18(February):557–568.

Wadsworth, P. and Khodjakov, A. (2004). E pluribus unum: towards a universal mechanism for spindle assembly. *Trends in cell biology*, 14(8):413–9.

Wang, J. C. (2002). Cellular roles of DNA topoisomerases: a molecular perspective. *Nature reviews. Molecular cell biology*, 3(6):430–40.

Wang, P. J. and Huffaker, T. C. (1997). Stu2p: A microtubule-binding protein that is an essential component of the yeast spindle pole body. *The Journal of cell biology*, 139(5):1271–80.

Xu, Y. X. and Manley, J. L. (2007). The prolyl isomerase Pin1 functions in mitotic chromosome condensation. *Molecular cell*, 26(2):287–300.

Yaakov, G., Thorn, K., and Morgan, D. O. (2012). Article Separase Biosensor Reveals that Cohesin Cleavage Timing Depends on Phosphatase PP2A Cdc55 Regulation. *Developmental cell*, 23:124–136.

Yanagida, M. (2009). Clearing the way for mitosis: is cohesin a target? *Nature reviews. Molecular cell biology*, 10(7):489–96.

Yang, S. S., Yeh, E., Salmon, E. D., and Bloom, K. (1997). Identification of a mid-anaphase checkpoint in budding yeast. *The Journal of cell biology*, 136(2):345–54.

Yeh, E., Skibbens, R. V., Cheng, J. W., Salmon, E. D., and Bloom, K. (1995). Spindle dynamics and cell cycle regulation of dynein in the budding yeast, Saccharomyces cerevisiae. *The Journal of cell biology*, 130(3):687–700.

Zapater, M., Sohrmann, M., Peter, M., Posas, F., and de Nadal, E. (2007). Selective requirement for SAGA in Hog1-mediated gene expression depending on the severity of the external osmostress conditions. *Molecular and cellular biology*, 27(11):3900–10.

Zhang, Y., Liu, T., Meyer, C. A., Eeckhoute, J., Johnson, D. S., Bernstein, B. E., Nusbaum, C., Myers, R. M., Brown, M., Li, W., and Liu, X. S. (2008). Model-based analysis of ChIP-Seq (MACS). *Genome biology*, 9(9):R137.

Zhao, X. and Blobel, G. (2005). A SUMO ligase is part of a nuclear multi-protein complex that affects DNA repair and chromosomal organization. *Proceedings of the National Academy of Sciences of the United States of America*, 102(13):4777–82.

Zhou, J. Q., Monson, E. K., Teng, S. C., Schulz, V. P., and Zakian, V. A. (2000). Pif1p Helicase, a Catalytic Inhibitor of Telomerase in Yeast. *Science*, 289(5480):771–774.

A

Genes deleted in LC

Relation of the different subtelomeric genes deleted while fusing chromosomes (Table A.1). Due to the homologous recombination at the subtelomeric regions, some ORFs were deleted during the chromosome fusion.

Chromosome	Gene	Function
IV	IRC4	unknown
IV	YDR541C	dihydrokaempferol 4-reductase (putative)
IV	PAU10	unknown
V	PUG1	uptake of protoprophyrin IX
V	YER184C	unknown
V	SLO1	vesicle-tethering at the Golgi
V	FMP10	unknown
V	FAU1	5,10-methenyltetrahydrofolate synthetase
V	RMD6	sporulation
V	DLD3	D-lactate dehydrogenase
V	DSF1	mannitol dehydrogenase (putative)
V	HXT13	hexose transport
VII	MAL12	maltase
VII	PAU12	unknown
VII	COS6	unknown
XV	PHR1	DNA photolyase
XV	YOR385W	unknown
XV	FRE5	ferric reductase (putative)
XV	FIT3	Mannoprotein from cell wall
XV	FIT2	Mannoprotein from cell wall
XV	YOR381W-A	unknown
XV	YOL164W-A	unknown
XV	YOL166W-A	unknown
XVI	HSP32	unknown
XVI	YPL277C	unknown
XVI	YPL278C	unknown
XVI	YPL279C	unknown
XVI	FDH2	Formate dehydrogenase

Table A.1: Genes deleted when fusing chromosomes.

B

Genetic interactions with LC

To look for mutations that reduced the viability in LC bearing cells, different genes were deleted or the thermosensitive mutations introduced in both wild type and LC cells (Figure B.1). Serial dilutions of the different strains were grown in rich media for 48 hours. The deletion strains were grown both at 25 ºC and 37 ºC. The strains with thermosensitive alleles were grown at 25 ºC, 30 ºC, 32 ºC, 35 ºC and 37 ºC.
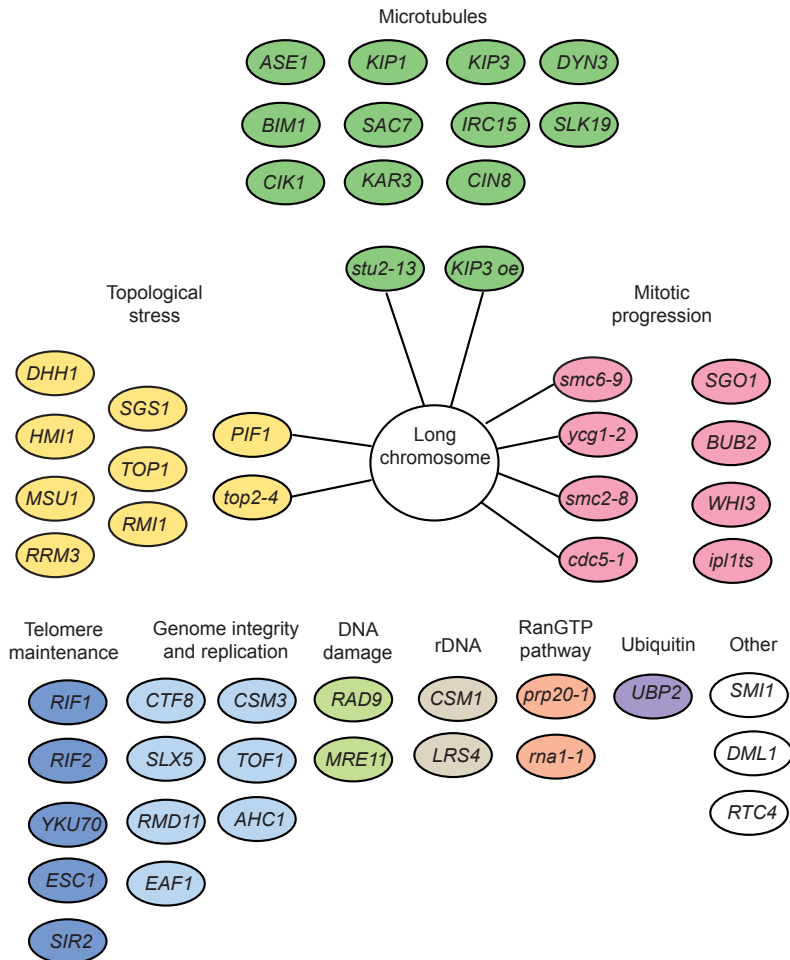
Figure B.1: Genetic interactions with long chromosome strains. The different genetic interactions tested so far are represented in the scheme. Line-connections show genetic interaction, the genes not connected were tested but no genetic interaction was present.

C

Strains used in the study

Table C.1 containing the yeast strains used in this study, all strains are α-mating type and derive from YMM409. Deletions and overexpressions to investigate genetic interactions with LC strains were constructed always using the kanMX4 marker, like 1470 and 1471 that are used as an example. The table contains the name of the strain, the correspondent identification number in the yeast database from the lab and the genotype.

Strain	Number	Genotype
WT	409	trp1::TetO::TRP1 lys4::LacO::LEU2 his3::LacR-GFP::HIS3 TetR-mRFP SPC42-GFP::hphNT1
pGAL:CEN4	413	trp1::TetO::TRP1 lys4::LacO::LEU2 his3::LacR-GFP::HIS3 TetR-mRFP SPC42-GFP::hphNT1 pGAL1-CEN4::kanMX4
pGAL:CEN4 IV:XV	1137	trp1::TetO::TRP1 lys4::LacO::LEU2 his3::LacR-GFP::HIS3 TetR-mRFP SPC42-GFP::hphNT1 pGAL1-CEN4::kanMX4 TEL4R-TEL15R::natNT2
IV:XV cen4Δ	1138	trp1::TetO::TRP1 lys4::LacO::LEU2 his3::LacR-GFP::HIS3 TetR-mRFP SPC42-GFP::hphNT1 TEL4R-TEL15R::natNT2 CEN4::URA3
pGAL:CEN4 IV:XV cen15Δ	1228	trp1::TetO::TRP1 lys4::LacO::LEU2 his3::LacR-GFP::HIS3 TetR-mRFP SPC42-GFP::hphNT1 pGAL1-CEN4::kanMX4 TEL4R-TEL15R::natNT2 CEN15::ble
pGAL:CEN4 IV:XV:V	1375	trp1::TetO::TRP1 lys4::LacO::LEU2 his3::LacR-GFP::HIS3 TetR-mRFP SPC42-GFP::hphNT1 pGAL1-CEN4::kanMX4 TEL4R-TEL15R::natNT2 CEN15::ble TEL15L-TEL5R::URA3
IV:XV:V cen4Δ	1379	trp1::TetO::TRP1 lys4::LacO::LEU2 his3::LacR-GFP::HIS3 TetR-mRFP SPC42-GFP::hphNT1 CEN4::ADE TEL4R-TEL15R::natNT2 CEN15::ble TEL15L-TEL5R::URA3
pGAL:CEN4 IV:XV:V cen5Δ	1386	trp1::TetO::TRP1 lys4::LacO::LEU2 his3::LacR-GFP::HIS3 TetR-mRFP SPC42-GFP::hphNT1 pGAL1-CEN4::kanMX4 TEL4R-TEL15R::natNT2 CEN15::ble TEL15L-TEL5R::URA3 CEN5::ADE
IV:XV:V cen5Δ	1387	trp1::TetO::TRP1 lys4::LacO::LEU2 his3::LacR-GFP::HIS3 TetR-mRFP SPC42-GFP::hphNT1 TEL4R-TEL15R::natNT2 CEN15::ble TEL15L-TEL5R::URA3 CEN5::ADE

Strain	Number	Genotype
pGAL:CEN4 *IV:XV:XVI*	1377	*trp1::TetO::TRP1 lys4::LacO::LEU2 his3::LacR-GFP::HIS3* *TetR-mRFP SPC42-GFP::hphNT1 pGAL1-CEN4::kanMX4* *TEL4R-TEL15R::natNT2 CEN15::ble* *TEL15L-TEL16L::URA3*
IV:XV:XVI *cen4Δ*	1380	*trp1::TetO::TRP1 lys4::LacO::LEU2 his3::LacR-GFP::HIS3* *TetR-mRFP SPC42-GFP::hphNT1* *TEL4R-TEL15R::NAT CEN15::ble* *TEL15L-TEL16L::URA3 CEN4::ADE*
IV:XV:XVI *cen16Δ*	1382	*trp1::TetO::TRP1 lys4::LacO::LEU2 his3::LacR-GFP::HIS3* *TetR-mRFP SPC42-GFP:hphNT1 pGAL1-CEN4::kanMX4* *TEL4R-TEL15R::NAT CEN15::ble* *TEL15L-TEL16L::URA3 CEN16::ADE*
IV:XV:XVI *cen16Δ*	1388	*trp1::TetO::TRP1 lys4::LacO::LEU2 his3::LacR-GFP::HIS3* *TetR-mRFP SPC42-GFP::hphNT1* *TEL4R-TEL15R:NAT CEN15::ble* *TEL15L-TEL16L::URA3 CEN16::ADE*
pGAL:CEN4 *IV:XV:V:VII*	1786	*trp1::TetO::TRP1 lys4::LacO::LEU2 his3::LacR-GFP::HIS3* *TetR-mRFP SPC42-GFP::hphNT1 pGAL1-CEN4::kanMX4* *TEL4R-TEL15R::natNT2 CEN15::ble* *TEL15L-TEL5R::URA3::natNT2 CEN16::ADE* *TEL5L-TEL7R::URA3*
IV:XV:V:VII *cen4Δ*	1788	*trp1::TetO::TRP1 lys4::LacO::LEU2 his3::LacR-GFP::HIS3* *TetR-mRFP SPC42-GFP::hphNT1* *TEL4R-TEL15R::natNT2 CEN15::ble* *TEL15L-TEL5R::URA3::natNT2 CEN16::ADE* *TEL5L-TEL7R::URA3::natNT2 CEN4::URA*
pGAL:CEN4 *IV:XV:V:VII* *cen7Δ*	1790	*trp1::TetO::TRP1 lys4::LacO::LEU2 his3::LacR-GFP::HIS3* *TetR-mRFP SPC42-GFP::hphNT1 pGAL1-CEN4::kanMX4* *TEL4R-TEL15R::natMX4 CEN15::ble* *TEL15L-TEL5R::URA3::natNT2 CEN16::ADE* *TEL5L-TEL7R::URA3::natNT2 CEN7::URA3*

Strain	Number	Genotype
IV:XV:V:VII	1793	*trp1::TetO::TRP1 lys4::LacO::LEU2 his3::LacR-GFP::HIS3*
cen7Δ		*TetR-mRFP SPC42-GFP::hphNT1 pGAL1-CEN4::kanMX4*
		TEL4R-TEL15R::natNT2 CEN15::ble
		TEL15L-TEL5R::URA3::natNT2 CEN16::ADE
		TEL5L-TEL7R::URA3::NAT CEN7::URA3
smc6-9	754	*trp1::TetO::TRP1 lys4::LacO::LEU2 his3::LacR-GFP::HIS3*
		TetR-mRFP SPC42-GFP::hphNT1 smc6-9:natNT2
IV:XV:V:VII	2411	*trp1::TetO::TRP1 lys4::LacO::LEU2*
cen4Δ		*his3::LacR-GFP::HIS3::kanMX4 TetR-mRFP*
smc6-9		*SPC42-GFP::hphNT1 TEL4R-TEL15R::natNT2 CEN15::ble*
		TEL15L-TEL5R::URA3::natNT2 CEN16::ADE
		TEL5L-TEL7R::URA3::natNT2 CEN4::URA3
		smc6-9::HIS3
cdc5-1	713	*trp1::TetO::TRP1 lys4::LacO::LEU2 his3::LacR-GFP::HIS3*
		TetR-mRFP SPC42-GFP::hphNT1 cdc5-1
IV:XV:V	1459	*trp1::TetO::TRP1 lys4::LacO::LEU2 his3::LacR-GFP::HIS3*
cen4Δ		*TetR-mRFP SPC42-GFP::hphNT1 CEN4::ADE*
cdc5-1		*TEL4R-TEL15R::natNT2 CEN15::ble*
		TEL15L-TEL5R::URA3 cdc5-1
IV:XV:XVI	1458	*trp1::TetO::TRP1 lys4::LacO::LEU2 his3::LacR-GFP:HIS3*
cen4Δ		*TetR-mRFP SPC42-GFP::hphNT1*
cdc5-1		*TEL4R-TEL15R::natNT2 CEN15::ble*
		TEL15L-TEL16L::URA3 CEN4::ADE cdc5-1
smc2-8	1210	*trp1::TetO::TRP1 lys4::LacO::LEU2 his3::LacR-GFP::HIS3*
		TetR-mRFP SPC42-GFP::hphNT1 smc2-8
IV:XV:V	1846	*trp1::TetO::TRP1 lys4::LacO::LEU2 his3::LacR-GFP::HIS3*
cen4Δ		*TetR-mRFP SPC42-GFP::hphNT1 CEN4::ADE*
smc2-8		*TEL4R-TEL15R::natNT2 CEN15::ble*
		TEL15L-TEL5R::URA3 smc2-8
ycg1-2	1619	*trp1::TetO::TRP1 lys4::LacO::LEU2 his3::LacR-GFP::HIS3*
		TetR-mRFP SPC42-GFP::hphNT1 ycg1-2::kanMX4

Strain	Number	Genotype
IV:XV:V	1620	*trp1::TetO::TRP1 lys4::LacO::LEU2 his3::LacR-GFP::HIS3*
cen4Δ		*TetR-mRFP SPC42-GFP::hphNT1 CEN4::ADE*
ycg1-2		*TEL4R-TEL15R::natNT2 CEN15::ble*
		TEL15L-TEL5R::URA3 ycg1-2::kanMX4
ase1Δ	1470	*trp1::TetO::TRP1 lys4::LacO::LEU2 his3::LacR-GFP::HIS3*
		TetR-mRFP SPC42-GFP::hphNT1 ase1::kanMX4
IV:XV:XVI	1471	*trp1::TetO::TRP1 lys4::LacO::LEU2 his3::LacR-GFP::HIS3*
cen4Δ		*TetR-mRFP SPC42-GFP::hphNT1*
ase1Δ		*TEL4R-TEL15R::natNT2 CEN15::ble*
		TEL15L-TEL16L::URA3 CEN4::ADE ASE1::kanMX4
stu2-13	1603	*trp1::TetO::TRP1 lys4::LacO::LEU2 his3::LacR-GFP::HIS3*
		TetR-mRFP SPC42-GFP::hphNT1 stu2-13::URA3
IV:XV:XVI	1604	*trp1::TetO::TRP1 lys4::LacO::LEU2 his3::LacR-GFP::HIS3*
cen4Δ		*TetR-mRFP SPC42-GFP::hphNT1*
stu2-13		*TEL4R-TEL15R::natNT2 CEN15::ble*
		TEL15L-TEL16L::URA3::hphNT1 CEN4::ADE stu2-13::URA3
IV:XV:XVI	2394	*trp1::TetO::TRP1 lys4::LacO::LEU2 his3::LacR-GFP::HIS3*
cen4Δ		*TetR-mRFP SPC42-GFP::hphNT1*
rad9Δ		*TEL4R-TEL15R::natNT2 CEN15::ble*
		TEL15L-TEL16L::URA3 CEN4::ADE RAD9::kanMX4
IV:XV:XVI	2394	*trp1::TetO::TRP1 lys4::LacO::LEU2 his3::LacR-GFP::HIS3*
cen4Δ		*TetR-mRFP SPC42-GFP::hphNT1*
stu2-13		*TEL4R-TEL15R::natNT2 CEN15::ble*
rad9Δ		*TEL15L-TEL16L::URA3::hphNT1 CEN4::ADE*
		stu2-13::URA3::natNT2 RAD9::URA3
IV:XV:XVI	1395	*trp1::TetO::TRP1 lys4::LacO::LEU2 his3::LacR-GFP::HIS3*
cen4Δ		*TetR-mRFP SPC42-GFP::hphNT1*
kip3Δ		*TEL4R-TEL15R::natNT2 CEN15::ble*
		TEL15L-TEL16L::URA3 CEN4::ADE KIP3::kanMX4

Strain	Number	Genotype
IV:XV:XVI	2414	*trp1::TetO::TRP1 lys4::LacO::LEU2 his3::LacR-GFP::HIS3*
cen4Δ		*TetR-mRFP SPC42-GFP::hphNT1*
stu2-13		*TEL4R-TEL15R::natNT2 CEN15::ble*
kip3Δ		*TEL15L-TEL16L::URA3::hphNT1 CEN4::ADE*
		stu2-13::URA3::natNT2 KIP3::URA3
top2-4	1780	*trp1::TetO::TRP1 lys4::LacO::LEU2 his3::LacR-GFP::HIS3*
		TetR-mRFP SPC42-GFP::hphNT1 top2-4::kanNT2
IV:XV:V	1782	*trp1::TetO::TRP1 lys4::LacO::LEU2 his3::LacR-GFP::HIS3*
cen4Δ		*TetR-mRFP SPC42-GFP::hphNT1 CEN4::ADE*
top2-4		*TEL4R-TEL15R::natNT2 CEN15::ble*
		TEL15L-TEL5R::URA3 top2-4::kanMX4
IV:XV:V:VII	1794	*trp1::TetO::TRP1 lys4::LacO::LEU2 his3::LacR-GFP::HIS3*
cen4Δ		*TetR-mRFP SPC42-GFP:hphNT1*
top2-4		*TEL4R-TEL15R::natNT2 CEN15::ble*
		TEL15L-TEL5R::URA3::natNT2 CEN16::ADE
		TEL5L-TEL7R::URA3::natNT2 CEN4::URA3
		top2-4::kanNT2
IV:XV:V:VII	1795	*trp1::TetO::TRP1 lys4::LacO::LEU2 his3::LacR-GFP::HIS3*
cen7Δ		*TetR-mRFP SPC42-GFP::hphNT1 pGAL1-CEN4::kanNT2*
top2-4		*TEL4R-TEL15R::natNT2 CEN15::ble*
		TEL15L-TEL5R::URA3::natNT2 CEN16::ADE
		TEL5L-TEL7R::URA3::natNT2 CEN7::URA3
		top2-4::kanMX4
top2-4	1849	*trp1::TetO::TRP1 lys4::LacO::LEU2::URA3*
		his3::LacR-GFP::HIS3 TetR-mRFP SPC42-GFP::hphNT1
		top2-4::kanMX4 pMET-CDC20::LEU2
IV:XV:V	2153	*trp1::TetO::TRP1 lys4::LacO::LEU2 his3::LacR-GFP::HIS3*
cen4Δ		*TetR-mRFP SPC42-GFP::hphNT1 CEN4::ADE*
top2-4		*TEL4R-TEL15R::natNT2 CEN15::ble*
kip3Δ		*TEL15L-TEL5R::URA3::hphNT1 top2-4::kanMX4*
		KIP3::URA3

Strain	Number	Genotype
top2-4 *esc1Δ*	2136	*trp1::TetO::TRP1 lys4::LacO::LEU2 his3::LacR-GFP::HIS3 TetR-mRFP SPC42-GFP::hphNT1 top2-4::kanMX4::URA3 ESC1::natNT2*
top2-4 *yku70Δ*	1870	*trp1::TetO::TRP1 lys4::LacO::LEU2 his3::LacR-GFP::HIS3 TetR-mRFP SPC42-GFP::hphNT1 top2-4::kanMX4::URA3 YKU70::natNT2*
IV:XV:V *cen4Δ* *top2-4* *esc1Δ*	2131	*trp1::TetO::TRP1 lys4::LacO::LEU2 his3::LacR-GFP::HIS3 TetR-mRFP SPC42-GFP::hphNT1 CEN4::ADE TEL4R-TEL15R::NAT CEN15::ble TEL15L-TEL5R::URA3::hphNT1 top2-4::kanMX4 ESC1::URA3*
IV:XV:V *cen4Δ* *top2-4* *yku70Δ*	2174	*trp1::TetO::TRP1 lys4::LacO::LEU2 his3::LacR-GFP::HIS3 TetR-mRFP SPC42-GFP::hphNT1 CEN4::ADE TEL4R-TEL15R::natNT2 CEN15::ble TEL15L-TEL5R::URA3::hphNT1 top2-4::kanMX4 YKU70::URA3*
SMC6-FLAG	2179	*trp1::TetO::TRP1 lys4::LacO::LEU2 his3::LacR-GFP::HIS3 TetR-mRFP SPC42-GFP::hphNT1 SMC6-FLAG::kanMX4*
IV:XV:V *cen4Δ* *SMC6-FLAG*	2153	*trp1::TetO::TRP1 lys4::LacO::LEU2 his3::LacR-GFP::HIS3 TetR-mRFP SPC42-GFP::hphNT1 CEN4::ADE TEL4R-TEL15R::natNT2 CEN15::ble TEL15L-TEL5R::URA3 SMC6-FLAG::kanMX4*
top2-4 *SMC6-FLAG*	2145	*trp1::TetO::TRP1 lys4::LacO::LEU2 his3::LacR-GFP::HIS3 TetR-mRFP SPC42-GFP::hphNT1 top2-4::kanMX4::URA3 SMC6-FLAG::kanMX4*
top2-4 *SMC6-FLAG* *esc1Δ*	2230	*trp1::TetO::TRP1 lys4::LacO::LEU2 his3::LacR-GFP::HIS3 TetR-mRFP SPC42-GFP::hphNT1 top2-4::kanMX4::URA3 ESC1::NAT SMC6-FLAG::kanMX4*
top2-4 *SMC6-FLAG* *yku70Δ*	2187	*trp1::TetO::TRP1 lys4::LacO::LEU2 his3::LacR-GFP::HIS3 TetR-mRFP SPC42-GFP::hph top2-4::kanMX4::URA3 YKU70::NAT SMC6-FLAG::kanMX4*

Strain	Number	Genotype
IV:XV:XVI *cen4Δ* *esc1Δ*	2175	*trp1::TetO::TRP1 lys4::LacO::LEU2* *his3::LacR-GFP::HIS3 TetR-mRFP* *SPC42-GFP::hphNT1 TEL4R-TEL15R::natNT2* *CEN15::ble TEL15L-TEL16L::URA3* *CEN4::ADE ESC1::KAN*
IV:XV:XVI *cen4Δ* *yku70Δ*	1394	*trp1::TetO::TRP1 lys4::LacO::LEU2* *his3::LacR-GFP::HIS3 TetR-mRFP* *SPC42-GFP::hphNT1 TEL4R-TEL15R::natNT2* *CEN15::ble TEL15L-TEL16L::URA3* *CEN4::ADE YKU70::kanMX4*
NUP49-mCherry	2391	*trp1::TetO::TRP1 lys4::LacO::LEU2* *his3::LacR-GFP::HIS3 TetR-mRFP* *SPC42-GFP::hphNT1 NUP49-mCherry::kanMX4*
NUP49-mCherry *esc1Δ*	2392	*trp1::TetO::TRP1 lys4::LacO::LEU2* *his3::LacR-GFP::HIS3 TetR-mRFP* *SPC42-GFP::hphNT1 NUP49-mCherry::kanMX4* *ESC1::URA3*
NUP49-mCherry *yku70Δ*	2393	*trp1::TetO::TRP1 lys4::LacO::LEU2* *his3::LacR-GFP::HIS3 TetR-mRFP* *SPC42-GFP::hphNT1 NUP49-mCherry:kanMX4* *YKU70::URA3*

Table C.1: Strains used in the study.